Final Technical Report (FTR)

a. Federal Agency	Department of Energy	
b. Award Number	DE-EE0009023	
c. Project Title	Risk-informed Hierarchical Control of Behind-the-Meter DERs with AMI Data Integration	
d. Recipient Organization	Eaton Corporation	
e. Project Period	*Start:* 04/01/2020	*End:* 12/31/2023
f. Principal Investigator (PI)	Name: Shakil Hossan Title: Technology Manager Address: Eaton Corporation 14142 Denver West Parkway, suite 345, Golden, CO Phone: 331-871-4637 Email: shakilhossan@eaton.com	
g. Business Contact (BC)	Name: Jill LeClaire Title: Manager, Government Contracts Email address: jleclaire@eaton.com Phone number: 262-352-8372	

Signature of Certifying Official — *Date* 6/24/2024

By signing this report, I certify to the best of my knowledge and belief that the report is true, complete, and accurate. I am aware that any false, fictitious, or fraudulent information, misrepresentations, half-truths, or the omission of any material fact, may subject me to criminal, civil or administrative penalties for fraud, false statements, false claims or otherwise. (U.S. Code Title 18, Section 1001, Section 287 and Title 31, Sections 3729-3730). I further understand and agree that the information contained in this report are material to Federal agency's funding decisions and I have any ongoing responsibility to promptly update the report within the time frames stated in the terms and conditions of the above referenced Award, to ensure that my responses remain accurate and complete.

ACKNOWLEDGEMENT:

This material is based upon work supported by the U.S. Department of Energy's Office of Energy Efficiency and Renewable Energy (EERE) Solar Energy Technologies Office (SETO) under the DE-FOA-0002064, Award Number DE-EE0009023

DISCLAIMER:

Executive Summary

This project addresses several key barriers to implement the next generation demand response applications and provides a clear understanding of implementing hierarchical and standalone control using AMI data. Through this program, Eaton has developed and tested a meter-as-a-controller prototype with the help of other partners--- National Renewable Energy Laboratory (NREL), Electric Power Research Institute (EPRI), Pecan St Inc. (PSI), and Delaware Electric Cooperative (DEC). The controller can utilize residential controllable loads such as heating, ventilation, and air conditioner (HVAC), electric water heater and distributed energy resources like solar PV and battery energy storage systems for off-setting the demand that is required from the grid, thus providing reliable grid-services for demand reduction or peak shaving. The controller is also capable of coordinating the resources of the premises for better management and energy efficiency while meeting the comfort bound of the premises owner as quality-of-service. The development has been demonstrated in a three virtual-home setup at system performance lab of NREL with real appliances (HVAC, electric water heater, solar PV, and battery). The technology has also been proved through laboratory and field demonstration with successful interconnectivity (e.g., end-to-end communication and data exchange) between the residential appliances and utility through the RF network at Delaware Electric Co-op (DEC) in Delaware.

Major Goals & Objectives: In a nutshell, the primary objective of this project was to develop and field-validate a first-of-its-kind TRL 6 control technology to enable optimal provision of high-value grid services from behind-the-meter (BTM) solar PV and other synergistic distributed energy resources (DER) such as battery storage, electric vehicles, and flexible loads. To achieve this objective, the following technologies have been developed:

- An advanced load disaggregation algorithm to significantly improve the accuracy of day-ahead and hour-ahead load forecasting to maximize the potential grid service capacity;
- A hierarchical control solution that leverages smart meters at the residential home level ("meter-as-a-controller") coordinated at the utility central level to enable optimal aggregate control of DERs while respecting the low bandwidth nature of existing utility communication;
- A smart meter with enhanced computational and communication capabilities. Such a meter will act as a "home energy services interface" to interact with diverse DERs, collect high-resolution energy consumption data, extract load disaggregation information, and execute optimal coordination control commands. Such a controller will help end-users to eliminate their consumptions and electricity bill without compromising comfortability while maintain utility constraints. Major accomplishments and technical effectiveness for the project are as follows:
  - Load Disaggregation: achieved a MAPE of 5.1% for aggregated Solar, 5.4% for aggregated EV and 8.5% for aggregated AC on the field data
  - Load Forecast: Day-ahead forecasting approach achieved 58% improvement in performance over the baseline method (naive persistence is used as the baseline method)
  - Comfort bound for meter-as-a-controller: Quality-of-service maintained over 90% of the time (customers temperature comfort bound doesn't violate over 10% of the time). Details validation of cost analysis is provided in task 12 of section 3.
  - Scalability of the deployed system: Scalable to more than 10000 meters with additional gateways than the standard meters

Table of Contents:

List of Contents

List of Figures

List of Tables

1. Background:

According to U.S Energy Information Administration (EIA) projection, the world's energy use will increase by 50% by 2050 [1]. This growth will occur mainly due to increasing population, climate change, paradigm shift in transportation sector, strong rising economy, and urbanization. To meet this increasing demand and reduce the dependencies on fossil-fuel based generation, climate and decarbonization strategies are being highly sought. Corporations, policy makers, and geo-political and economic leaders are advocating net-zero greenhouse emission route as a critical goal for electricity sector. International Energy Agency (IEA) predicts that integration of distributed energy resources (DERs) and energy efficiency techniques will play a key role in achieving this net-zero goal, and a fundamental transformation will take place in global energy systems by 2050 [2]. During this fundamental transformation, annual solar and storage capacities are estimated up to 630 GW and 380 GW, respectively [2],[3]. Furthermore, 240 million households are expected to install rooftop solar PV which are contributing to significant behind-the-meter (BTM) DER assets [2],[4]. These DERs along with other controllable loads will alter the landscape of current distribution systems operations and pose different challenges and opportunities. Utilities will have to face various challenges to control these end-user appliances to receive optimal operations due to:

1. Distributed and geo-stochastic nature of BTM DERs (e.g., household solar and storage) penetration, climate, human-behavior dependent controllable load (e.g., electric water heater, air conditioner) consumption, and EV charging or discharging needs increased visibility to have precise controllability through advanced forecasting and flexibility estimation [5],[6].

2. Coordination of all various BTM DERs and controllable loads require edge control algorithms those can fulfill the objective of energy and cost reduction by considering constraints from both homeowners and utility to provide grid-services and economic operations [7],[8].

3. One-to-one secured exchange of data-streams and state maintenance between a utility controller such as Demand Response Management Systems (DRMS), Distributed Energy Resources Management Systems (DERMS), Advanced Distribution Management Systems (ADMS) and individual premises devices will make the system unscalable unless a mechanism of grouping or premises aggregation of messages (e.g., broadcast, unicast, multicast) is not present for specified messages [9].

In addressing these challenges of visibility, user preferences, and scalable coordination and control, this project develops a hierarchical control and communication architecture for optimal operations of edge controller, embedded in a hardware prototype called meter-as-a-controller, that can optimize and schedule the BTM appliances autonomously. In addition, this meter-as-a-controller can take the utility signal from a central controller to drive the coordination of the premises appliances when required to provide grid-services. Below are the main algorithms developments in this project:

a. Load disaggregation algorithm: U.S residential customers consumed the most end-use electricity according to the U.S. Energy Information Administration [10]. Given such huge end-

use electricity consumption from the residential sector, there is an urgent need to develop an efficient load disaggregation methodology that can provide higher resolution for end-use electricity estimation than house-level load estimation. The methodology needs to accurately estimate the electricity usage of appliances/devices that consume most of the electricity in typical homes. Meanwhile, with ever-evolving smart grids and artificial intelligence technologies [11], the methodologies for demand response (DR) and load shifting are being developed based on various cutting-edge techniques. Among the newly developed algorithms [12], the assumptions for loads are always ideal. In [13], the authors proposed an algorithm based on artificial intelligence; however, the algorithm is for load disaggregation at the bulk supply point, and it can help DSM on the transmission grid. Research on load disaggregation at the house level has also been conducted. A voltage-based method has been designed [14], but it is based on the voltage changes, and the performance might degrade with high penetrations of DERs because the methodology requires a device installed behind a smart meter. Therefore, two aspects need to be addressed. The first is to utilize limited information collected by AMI to achieve accurate load disaggregation. The second is to consider the real-world application scenarios that the algorithm will be implemented at the edge so it has to be computational friendly. In this project, residential load disaggregation is tasked at the metering point of the home to develop further control application within the residences in the subsequent tasks. Efficient and accurate load disaggregation algorithm is developed with two-phase electrical service data of a home as inputs. Without additional information, our proposed algorithm efficiently and fully uses the input data, and the load disaggregation results meet the goals. For large communities with various types of houses and load patterns, we also developed the classification algorithm to classify houses into different clusters and train one load disaggregation model for each cluster. The classification algorithm and the load disaggregation algorithm are tested at different locations and seasons and the performances are good.

b. Load forecasting algorithm: The forecast model provides the central controller algorithm with day-ahead values of the aggregate uncontrollable load for each node in the system. The central controller decisions are influenced by the day-ahead forecasts and the associated errors. Most of the earlier research in the area focused on aggregated residential load forecasting using methods such as random forest regression [15], long short-term memory (LSTM) [16], Bayesian deep learning [17] and forecast of net metered residential load using Bayesian Neural Network [18], LSTM [19] etc. Not much work has been conducted on the forecast of uncontrolled residential load which is volatile and heavily dependent on customer behavior. In this project, we developed an approach suited to the forecast of aggregated uncontrolled residential load based on the output of load disaggregation algorithm from individual meter-as-a-controller.

c. Edge control algorithm: The first aspect of edge control algorithm is the development of the edge-level DERs and loads models. The DERs and loads are classified as controllable and uncontrollable assets. Controllable assets behavior can be modified through an external control signal, whereas uncontrollable loads do not have this flexibility and are usually more critical to the consumer. Based on literature, asset models have the following characteristics – comprehensive, considering physical and operational characteristics of appliances and will

allow external control signals to interact to simulate demand response operations [20]. For this project, the following assets will be considered – solar photovoltaic and inverter (PV), residential-energy-storage-system (RESS), electric-water-heater (EWH), heating-ventilation-and--air-conditioner (HVAC), and electric vehicle (EV). The second aspect is the development of the coordinated edge-level controller. From literatures [21-23], it is found that an optimization-based edge-controller with a flat day-ahead time-of-Use tariff will generally result in the following operations : the electrical energy from the grid is consumed and stored in the batteries (for EV and RESS) during off-peak hours when the electricity cost is low and utilized during on-peak hours when the electricity cost is high. Additionally, considering the limited processing capability of the edge-level hardware, a Rule-Based method is deemed to be more feasible and practical. Furthermore, an optimization-based controller is also investigated for the purpose of precision. To this end, an optimization formulation to optimally control the DERs are identified. The total electricity cost to the homeowner is defined as the optimization cost function. The DERs model identified will be used to calculate the model-states at every time-step, which are defined as the inside temperature of the house (for HVAC), the hot water temperature (for EWH), and the batteries State-of-Charge (for EV and RESS). The Quality-of-Service, which defines the minimum and maximum values of the system-states for user comfort, are defined as the inequality and equality states-constraints in the optimization problem. It is also identified that some DERs, such as the electric-water-heater and HVAC system, can only be controlled in an On or Off manner, which influences the optimization problem formulation and solver. Therefore, a mixed-integer problem formulation and solver is selected to handle such DERs. The edge-controller modes of operation are also identified to address both demand response (DR) and non-DR events. To this end, a two-mode operation of the edge-level controller is considered. The first mode is called the DR-mode, a pseudo-price electricity tariff is sent by the central-level to the edge-level. During this mode, the edge-level controller objective is to manage its local DERs to address the power requirement from the grid, which is represented by the pseudo-price, without sacrificing the Quality-of-Service in the residential unit. The second mode is called the Idle-mode, where the electricity tariff is represented by the flat Time-of-Use tariff. During this mode, the edge-level controller objective is to manage its local DERs to minimize the cost of electricity for the homeowner. To this end, the optimization methods discussed above are implemented.

d. Central control algorithm: The goal of the central controller is to keep voltage magnitudes within bounds and support grid-service events (e.g., peak shaving). It works in a day-ahead fashion in that it takes historical day-ahead forecast errors of nodal loads on a distribution network, the next day's nodal load forecasts, and nodal load flexibility bounds as inputs, and outputs day-ahead pseudo-prices for each edge controller to use as a control signal in the demand response mode. The pseudo-prices are intended to guide nodal loads to meet the central controller's goals. The reason behind this daily batch collection of input data and communication of pseudo-prices is that it requires data from smart meters that are typically collected by utilities in batches [24,25]; whereas feedback-based central control algorithms require a continuous bidirectional flow of data that is not currently supported by most smart meter communication systems [26]. The main development is the internal calculation of

dispatch bounds that determine if the central controller's goals can be met with only the nodal load flexibility bounds and sends out node-specific pseudo-prices when they are insufficient.

All these algorithms listed above have been packaged in firmware and integrated in different platforms. Algorithm(s) listed in (1), (2), and (3) have been unified in meter-as-a-controller, solely developed for this project. Algorithms developed in (4) has been incorporated in the cloud that has readily available integration with Eaton Yukon DRMS. All these developments have been comprehensively tested in a unique lab setup at NREL with real home appliances and DERs. Then, a subset of the development has be demonstrated in a real utility setup and volunteer homes in Delaware. Figure 1 below shows the difference between state-of-the-art solution versus meter-as-controller solution that has been developed in this project. As shown in the figure, meter-as-a-controller can coordinate with all the residential resources and is able to communicate back and forth with the utility. On the other hand, current solution is only able to control the loads without any coordination with DERs which compromises the quality-of-services (e.g., temperature preference is not maintained by air conditioner or not enough hot water reserve) of the homes.

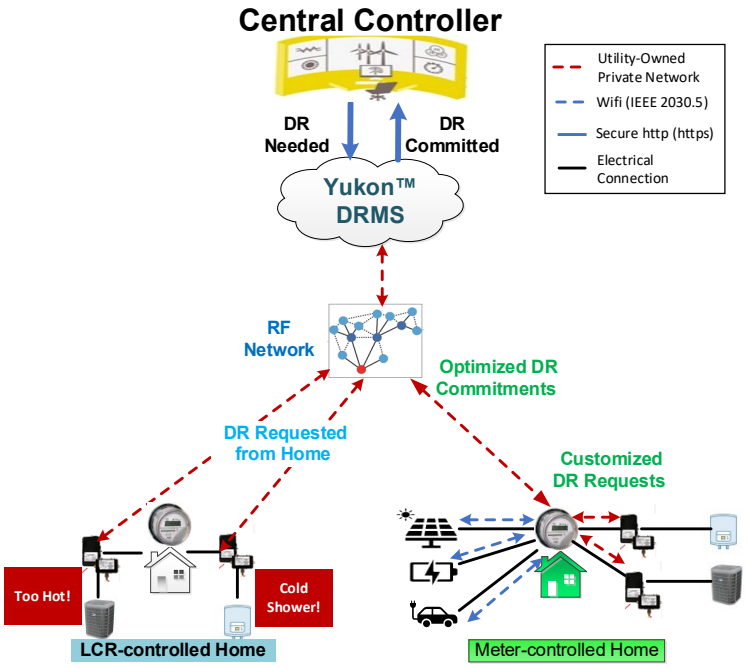

Figure 1. State-of-the-art Solution Vs Proposed solution with meter-as-a-controller.

2. Project Objectives:

Technical approaches and scopes

The nation aims to achieve net-zero greenhouse gas emissions by 2050 and this involves reducing emissions across all sectors of the economy; Furthermore, the U.S. is committed to reducing net GHG emissions by 50-52% below 2005 levels by 2030 [27]. This decade is crucial for implementing

policies and technologies to accelerate emissions reduction. Therefore, the federal government is investing in clean energy and climate solutions, with initiatives projected to reduce U.S. climate pollution by up to 40% below 2005 levels by 2030 [28]. As part of this continuous investment, Eaton along with its partners received funding from DOE SETO office to develop a hierarchical control platform using the AMI data integration to take advantage of residential DERs for improving the quality of grid services. With the background, there are specific technical objectives accomplished during three budget periods. These activities have led clean energy utilization, consumption cost, and CO_2 emission reduction by leveraging residential DERs and minimizing the demand and energy consumption of the appliances (e.g., HVAC, EWH) within a home as well as in a distribution system in an aggregated manner through the innovation of meter-as-a-controller and next generation demand response application. Details of the development, validation, and economic benefits are provided in later sections with the comparison of target and achieved quantifications. High-level summary of the tasks, corresponding milestones, and go-no go (GNG) decision per SOPO are listed below by the budget periods to highlight the significant work done during the project lifetime to contribute to the net-zero goal.

I. **Budget Period 1 (BP1)**

Task(s) summary: In this BP, team focused on algorithm development and overall architecture design for the hardware and firmware. Ground truth data from whole house consumption for different home appliances from over 140 homes from three different regions (TX, NY, and CO) was made available to the team. The datasets had a resolution of 1-minute and a yearly duration (availability from 2017 to 2020). The collected data were used for developing load disaggregation and control algorithms. Different use cases and strategy was developed for control purposes. Besides, RF network to interact with controllable loads and utility via load control relay and solar PV/storage via IEEE 2030.5 over WiFi was designed.

Milestones summary: Associated milestones for the tasks completed in this BP are- collect ground truth data from more than 100 homes, develop load disaggregation algorithm with RMS error <5% at aggregated level, use cases for home operations and utility grid services are approved by IAB, simulation validation of the use cases, communication architecture design to meet sunspec alliance requirement, and conduct IAB meetings.

GNG summary: Passing GNG criteria for this budget period was to validate the load disaggregation with <5% RMS error for individual homes and <30% RMS error for aggregated appliances; Besides, team required to submit a formal commitment letter to DOE from a utility partner to support the field demo.

II. **Budget Period 2 (BP2)**

Task(s) summary: During BP2, team concentrated on developing the hardware and firmware for the meter-as-a-controller. The development focused on multiple applications that include RF node, premises controller, and IEEE 2030.5 server. Besides, the algorithm developed for central controller that is capable of aggregating large number of meter-as-a-controllers has been integrated with Eaton's Yukon demand response management system (DRMS). The entire system has been placed in a three-home testbed at NREL to validate the communication and control before deploying the field.

Milestones summary: The milestones associated with the tasks during BP2 were to complete integrated quasi-static simulation validation of a distribution feeder with sample residential homes to quantify the grid services, develop and lab testing of hardware/firmware for meter-as-a-controller with the communication link to central controller through Eaton's Yukon demand response platform, and conduct IAB meeting to come up with conclusive field-testing plan.

GNG summary: GNG criteria to meet this BP was to complete simulation validation with that promised grid services don't violate the more than 90% of the operational time and detailed test plan vetted by IAB members and host utility.

III. **Budget Period 3 (BP3)**

Task(s) summary: In budget period 3(BP3), team validated the hardware and firmware development and fixed the necessary bugs. Beyond that, team has recruited ~20 volunteers in the DEC territory to deploy the meter-as-a-controller and associated control and communication devices (e.g., LCR, IEEE 2030.5 gateways). Communication link between meter-as-a-controller and central controller has been established. Finally, Eaton team along with Pecan St and DEC was able to test and demonstrate the interconnectivity with 11 residences through the meter-as-a-controller. The interconnectivity included data exchange between the home appliances and meter-as-a-controller to estimate the demand flexibility and transport it to central controller. It also included the operating status of each appliance to ensure the estimated demand flexibility is accurate and control can be enforced, if warranted. Demonstration did not include any controllability as the volunteers were not willing to have controllability on the home appliances for extended period of time as per the requirement of meter-as-a-controller.

Milestones summary: Milestones for this BP were to complete the lab and field testing – thorough lab testing needs to be completed prior to field deployment; Communication interconnectivity should be established with flexible loads and DERs using the protocols considered on this project (e.g., IEEE 1815, IEEE 2030, Sunspec etc.) and field demonstration needs to showcase the scalability to more than 10,000 meters- as-a controller.

End of project Goal: Project needs to showcase a commercial-grade hierarchical control solution that is field-demonstrated on real utility feeder systems. Project will leverage meter-as-a-controller and DRMS to enable aggregate control of BTM DERs to provide grid services and meter-as-a-controller will be able to interact with diverse DERs within the home through a field-demonstration. Further, a risk-based framework will be developed to utilize the available flexibility of BTM DERs.

3. Project Results and Discussion:

This section discusses the tasks, associated subtasks, and milestones to accomplish the project objective with detail clarity to showcase the development, testing, and validation of meter-as-a-controller and demand response application. The activities include data collection and cleaning, load disaggregation and forecasting algorithm development, controller development to operate in both grid-event or demand response and idle-mode to reduce demand, energy, and cost, hardware/firmware development, lab testing and validation, and field pilot. Besides, the

conversations with stakeholders have been discussed which have helped to shape the outcome of this program and paths forward. Before diving into the details, Table 1 below highlights the sub-tasks by budget period.

Table 1. Subtasks listed for three budget periods.

Budget Period	Task #	Task	Sub-task #	Sub-task
1	1	Machine learning based load disaggregation and load forecasting algorithm development	1.1.1	Historical meter data collection, selection, filtering, and analysis
			1.1.2	Development of a machine learning method for load disaggregation
			1.1.3	Enhanced load forecasting using load disaggregation information
	2	Hierarchical grid services control algorithm development	1.2.1	Development of applications and use cases for DER edge intelligence
			1.2.2	Edge-level control algorithm development
			1.2.3	Coordinated control between central and edge layers
	3	Development of the risk-based DER dispatch bounds calculation framework	1.3.1	Developing probabilistic profiles for BTM DERs
			1.3.2	Stochastic optimization algorithm to calculate DER dispatch bounds
	4	Advanced metering hardware, firmware, and software development	1.4.1	System communications and security architecture development
			1.4.2	Advanced smart meter node hardware platform development
			1.4.3	Design specification of advanced smart meter
	5	Stakeholder engagement	1.5.1	Stakeholder engagement
2	6	Coordinated control between central and edge layers	2.6.1	Coordinated control between central and edge layers
	7	Development of the risk-based DER dispatch bounds calculation framework	2.7.1	Risk-based framework implementation in REopt and testing
	8	Advanced metering hardware, firmware, and software development	2.8.1	Advanced smart meter node communications interworking firmware development
			2.8.2	Advanced smart meter node analytics and control application firmware integration
			2.8.3	Headend system control application software integration and communications interworking

	9	Lab testing and end-to-end integration testing	2.9.1	Unit level testing in the lab
			2.9.2	End-to-end system integration testing in the lab
	10	Field deployment and demonstration	2.10.1	Pilot site selection, volunteer recruitment, and test planning
	11	Stakeholder engagement	2.11.1	Stakeholder engagement
3	12	Lab testing and end-to-end integration testing	3.12.1	End-to-end system integration testing in the lab
	13	Field deployment and demonstration	3.13.1	Field tests and evaluation of overall solution
			3.13.2	Final report of the field demonstration of the proposed AMI based grid service using BTM DERs.
	14	Stakeholder engagement	3.14.1	Stakeholder engagement

Tables below shows the associated success values and target metrics per SOPO, and actual performance achieved for each milestone including GNG and end of project goal. Quantitative comparison have been discussed in detail in the later sections, wherever applicable, to demonstrate the effectiveness of the outcomes of different technologies developed in this project.

Table 2. Description of milestones associated with tasks and success criteria.

Tasks	Milestone #	Performance Metric	Success Value	Actual performance achieved
Machine learning based load disaggregation and load forecasting algorithm development	1.1.1	Data collection and cleaning	Data collected for >100 residential homes from 3 geographically dispersed states	Data has been gathered from about 140 homes in TX, NY, and CO
	1.1.2	RMS error	<30% at individual home level, <5% at aggregated level	The developed load disaggregation approach is neural network based and shows an error of <30% for individual appliance within a home and between 5%-9% at the aggregated level which is close to target; different customer behavior due to geography and other random usage factors have made it difficult to reach exactly to the target
	1.1.3	Forecast error reduction	>10% reduction in error over persistence model	A load forecast model was developed to generate day-ahead values of the uncontrolled residential load at every node in the system. The central controller makes use of these forecasts to account for the uncontrollable loads

				to maintain grid voltage profile within acceptable range. The developed adaptive persistence model achieved a 58% improvement in performance over the baseline method (naïve persistence) which is also well above the target.
Hierarchical grid services control algorithm development	1.2.1	Application and use case definition	Approved by IAB	For this project, hierarchical control is referred as utility interactions with residential meter-as-controllers. Two use cases have been discussed with and approved by IAB: a) Grid-event case where the utility provides signal to reduce demand, b) Idle-mode when the home appliances are scheduled for economic operation for the homeowner; in both cases Quality-of-Services (QoS) are the priority.
	1.2.2	Simulation validation	Meeting specification developed in M 1.2.1	Model-based edge-level controls were developed to optimally manage local DERs in coordination with a central-level controller to meet peak load reduction during grid-event and minimize electricity usage for homeowners in idle mode as discussed in 1.2.1 to conduct simulation.
Development of the risk-based DER dispatch bounds calculation framework	1.3.1	Simulation and data mining	Conforming risk threshold based on best engineering judgement	Dispatch bounds are the subset of load flexibility bounds that can guarantee voltage magnitudes are within their bounds if the dispatch bounds/thresholds are respected. Otherwise, pseudo-prices can be set to guide controllable loads to bring nodal voltage magnitudes back within bounds and support grid-events. Pseudo-prices were shown to be successfully calculated under many scenarios and distribution networks.
Advanced metering hardware, firmware, and software development	1.4.1	Data rate and specs	>9.6 Kbps over up to six (6) link hops; meet Sunspec Alliance requirement	A compatible controller is developed that can be integrated with commercial meters, known as meter-as-a-controller, to interact with residential assets , DERs, and utility central controller; this task also covers the development of customized information model to communicate and exchange information between utility and the homes to meet the target metrics
Stakeholder engagement	1.5.1	Frequency and outcome	Once every quarter	In this task, a utility advisory board was formed to discuss the use cases, field

				integration and test plan of meter-as-a-controller along with the future development plans
	GNG-1A	RMS error	<30% at individual home level, <5% at aggregated level	The performance was met closely as discussed in milestone 1.1.2
	GNG-1B	Commitment letter and initial test plan	Receive formal commitment letter from at least one utility company for field demonstration	Received a commitment letter from Delaware Electric Co-op to host the pilot
Hierarchical grid services control algorithm development	2.6.1	Simulation validation	Single feeder simulation	Batch simulation using field data from the selected feeder shows potential 15%-45% energy savings for homeowners in summer months and up to $1.15M annual saving for utilities from coincidental-peak load reduction.
Development of the risk-based DER dispatch bounds calculation framework	2.7.1	Simulation validation	No violation of promised grid service for >90% of the operation hours in a period of one year; Provided reserve is no less than 90% of the total available reserve in the system	The simulation and HIL setup shows that more than 90% of the time during grid-event, no temperature violation has occurred in customers premises and threshold of load reduction was maintained as commanded by the central controller to maintain no voltage violation for >90% of the operational instants; team discussed with DOE about the reserve and decided not to look at this based on the problem formulation
Advanced metering hardware, firmware, and software development	2.8.1	Firmware functionalities	Support specified edge-node inter-communication requirement	Firmware was developed to meet the need for edge level communications with assets using RF and IEEE 2030.5 protocol
	2.8.2	Hardware/software integration	Successful integration	Meter-as-a-controller hardware was integrated with node applications software
Lab testing and end-to-end integration testing	2.9.1	Hardware/software function test	Performance meeting specification	Performance was tested on the stability of the prototype; ran over a 3-4 day period without any interruptions before validating in the lab
Stakeholder engagement	2.11.1	Frequency and outcome	Once every quarter	In this task, the development of the hardware was reported and test plan in the field was developed to align with the expectation of the advisory board
	GNG-2A	Simulation validation	No violation of promised grid	Simulation criteria was met as discussed in milestone 2.7.1

			service for >90% of the operation hours in a period of one year; Provided reserve is no less than 90% of the total available reserve in the system	
	GNG-2B	Detailed field demonstration plan	Committed by the utility company, approved by IAB and DOE	Test plan developed in 2.11.1 was approved by the stakeholders
Lab testing and end-to-end integration testing	3.12.1	Hardware/software function test	Performance meeting specification	To de-risk the technology, a setup like the field was mimicked in system performance lab at NREL where both control and communication testing were done to check the specified requirements; an in-person demo was also shown to DOE TM
Field deployment and demonstration	3.13.1	Status report	Progress towards field deployment	Field installation updates were provided
	3.13.2	Field test	Performance meeting specification	Details interconnectivity testing was conducted between utility demand response management systems (DRMS) and meter-as-a-controllers at 13 volunteer homes; the controller was able to exchange the solar inverter, HVAC, and EWH information to the DRMS; demonstration of the system was shown to DOE
Stakeholder engagement	3.14.1	Frequency and outcome	Once every quarter	Field test results were shown and pathway to add more features/functionalities were discussed
EOP	EOP	Connectivity and scalability	1) the newly developed smart meters show proven interconnectivity with all DER and flexible load communication protocols under consideration on this project (e.g., IEEE 1815, IEEE 2030, SunSpec); 2) the control system	The EOP goal was met by the interconnectivity in the field validation as discussed in milestone 3.13.2; The analysis show that such a control system is scalable to more than 10000 meter-as-a-controller with additional gateways to Eaton Yukon DRMS

			demonstrates capability to scale to a field system of more than 10,000 meter interfaced end points.	

Task 1.0: Machine learning based load disaggregation and load forecasting algorithm development

Meter data collection: The raw field data is collected by Pecan St. in multiple locations and different time windows, and the raw data is preprocessed by Eaton before shared with NREL team.

Data preprocessing: The raw data from the households will have data quality issues. The appliance-level data is sent through a preprocessing module to resolve the inconsistencies in the data. The data preprocessing module performs the following tasks:

1. Handle missing timestamps: It is common to have missing observations from time series data. The first stage of the preprocessing module will fill in the missing timestamps to ensure clean time series data. The missing data points were filled using the approach of linear interpolation.
2. Data format checking: The module ensures a uniform date and time format to do an accurate aggregation of the residential data.
3. Outlier detection: In time series data, an anomaly or outlier is a data point that does not follow the common trend or is significantly different from the rest of the data. The approach of percentiles is utilized to detect anomalies and replaced with the mean of the previous data points. As the approach is utilized using the historical data from the same location/meter, it is expected to be precise.

Load disaggregation algorithm development: For this task, we designed and developed a specific neural network to realize the load disaggregation algorithm. The neural network contains 5 layers with 3 hidden layers, one input layer and one output layer. The algorithm is tested on different locations and various time window. The locations include Texas, New York state, and Delaware. Among all the previous scenarios, our developed load disaggregation (LD) algorithm demonstrated accurate and robust performances under different conditions. The most recent testing scenario locates in Delaware, and the data is collected in June. Three major appliances are tested, which are air conditioner (AC), solar panels, and electric vehicles (EV).

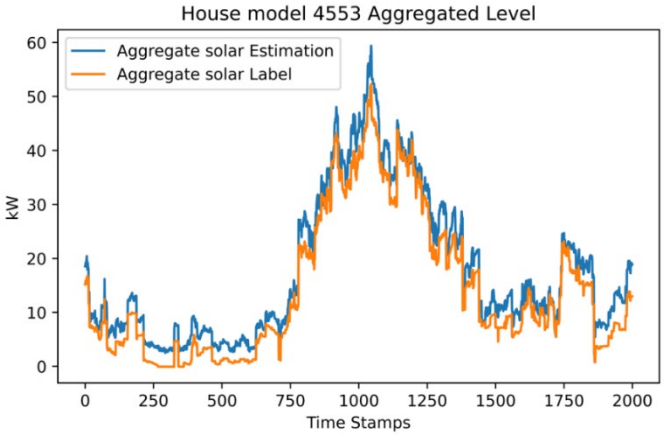

Figure 2. Solar model performance at aggregated level.

For each appliance, one house will be selected to train the model, and the trained model will be applied to all the houses that have the same appliance. For example, in the Delaware dataset, there are 15 houses with valid full month data for solar, and house 4553 is selected as the model house to train the solar LD model. The trained model is then applied to the rest houses. The Figure 2 shows the model performance at aggregated level. The mean absolute error (MAE) is 2.88 kW, and the mean absolute percentage error (MAPE) is 5.12%.

For AC there are 18 houses with valid data, and house 9464 is selected to train the model, the aggregated level MAE is 2.62 kW, and the MAPE is 8.56%. For EV there are 7 houses with full month valid data, house 10867 is selected to train the model. At aggregated level, the MAE is 1.06 kW, the MAPE is 5.48%. Table 3 shows the evaluation results for each appliance at aggregated level. And Table 2 shows the maximum and minimum MAE for a single house among all the houses with valid data for each of the appliances.

Table 3. Evaluation results for each appliance

Appliance	Valid house	Model house	MAE (kW)	MAPE
AC	18	9464	2.62	8.56%
Solar	15	4553	2.88	5.12%
EV	7	10867	1.06	5.47%

Table 4. Evaluation results for each appliance cont.

Appliance	Model house	MAX MAE(kW)	Min MAE (kW)
AC	9464	0.615	0.106
Solar	4553	0.604	0.180
EV	10867	0.279	0.027

Besides testing the LD algorithm, we've also developed a clustering algorithm in case that there are vast houses, and the locations are distant, so the household consumption varies a lot, and one model may not cover all the scenarios. In our testing case, there are 141 houses, and the

developed clustering algorithm can successfully classify the houses into different clusters and improve the overall performance.
Figure *3* shows 3D visualization of five clusters.

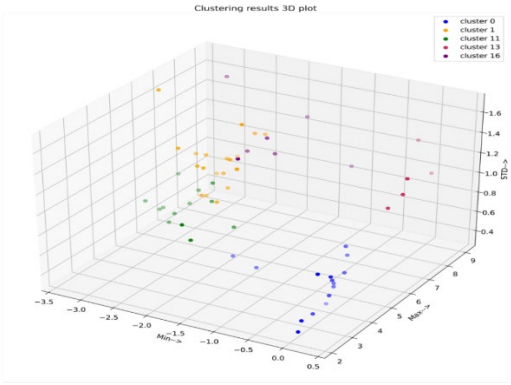

Figure 3. 3D visualization of the clustering algorithm

Data aggregation: The cleaned time series data is aggregated to generate the load profiles. The aggregation is performed on the selected households at an appliance level while ensuring the data points in the same timestamps are only added. The load profile for an air conditioning unit for a single residential household (home ID 1642), on August 17th, 2020, is shown in Figure 4. The figure represents an example of raw data before preprocessing and aggregation. The appliance level data for the selected households goes through the preprocessing and aggregation modules and the aggregated air conditioning load for the system on the same day (Aug 17th, 2020) is shown in Figure 5.

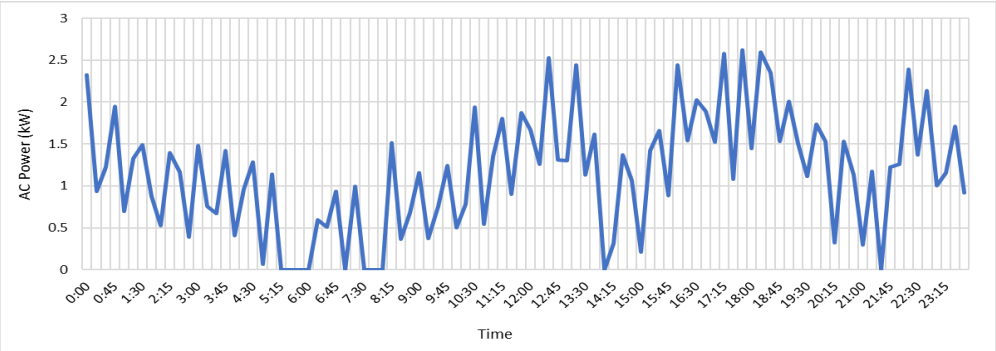

Figure 4. Load profile of an air conditioner for a single residential unit

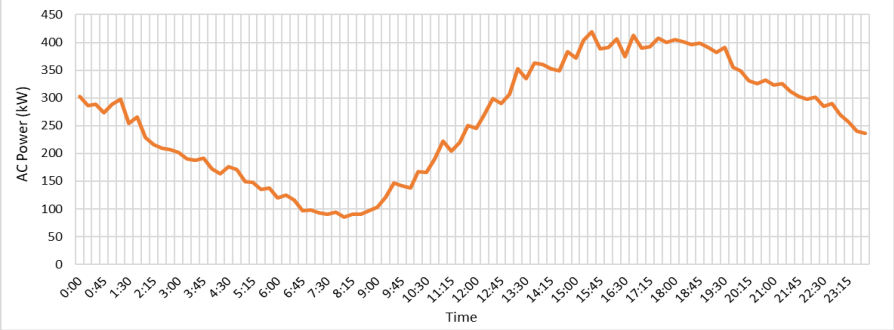

Figure 5. Aggregated profile for the air conditioning load

Forecasting algorithm to predict appliance-level consumption: The development of the forecast algorithm to predict day-ahead values with 15-minute resolution is performed on the aggregated appliance level data. Methods such as Random Forest (RF), Support Vector Machines (SVM), K Nearest Neighbor's (KNN), gradient boosting, and the different version of the novel modified persistence model (D-N) are tested to find the best method for each appliance. The steps followed for the modified persistence are shown in the block diagram below. The equation for modified seasonal persistence is given in equation (1), and the error from these predictions are evaluated using MAPE (Mean Absolute Percentage Error), as show in equation (2). Here, $P(t+\Delta t\,|t)$ is the forecast for a period of Δt made at time t; n represents the number of past measurements; and δ_i are the different lag values for selecting the past measurements. In equation (2), $\hat{y}_t$ represents the forecasted value, y_t the actual value and n the number of data points in the forecast.

$$P(t+\Delta t \mid t) = \frac{1}{n}\sum_{i=1}^{n} P(t-\delta_i t) \quad (1)$$

$$MAPE = \frac{1}{n}\sum_{t=1}^{n} \frac{|\hat{y}_t - y_t|}{y_t} \quad (2)$$

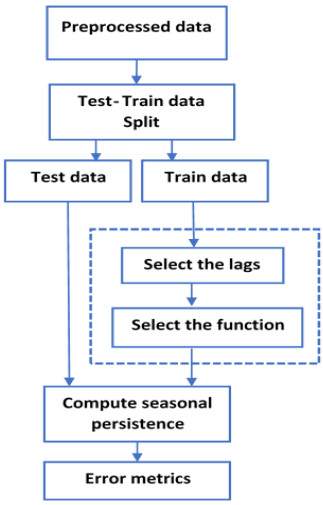

Figure 6. Sequence for adaptive persistence forecasting approach.

Table 5. Comparison of forecasting approaches for individual appliances

Appliances	RF	SVM	KNN	Gradboosting	D-1	D-1,2,3	D-1..7	D-1,7,14,21	D-7,14,21
AC power	525.11	495.52	461.78	420.44	69.33	87.16	102.42	213.68	271.56
Bedroom	13.36	15.4	15.43	13.55	9.26	8.48	8.55	9.41	10.93
Furnace	91.87	78.5	98.99	74.39	20.85	24.97	29.98	44.19	55.59
Kitchen	12.72	29.33	13.96	12.95	16.26	14.20	13.14	13.05	13.89
Pool	66.8	122.29	56.82	64.94	19.51	21.69	27.31	36.30	44.05
Refrigerator	7.49	12.83	9.5	8.08	6.72	6.24	5.94	6.39	7.19
Others	20.73	29.15	22.17	21.19	26.89	22.92	20.33	20.79	21.18

The MAPE from the day-ahead forecast using the 9 different approaches are listed in the table above. The acronym 'D-1,2,3' represents the lags in days used for the modified persistence, data from the previous 3 days are utilized for this model, similarly for all other persistence models listed in the table. The values highlighted in red represent the method selected for each appliance based on the error and run-time. The performance improvement in forecasting aggregate residential load at an appliance level using APM in comparison with traditionally used approached is validated using the tests conducted as shown in Table 5. The performance of APM in forecasting load at an aggregate level is shown in Table 6, where it displayed a 58% improvement in performance over classical persistence (baseline), and 10.6% improvement over support vector machines (SVM).

Table 6. Comparison of forecasting approaches

Forecasting method	MAPE
D-1,7,14,21,28	10.86
Mode, D-1,7,14,21,28	10.9
Mode, D-7,14,21,28	11.19
D-7,14,21,28	11.23
SVM	12.15
RF	12.67
KNN	13.82
D-1…7,14,21,28	15.56
Classic persistence	25.93

Performance of the forecasting methods on the uncontrollable load profile: The developed forecasting method is tested on the appliance level value acquired from the load disaggregation algorithm. The disaggregated information of 3 residential households is aggregated and the results are shown in
Figure 7.
Figure 7(a) represents the aggregated air conditioning load and
Figure 7(b) shows the uncontrollable part of the residential households. In this task, the major item that was validated is the performance of APM method on the aggregate residential load generated from the output of load disaggregation.

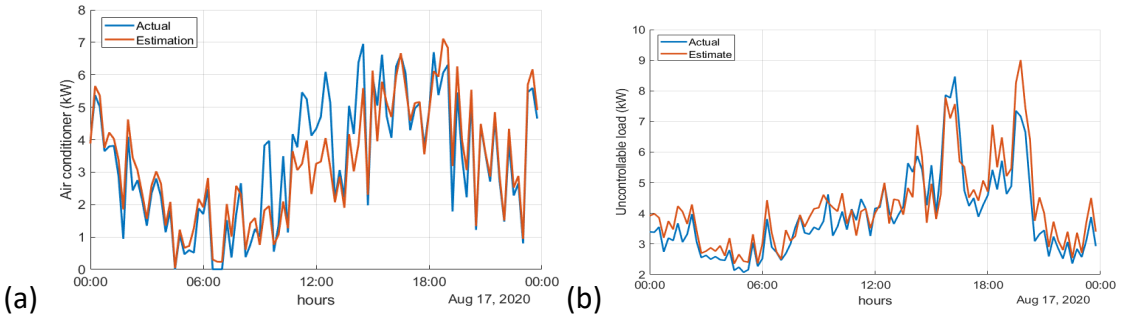

Figure 7. (a) Aggregated air conditioner load profile generated from the LD output of 3 residential households, (b) Aggregated uncontrollable load profile generated from the LD output of 3 residential household

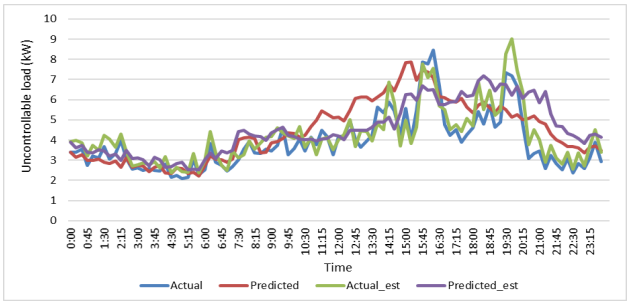

Figure 8. Day-ahead forecast of uncontrollable load.

The day-ahead predictions with a 15-minute resolution on August 17th on the uncontrollable part of the aggregated residential load are represented in Figure 8. The modified persistence method of D-1...7 was used to generate the predictions. The graph portrays the effect of load disaggregation on the forecast. The legend 'Actual_est' and 'Predicted_est' represent the actual and predicted values using the data from disaggregation, while the lines 'actual' and 'predicted' show the real and predicted values using the Pecan St appliance level values. The test was extended to 22% of the dataset yielded a MAPE of 19.7 for the predictions based on the actual Pecan St appliance data and a MAPE of 18.71 for the predictions based on disaggregated load.

The developed forecasting methodology is applied to predict the day-ahead aggregate uncontrollable load values on the central controller. The forecasts were performed for a period of 24 hours with a 15-minute resolution and the error values at each datapoint for the predictions on 4 different days at the controllable node are given in Figure 9.

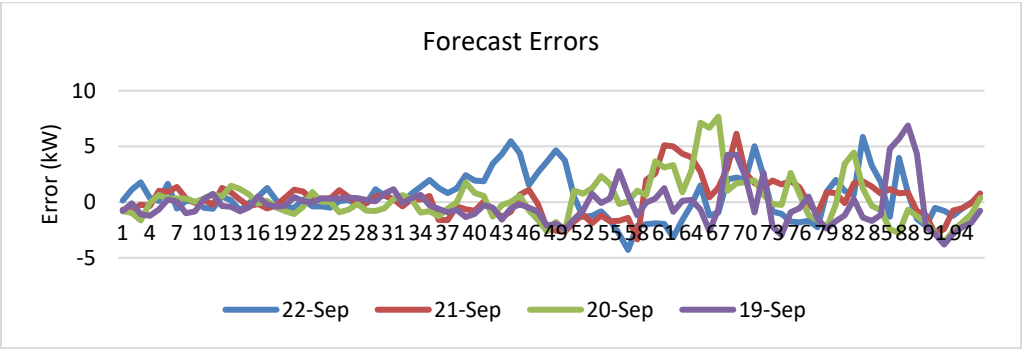

Figure 9. Performance of the forecast method on the controllable node

The home load is the aggregate of uncontrollable load values from 5 different homes. The average MAE values for predictions conducted on the 4 days ranged from (1.2 to 1.5 kW).
The performance of the forecast method on the load values of uncontrollable nodes are given in Figure 10. There are 20 uncontrollable nodes with 10 homes each and the average prediction errors for the 4 days (19- Sept to 22-Sept) for all the 20 nodes are 3.25, 3.17, 3.54, and 3.75.

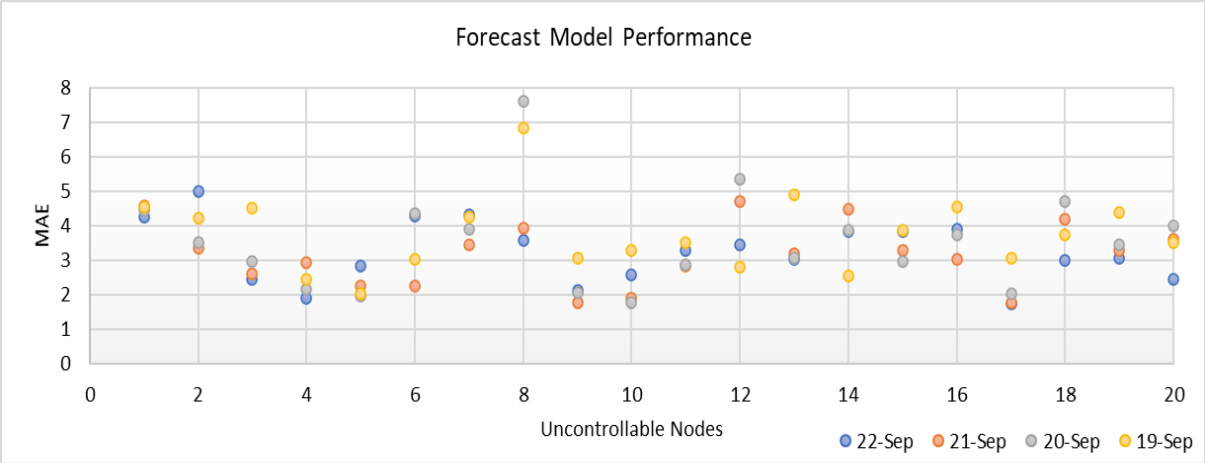

Figure 10. Performance of the forecast method on the uncontrollable nodes

Task 2.0: Hierarchical grid services control algorithm development

The first use case in a simulation environment is the DR event. In a DR event, the central-level controller will gather disaggregated load data from the edge-level controller and calculate potential PV energy generation from weather forecast, to predict future energy reserve and compute the corresponding energy pseudo-pricing that is broadcasted to the edge-level controllers. Pseudo-price, as the name suggest, is not a real energy pricing. It is a simplified pricing-value, based on the normal energy-pricing, that is used by the central-level controller to communicate the expected loads to the edge-level controller during a DR event. First, the central-level controller would perform its analysis and estimate the desired peak loads from the homes during a DR event. Then, using the averaged historical aggregated load profile and the historical energy-pricing, a simple correlation between energy-price and home loads is derived. The pseudo-price is then calculated by using this price-to-load correlation with the desired peak loads from the homes during the DR event and sent to the edge-level controllers. The edge-level controller will then perform similar conversion using the home's historical load profile and historical energy-pricing to translate the pseudo-price into the expected maximum home load during a DR event.

Each edge-level controller receives the pseudo-pricing data and manages its local DERs to meet the energy/power demanded from the central-level controller, based on the pseudo-pricing, while reporting back the disaggregated load data to the central-level controller. DR event use case is selected as the starting point to evaluate the development of central-level and edge-level

controllers in this program because it represents the most basic scenario where grid-level demands are met by the edge-level responses through DERs participations and intelligence.
In a specific grid-service use-case for a hierarchical Distributed-Energy-Resources (DERs) management strategy, a centralized controller (usually electrical utility provider) may send signals to individual homes to limit their maximum net-power consumptions for a specific time-duration. However, in conventional homes, multiple DERs operate independently and may turn on at the same time to ensure the Quality-of-Services (QoS) are met for the homeowner. For example, the AC needs to cool the indoor air, the electric water heater needs to heat the water tank and the electric vehicle needs to be charged, all at the same time, which may cause a spike of power usage at the home level. The challenge is then on scheduling the different DERs On and Off statuses to limit the maximum net-power consumption of the home is below a certain power threshold limit all the time during a grid-service event, while maintaining the Quality-of-Services controlled by the DERs. The controller's objective is also expanded to minimize total energy use for the home and schedule the DERs outside of grid-service event, given the day-ahead Time-of-Use (TOU) tariff, while also maintaining the Quality-of-Services controlled by the DERs. By formulating the problem to consider pre-determined TOU tariff to minimize the energy cost, on top of grid-even that can occur at any hours at any given day, the controller is guaranteed to minimize the peak load during a grid-event for the utility, while at the same time minimizing the energy cost for homeowners. This works in either scenarios of when the grid-event hours coincides with the pre-determined peak-pricing hours or when they do not coincide.

Edge-Controller Overview: The first aspect is the development of the edge-level DERs loads models. The DERs loads are classified into controllable and uncontrollable loads. Controllable loads are loads whose behavior can be modified through external control signals, whereas uncontrollable loads do not have this flexibility and are usually more critical to the consumer. For this project, the following DERs loads will be considered – solar photovoltaic and inverter (PV), residential-energy-storage-system (RESS), electric-water-heater (EWH), heating-ventilation-and--air-conditioner (HVAC), and electric vehicle (EV). While the main input into these models is the energy/power consumed, each model has a different set of inputs/parameters depending on customer comfort and thermal dynamics; PV - solar irradiation data, HVAC - ambient air temperature, thermostat set point based on consumer comfort, allowable temperature deviation or dead band and data pertaining to the structure of the house, with room temperature as the model-state, EWH – ambient air temperature, outlet hot water set point based on consumer comfort, allowable temperature deviation, tank characteristics, rated power and hot water usage profile, with hot water temperature as the model-state, and RESS/EV – rated charging power and plug in time, with battery State-of-Charge as the model-state. The challenge in EV modeling is that the SOC is unknown; EV manufacturers do not typically allow SOC to be communicated to the charger. The challenge in water heater modeling is estimating the daily usage, therefore the total energy available is modeled instead of usage. From a control standpoint, water heater is a one-way load, load can be increased but not decreased. These models are driven by the power/energy inputs from the edge-level control algorithm.
The second aspect is the development of the edge-level controller. From literatures, it is found that an optimization-based edge-controller with a flat day-ahead Time-of-Use tariff will generally

result in the following operations : the electrical energy from the grid is consumed and stored in the batteries (for EV and RESS) during off-peak hours when the electricity cost is low and utilized during on-peak hours when the electricity cost is high. Additionally, considering the limited processing capability of the edge-level hardware, a Rule-Based method is deemed to be more feasible and practical. Additionally, an optimization-based controller will also be investigated. To this end, an optimization formulation to optimally control the DERs are identified. The total electricity cost to the homeowner is defined as the optimization cost function. The DERs model identified will be used to calculate the model-states at every time-step, which are defined as the inside temperature of the house (for HVAC), the hot water temperature (for EWH), and the batteries State-of-Charge (for EV and RESS). The Quality-of-Service, which defines the minimum and maximum values of the system-states for user comfort, are defined as the inequality and equality states-constraints in the optimization problem. It is also identified that some DERs, such as the electric-water-heater and HVAC system, can only be controlled in an On or Off manner, which influences the optimization problem formulation and solver. Therefore, a mixed-integer problem formulation and solver is selected to handle such DERs. The edge-controller modes of operation are also identified to address DR and non-DR events. To this end, a two-mode operation of the edge-level controller is considered. The first mode is called the DR-mode, a pseudo-price electricity tariff is sent by the central-level to the edge-level. During this mode, the edge-level controller objective is to manage its local DERs to address the power requirement from the grid which is represented by the pseudo-price, without sacrificing the Quality-of-Service in the residential unit. The second mode is called the Idle-mode, where the electricity tariff is represented by the flat Time-of-Use tariff. During this mode, the edge-level controller objective is to manage its local DERs to minimize the cost of electricity for the homeowner. To this end, the optimization methods discussed above will be implemented.

DERs Control Models Development: In total there are five DERs under consideration for the simulation efforts which are Air-Conditioner (AC), Electric Water Heater (EWH), EV-charger (EVC), PV-solar (PV) and Residential Energy Storage System (RESS). Control-models for the DERs are developed to predict the amount of electrical power each DER can consume or generate during a DR-event, while minimizing the impact on the Quality of Service (QoS) for the users. The models are calibrated based on DERs historical data, which are assumed to be collected in a database at the edge-level, to ensure good representations of the actual DERs.

Home Thermal Parameters Estimation with Indoor Temperature Reading for Air-Conditioner (AC): The objective of the AC control-model is to predict the home indoor temperature variations when the AC is turned on or off. By knowing this, the edge-level control can then allocate the on and off timings of the AC during a DR-event without violating the Quality-of-Service based on the temperature set-points by the user. First, the thermal model of a residential unit is represented as a simple RC-circuit as shown in
Figure 10 as discussed in [20,21]. A simple, but well-calibrated model, is first proposed that can be used in a wide variety of users homes. More complex model can also be utilized – however this requires detailed information about the house such as walls insulation materials, number of rooms and their locations with respect to the outer home walls. This information may be hard to

collect may complicate the development of the controller if each house has its own different model to be calibrated. The objective is therefore to have a common model that can be calibrated to specific homes using data collected on-site. To this end, a simple model was found to be sufficient to capture the indoor temperature dynamics, as will be presented in here. R_{th} and C_{th} represent thermal resistance and capacitance of the home respectively, while T_{in} and T_{out} represent the indoor and outdoor temperatures. P_{AC} represents the electrical power used by the AC.

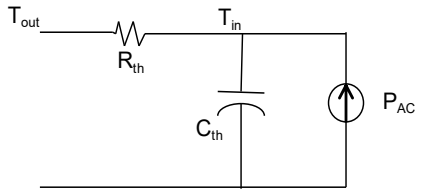

Figure 10. Simple RC-circuit Representation of Home Thermal Model.

The dynamics of the indoor home temperature is given by (1)

$$\dot{T}_{in} = \left[\frac{T_{out} - T_{in}}{R_{th} C_{th}}\right] - \left[\frac{P_{AC}}{C_{th}}\right] \quad (1)$$

The thermal constants R_{th} and C_{th} are calculated during on and off cycles of the AC based on T_{in}, T_{out} and P_{AC} from historical data collected at the edge-level, as shown in Figure 11.

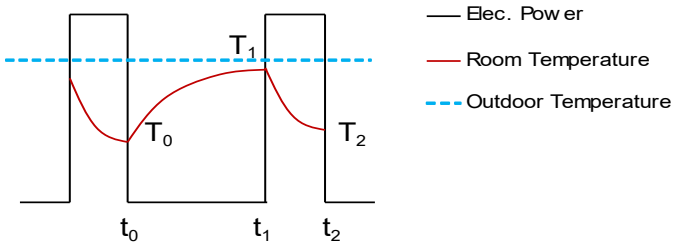

Figure 11. On and Off cycles of AC for Thermal Constants Calculations.

$R_{th}C_{th}$ is estimated during off-cycles with (2) while C_{th} is estimated during on-cycles with (3). R_{th} is then calculated by dividing $R_{th}C_{th}$ with C_{th}.

$$R_{th} C_{th} = \frac{\int_{t0}^{t1} (T_{out} - T_{in}) dt}{(T_1 - T_0)} \quad (2)$$

$$C_{th} = \frac{\int_{t1}^{t2} P_{AC} dt}{(T_1 - T_2) + \frac{\int_{t1}^{t2} (T_{out} - T_{in}) dt}{R_{th} C_{th}}} \quad (3)$$

Once the thermal constants are estimated, the On-delay-time and On-duration for an AC can be estimated, such that the indoor temperature does not exceed the maximum and minimum temperatures set by the user. It is assumed historical data of forecasted outdoor temperature, estimated/measured indoor-temperature and measured AC-power consumption are stored on

the edge-level and can be used for model calibration. During simulation development, actual residential historical data from Pecan St were unavailable and therefore were manually generated. Note that these will be replaced with actual historical data when they are available. The indoor temperature is represented by a sinusoidal function between 18°C and 33°C, while the outdoor temperature is 35°C, both with added random noise, shown in Figure 12 (a). The rated AC-Power is assumed to be 4 kW, where the AC is turned-on when indoor temperature decreases and turned-off when the temperature rises, shown in Figure 12 (b).

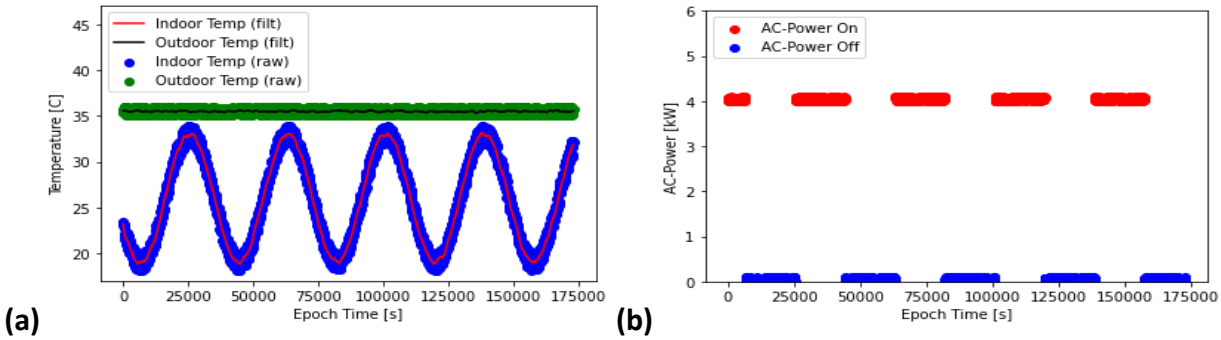

Figure 12.(a) Manually Generated Data of (a) Indoor & Outdoor Temperatures; (b)AC-Power

First, the user temperature set point is estimated to be 25.96°C from the mean of indoor temperature variations. The thermostat temperature deadband is estimated to be 7.13°C from the temperature variation from the mean to the maximum and minimum indoor temperatures, based on data collected from users in Austin TX as shown in Figure 13. The temperature set point & deadband are used to determine the minimum and maximum allowable indoor temperatures, in this case are 18.83°C and 33.09°C respectively. The thermal resistance R_{th} and thermal capacitance C_{th} are calculated using equations (2-3) for each on-cycle and off-cycle and are averaged. Using R_{th}, C_{th} and actual AC-Power, the indoor temperature is simulated. Simulation results in Figure 13 show good estimation of the indoor temperature variation using an RC-circuit.

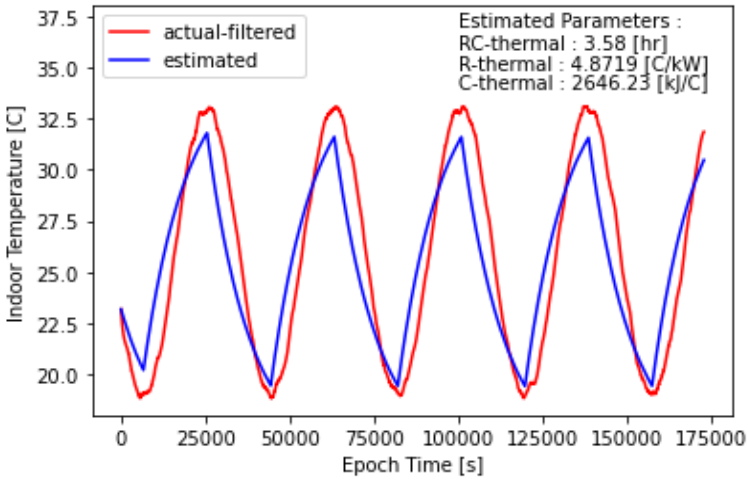

Figure 13. Indoor Temperature Simulation with Estimated Thermal Constants.

Home Thermal Parameters Estimation without Indoor Temperature Reading for Air-Conditioner (AC): Previous method to calibrate home thermal parameters relies on the availability of home indoor temperature. However, unless if a home has a smart thermostat, indoor temperature sensor may not be available in all SETO homes. Therefore, an indoor temperature estimation method without relying on historical measurement of indoor temperature is proposed. Several assumptions are made in the proposed method as shown in Figure 14. In this method, only the AC power consumption is known from Load Disaggregation output. First, it is assumed that the AC will turn on when the maximum allowable indoor temperature T_{hi} is reached. Second, the AC will turn off when the minimum allowable indoor temperature T_{lo}. Third, the increasing temperature trajectory f can be approximated as a polynomial function of T_{lo}, T_{hi} and AC-off times. Fourth, the decreasing temperature trajectory g can also be approximated as a polynomial function of T_{lo}, T_{hi} and AC-on times.

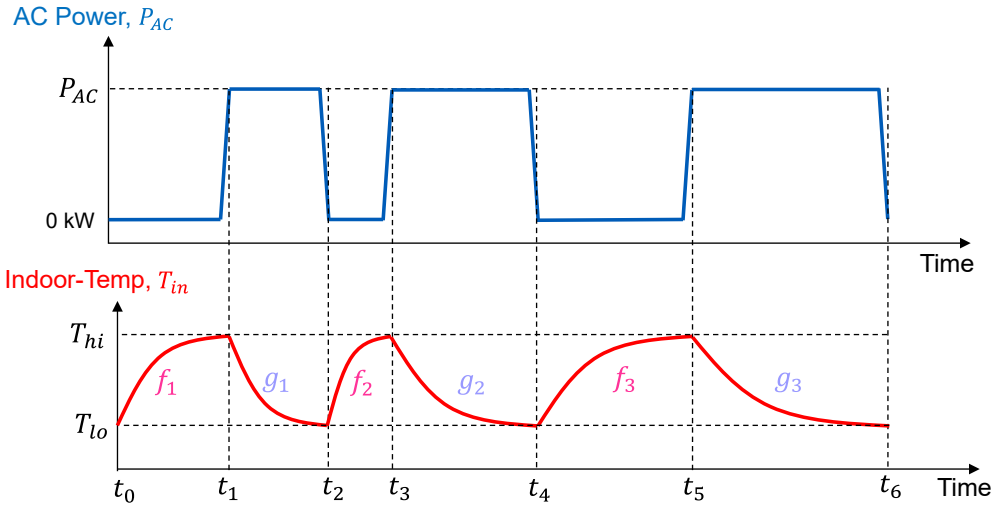

Figure 14. Indoor Temperature Estimation

It was found that a 2nd order polynomial best represents the increasing and decreasing temperature trajectories f and g with a fitting K-factor to ensure the end temperature is reached by the end of the temperature increase or decrease durations as shown in (5). (4) represents the increasing temperature function f, while (5) represents the decreasing temperature function g. Note that there are multiple cycles of temperature increase and decrease durations during the calibration period. With historical virtual indoor temperature, the home thermal parameters RC_{th} and C_{th} can be calculated and used as model parameters to estimate future indoor home temperature variations.

$$T_{in} = K \cdot time^{\frac{1}{2}} + T_{lo} \quad (4)$$

$$T_{in} = T_{hi} - K \cdot time^{\frac{1}{2}} \quad (5)$$

Once the historical virtual temperature estimates are available, the home thermal parameters can be calculated using (6) during AC off-cycles and (7) during AC on-cycles.

$$R_{th}C_{th} = \frac{\int_{time\_start}^{time\_final}(T_{out} - T_{in})dt}{(T_{in\_final} - T_{in\_start})} \quad (6)$$

$$C_{th} = \frac{\int_{time\_start}^{time\_final} Power_{AC} dt}{(T_{in\_start} - T_{in\_final}) + \left(\frac{\int_{time\_start}^{time\_final} (T_{out} - T_{in}) dt}{R_{th} C_{th}} \right)} \quad (7)$$

Past fourteen days of historical AC power consumption were utilized to test the indoor temperature estimation using virtual temperature. First, T_{lo} and T_{hi} were selected as [22,25] °C, based on historical actual indoor temperature. In actual implementation, the temperature bound values can be identified using user surveys. Next, the virtual indoor temperature trajectory during AC on and off-cycles are estimated using (4) and (5). Home thermal parameters can then be calculated using the virtual temperatures using (6) and (7). Note that since there are multiple on and off AC durations during the fourteen days, the average RC_{th} and C_{th}, after removal of statistical outliers, are calculated to represent the thermal home parameters.

Table 7. Indoor Temperature Estimations using Actual Temperature and Virtual Temperature

Calibration Dates	Est using Actual Indoor Temp			Est using Virtual Indoor Temp			
	RC-th [hr]	C-th [kJ/C]	T_{in} RMSE [C]	RC-th [hr]	C-th [kJ/C]	T_{in} RMSE [C]	ΔT_{in} Max [C]
08/16/2020	2.59	1621.58	0.2775	1.46	892.24	0.5287	0.9667
08/17/2020	2.51	1590.07	0.3960	1.03	660.75	0.5886	0.9425
08/18/2020	2.48	1554.52	0.4138	1.00	587.05	0.6973	1.2610
08/20/2020	2.48	1535.15	0.4272	1.59	888.48	0.6435	1.4871
08/21/2020	2.74	1639.96	0.4616	1.64	905.12	0.8917	1.4584
08/25/2020	3.18	1848.09	0.2627	1.84	992.53	0.1333	0.3615
08/26/2020	2.66	1592.63	0.4206	1.69	882.06	0.9903	1.6945
08/27/2020	2.46	1486.25	0.2041	1.26	683.33	0.3266	0.5993
08/28/2020	2.48	1509.36	0.4869	1.27	737.46	0.7912	1.3230
08/29/2020	3.72	2258.48	0.4200	1.64	892.29	0.3284	0.5572

Test days are selected in August as shown in Table 7. In general, both indoor temperature estimation using actual temperature and virtual temperature provide thermal parameters that are consistent across different days, with reasonable variations. The variations may be attributed to homeowner activities such as windows not being shut properly or error in actual localized outdoor temperature, which were captured by the calibration variations and resulted in low RMS-error below 1°C. The thermal parameters estimated using virtual temperature in general is lower than using actual temperature, which may be attributed by a lower temperature range of the virtual temperature compared to actual average temperature range. Despite having lower estimates of thermal parameters, estimation using virtual temperature is able to maintain good level of RMS-error with a maximum RMSE of 0.9903 °C. Additionally, the maximum absolute temperature error ranges between 0.35 to 1.69 °C, which is only 1.5-7.2% of the mean average temperature being controlled inside the home of 23.5 °C. Comparisons of temperature estimation results using actual and virtual temperature on August 25th 2020 are shown in Figure 15.

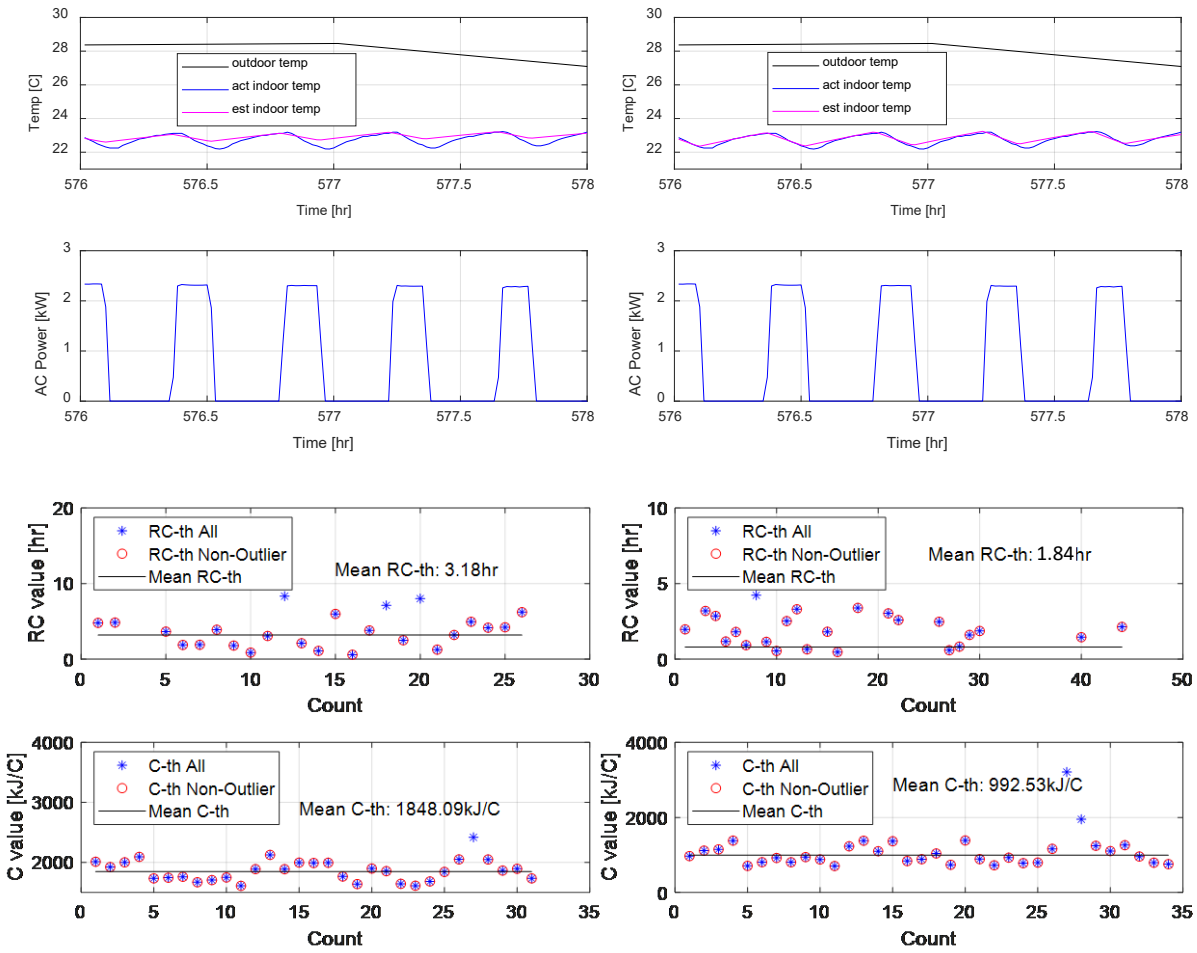

Figure 15. Indoor Temperature Estimations using Actual Temperature (top) and Virtual Temperature (bottom) for August 25th 2020.

Electric-Water-Heater (EWH): This task involves control design specification of an electric water heater (EWH) of an individual household such that the consumed power can be controlled from the edge level in response to a grid service event. This task has continued from the last quarter and presently the revised model and control strategy allows the EWH to be a fully controllable load. Through intelligently delaying the turning on of the EWH, a certain reserve capacity of power is obtained during a grid service event. This reserve capacity adds to the aggregate reserve of controllable loads in a household allowing the edge controller to take part in responding to a grid service event as requested by the central utility level control.

EWH can be considered as a potent source of energy reserve in a household as it is designed to always store a certain volume of hot water for ready usage. This reserve can be exploited by the edge control to respond to a grid service event. In a typical EWH as illustrated in Figure 16(a), cold water is circulated from the bottom of the tank while hot water outlet is at the top. Usually there are two heating elements, one located near the top and the other near the bottom. The control of each heating element is managed by their respective thermostats in a way that the elements heat up the water when temperature falls below a preset threshold. The lower heating

element heats up the inlet cold-water to an intermediate hot temperature, while the top one maintains the hot water temperature at the top outlet. The top heating element has the priority over the bottom one. The resultant behavior is thus like an on off control maintaining the temperature at both the top and bottom half of the chamber within certain bounds. The temperature distribution in a water heater is shown in Figure 16(b) through a 40-layer Eaton developed EWH model represented in Excel tool.

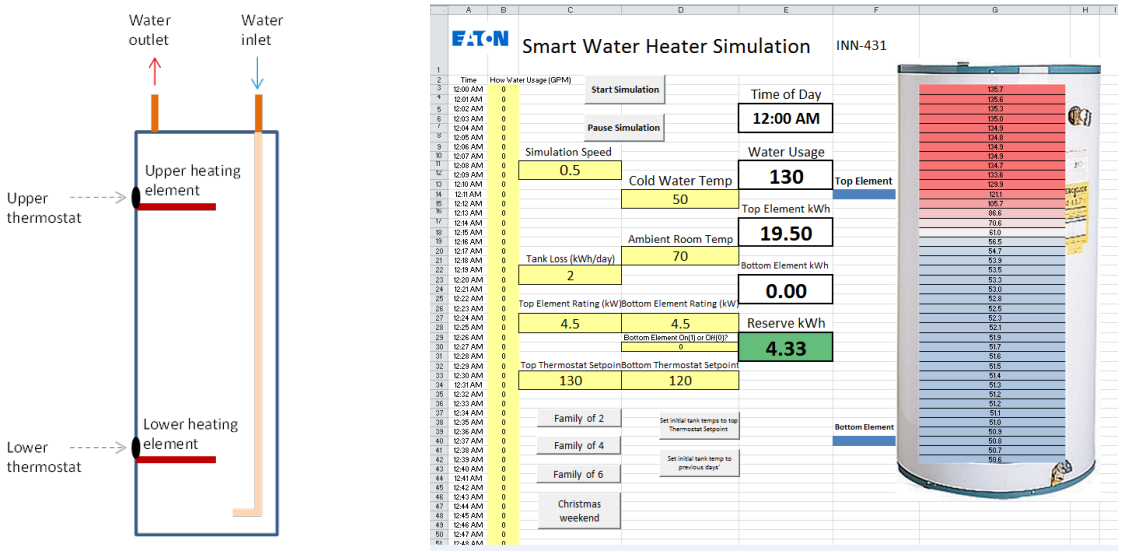

Figure 16. (a) Simple EWH Representation, (b) 40-layer EWH model represented in Excel tool (right)

There are substantial challenges in controlling such an EWH some of which are listed as below:

1. The turning on of the EWH is uncertain and is triggered by random human behavior.
2. During hours of substantial hot water usage (e.g. when dishwasher is running), responding to grid service event may lead to customer discomfort like cold showers.
3. EWH, compliant with CTA 2045 standard provides reserve capacity as a measurement. In others, no measurements are available, installation of additional sensors may lead to tampering the manufacturer's warranty for the EWH.
4. Controllability is only available in the form of blocking of the heating elements.

In order to tackle these challenges, an innovative control strategy is developed. Some of the simplifying assumptions are as follows:

1. The EWH is a two-mass system, upper and lower chamber with uniform temperature.
2. Temperature of the hot water at the outlet, ground water at the inlet, ambient temperature, power rating and tank capacity are known or can be estimated.
3. Parameters like specific heat and density of water is known.

A brief overview of all the steps involved in the control of the EWH is shown in Figure 17. The principal steps are mentioned below:

1. Data Historian
2. Stochastic Modeling
3. Reserve Capacity Estimation using two-mass model

4. Safe Deferred Time Computation.

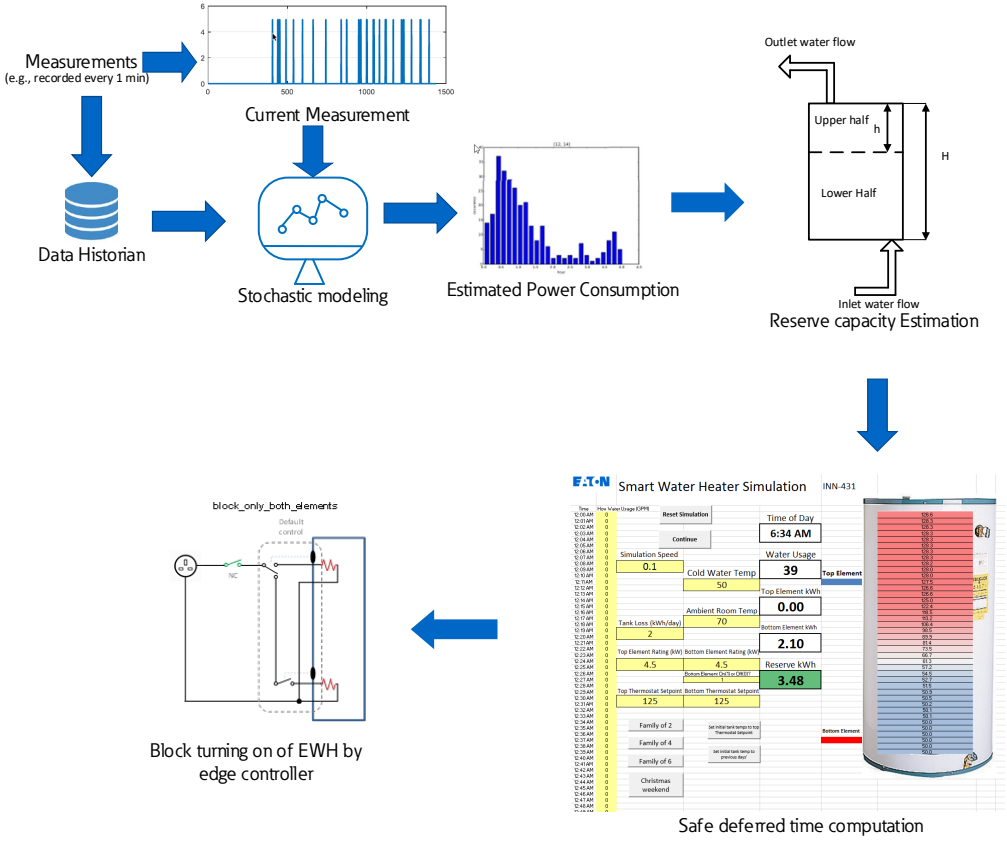

Figure 17. Control Overview of Edge Control Algorithm of Electric Water Heater.

The steps mentioned in the overview are detailed in this section:

Data Historian: Historical 1- min power consumption data of EWH from a single household is obtained as shown in Figure 18. The Edge controller uses a Historian function to store this data in a database and then retrieve it as required for the algorithm. The EWH either consumes its rated power of 4.5 kW or is zero.

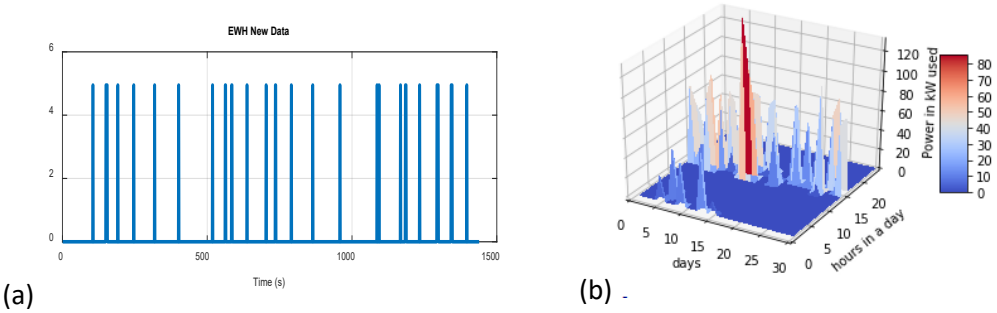

Figure 18. (a) 1-mn power consumption of EWH , (b)Hourly variation of power of EWH

From this data, the number of minutes EWH is turned on in a certain period (say 15 min) can be derived, which in turn provides exact consumed power $P_{EWH\_his}[n]$.

Stochastic Modeling: The historical power usage $P_{EWH_his}[n]$as determined above can be fed into a stochastic prediction model which can forecast an expected kWatt consumption$P_{EWH_est}[n]$. It is observed that there is some correlation between daily power usage of EWH with that of the hour of operation. The 3-d plot in Figure 18(b) shows power in kW used in all hours of the day in all days of July 2018 from a certain household. It clearly shows concentration of power consumption in a few hours in the morning. Based on this understanding, a Pearson correlation coefficient is computed between the power usage in the current period n and that of the previous period $n_1$for a certain length of days (typically 14 days).

$$Corr(P_{EWH}[n], P_{EWH}[n_1]) = \frac{\sum_{j=1}^{14}(P_{EWH,j}[n]-\bar{P}_{EWH,j}[n])(P_{EWH,j}[n_1]-\bar{P}_{EWH,j}[n_1])}{\sqrt{\sum_{j=1}^{14}(P_{EWH,j}[n]-\bar{P}_{EWH,j}[n])^2}\sqrt{\sum_{j=1}^{14}(P_{EWH,j}[n_1]-\bar{P}_{EWH,j}[n_1])^2}} \quad (8)$$

Based on the calculated correlation coefficient and the measured power in the previous period n_1, the power that will be consumed in the next period n can be predicted following the relation as shown below.

$$P_{EWH\_est}[n] = Corr(P_{EWH}[n], P_{EWH}[n_1])P_{EWH}[n_1] \quad (9)$$

Reserve Capacity Estimation using two-mass model: In a certain interval if estimated power usage $P_{EWH_est}[n]$is known, that information can be used to delay the turning on of the EWH by a certain number of minutes. This facilitates the edge controller to minimize the aggregate power demand in the household during grid service events. But for that a reserve capacity of hot water needs to be estimated in real time so that customer comfort bounds are not violated. The problem is thus transformed to a determination of reserve capacity of hot water in the tank with obtained power measurements.

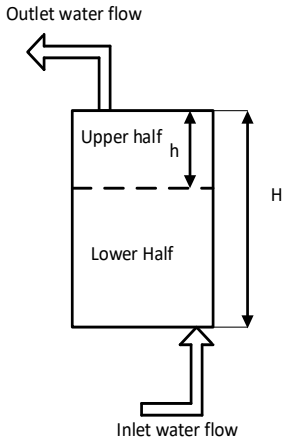

Figure 19. 2 mass model.

The temperature distribution in the EWH tank follows a pattern as shown in Figure 16(b). As observed, there is a sharp change in water temperature along the length of the water tank. Consequently, the energy balance in the water tank can be captured approximately as a two-mass model shown in Figure 19. In the approximate 2-mass model, the top mass has an average temperature of T_u while the bottom mass has an average temperature of T_l. Water is injected into the tank through the inlet at a bottom while hot water leaves from the top at a mass flow

rate of $\dot{m}$. Ambient temperature is provided by T_{amb}. UA_{WH} is the heat loss coefficient of the tank, Q_{elec} is the electrical energy input, C_p is the specific heat of water and C_W is the thermal capacitance of water. The dynamics of the height of the top hot water mass is defined by the following differential equation,

$$\frac{dh}{dt} = \frac{Q_{elec}+UA_{WH}(T_{amb}-T_l)}{C_W(T_u-T_l)} * H - \frac{\dot{m}C_p}{C_W}H - \frac{UA_{WH}}{C_W}h \quad (10)$$

Considering steady state operation when the amount of hot water in the tank is not changing,

$$\frac{dh}{dt} = 0 \rightarrow \frac{Q_{elec}+UA_{WH}(T_{amb}-T_l)}{C_W(T_u-T_l)} * H - \frac{\dot{m}C_p}{C_W}H = \frac{UA_{WH}}{C_W}h_{ss} \quad (11)$$

Now, if initial steady level of hot water

$$h_{ss} = \alpha H \quad (13)$$

This leads to the following relation,

$$\frac{Q_{elec}+UA_{WH}(T_{amb}-T_l)}{(T_u-T_l)} - \dot{m}C_p = \alpha UA_{WH} \quad (14)$$

The above relation is valid in case when water is used, and water is not used in steady state. Considering the scenario when hot water is not used, $\dot{m}C_p = 0$

$$Q_{elec,nouse} = \alpha UA_{WH}(T_u - T_l) - UA_{WH}(T_{amb} - T_l) \quad (15)$$

On the other hand, when hot water is being used

$$Q_{elec,use} = \alpha UA_{WH}(T_u - T_l) - UA_{WH}(T_{amb} - T_l) + \dot{m}C_p(T_u - T_l) \quad (16)$$

$Q_{elec,nouse}$ is basically the energy used the EWH if hot water is not used at all. It can be computed daily based on the computations of low power surges used by the EWH through out the day. So, the unknown parameters of tank loss coefficient and mass flow rate of hot water can be estimated as,

$$UA_{WH} = \frac{Q_{elec,nouse}}{(\alpha T_u+(1-\alpha)T_l-T_{amb})} \quad (17)$$

$$\dot{m}C_p = \frac{Q_{elec,use}-Q_{elec,nouse}}{(T_u-T_l)} \rightarrow m = \int \frac{Q_{elec,use}-Q_{elec,nouse}}{C_p(T_u-T_l)}dt \quad (18)$$

$T_{upper}, T_{lower}, T_{amb}$ can be respectively considered as 125 °F, 50°F, 70°F in approximate terms. Provided measurement of energy is known in a certain period, one can thus estimate the new reserve capacity of hot water in real time following the relations:

i. If energy usage > a preset threshold (10% of rated energy in a period)

$$\alpha_{esti} = \alpha_{old} - \left(\frac{m_{esti}}{\rho * tank\_capacity}\right) \quad (19)$$

ii. If energy usage <a preset threshold (10% of rated energy in a period)

$$\alpha_{esti} = \alpha_{old} = preset\ bottom\ sensor\ location$$

Safe Deferred Time Computation: Once the reserve capacity is estimated, the safe deferral time for turning on the electric water heater at the beginning of a grid service event can be computed. Say for example if full tank (say 50 Gallon) of hot water needs to be heated up the energy required can be computed as below,

$energy = \rho * \text{tank\_capacity} * (T_u - T_l)$ =8.337 gal/lb*50 gal*(125-50) ˚F=31275 BTU=9.16kWh

For the same EWH with 4.5 kW rated power if there is a full tank of hot water, the number of minutes, the turning on of the EWH can be deferred by

safe deferred time= 9.16kWh/4.5kW=2.04 hours= 122 mins

If only α is the fraction of hot water is estimated to be left at the end of the grid service event,

safe deferred time= 122* α mins

Also, If α<0.25, EWH doesn't participate in grid service event, safe deferred time= 0 mins. This guarantees a minimum reserve capacity of 0.25 at the end of each grid service event, preventing customer discomfort or cold showers. The Control logic engine in Figure 20 shows the implementation of the algorithm in the edge controller. In this way based on the reserve capacity estimated at the beginning of grid service event, the edge controller determines a safe deferred time for blocking the turning on of the EWH.

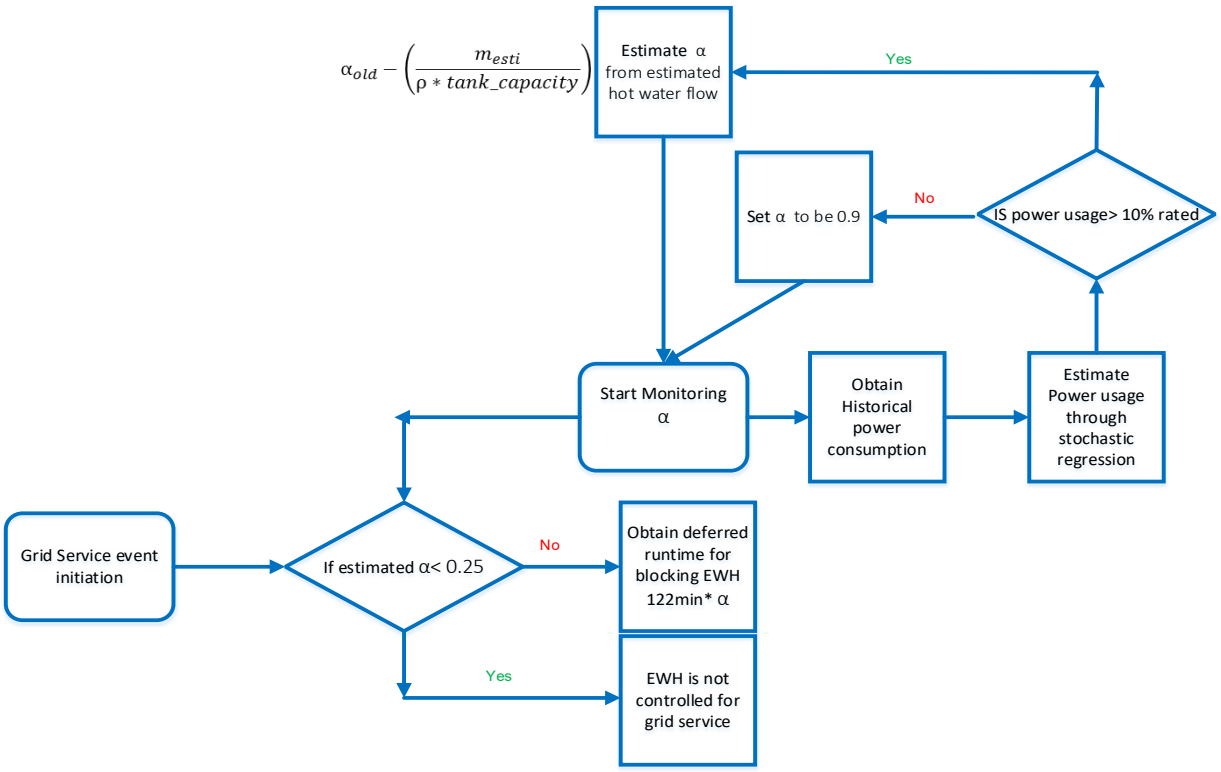

Figure 20. Control Logic Engine.

Results: The method mentioned above is used to forecast power usage of a single household EWH based on historical data. Figure 21(a) shows forecasted mins of usage of an EWH for an entire day considering a 10 min of forecasting horizon. Figure 21(b) shows forecasted power for an hour with 10 min intervals considering a 60 min forecasting horizon. In this task, the correlation between EWH energy consumption and the mass of hot water leaving the tank is performed. Therefore, the input required is the EWH energy consumption - which is the integration of the EWH power profile in Figure-21b. Despite not capturing the peak power, the forecasted EWH power stays longer (Figure 21b), due to the forecasting method that utilize

averaged 10-minutes historical EWH power profiles. Therefore, as shown in Figure 22 which utilized averaged 1-hour historical EWH power profiles for the whole day, the estimated hot water usage using EWH energy consumption is shown to be correlated with the actual hot water usage.

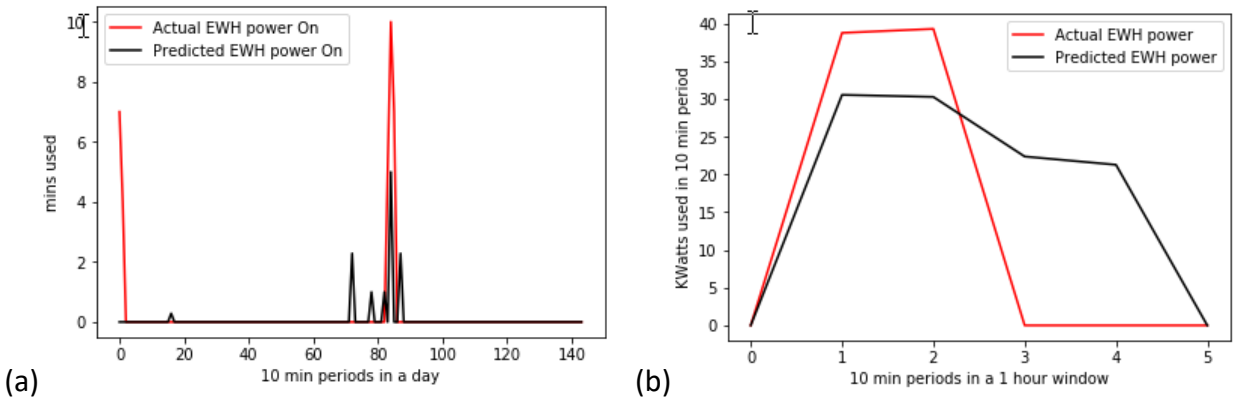

(a) (b)

Figure 21. (a) 10-min forecasting horizon, (b) 60-min forecasting window

The next set of results are for estimation of the usage of hot water in a household based on simple power measurement. This estimation is critical for computing the reserve estimate which determines the safe deferment of the turning on of the EWH. Figure 22(a) shows the hourly usage prediction of a household having family of 2 with a 40 Gallon water tank. Likewise, Figure 22(b) shows the hourly usage prediction of a household having family of 4 with a 60 Gallon water tank. In either case the estimator can capture the peak usage time which is required for the implementation of the control logic engine of Figure 20.

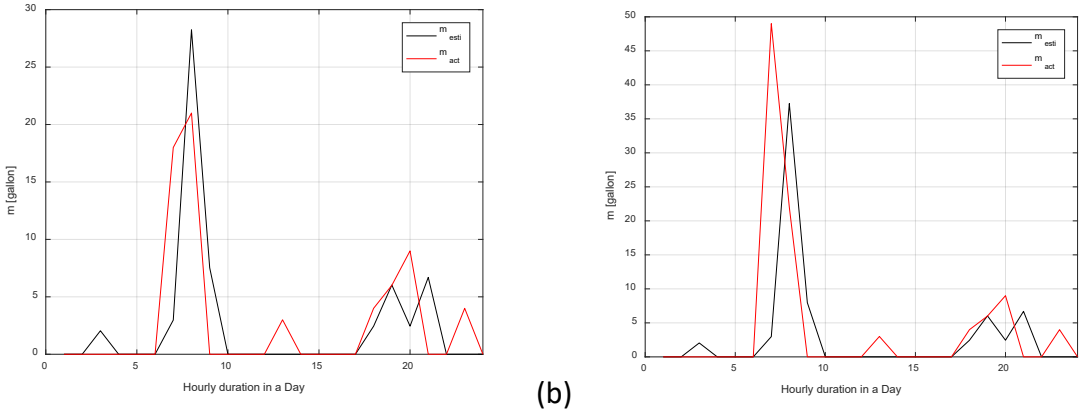

(a) (b)

Figure 22. (a) Family of 2, 40 Gallon Water tank; (b) Family of 4, 60 Gallon Water tank

Conclusions and Insights:

The development of this control oriented EWH model has further be quantified and validated during lab tests in Task 12: Lab testing and end-to-end integration testing. However, the following insights were found:

- The correlation pattern in historical usage can be exploited for long term forecast and usage profile.
- The simple model and control strategy maximizes the utility of EWH reserve in grid service events such as demand response.
- Automatic tuning of minimum safety reserve can further help avoid customer discomfort.
- The method is applicable in all EWH irrespective of CTA-2045 compliant or not
- Overestimating the usage in peak times, provides safety against cold showers.

EV-Charger (EVC): The objective of the EVC control-model is to predict the ON/OFF times and power consumption of the EVC within certain time period in the future when a DR-event kicks off. With the predicted EVC information, the edge-level control can then allocate the on and off timings of other DERs during a DR-event without violating the Quality-of-Service based on the charging need set by the user.

EV charger consists of a power converter and a battery pack, where the characteristics of both should be considered for physical modelling. The electrical parameters of the battery, e.g., internal voltage and resistance, vary with various factors such as temperature or state-of-charge (SOC). All the parameters and state variables are needed in a physical battery model. It comes to our attention that the battery SOC, as an important state variable in the physical battery model, is typically not accessible in majority of the EVs. Therefore, the data based EVC load forecast models which do not rely on SOC and other physical measurements are adopted to achieve the objectives. Similar to EWH modelling, two data-based modelling approaches were developed for EVC, i.e., time-series characteristics and statistical analysis approaches.

Time-series weighted forecast model: The time-series weighted forecast model takes the real-time power consumption data before the DR event and conducts the weighted mean of the measurements of the day as well as the historical data of a similar day. The historical load data is classified through qualitative inspection into the following patterns: day-wise pattern; weekly pattern (weekdays vs. weekends); and seasonal pattern. Figure 23 shows the day-wise EV charging profile in two weeks with x-axis unit being hour. The sample data is collected in a household in New York and is provided by Pecan Street. It can be clearly observed that there is a day-wise pattern in the charging profile of the EV owner. The EV was charged most often after 3pm every day.

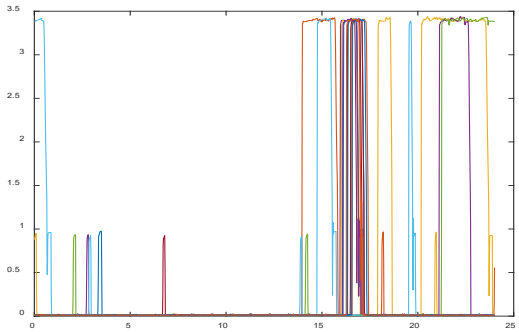

Figure 23. The daily charging load profile of an EV owner within 2 weeks.

Similar to EWH, the mathematical expression of the short-term (in this case 0.5 hour ahead) time-series EVC forecast model can be written as:

$$P_{EVC\_est}[n] = (1-k)\cdot Mean\big(P_{EVC\_rt}[n-59,\ n-30]\big) + k\cdot P_{EVC\_his}[n] \qquad (20)$$

where $P_{EVC\_est}[n]$ is the estimated power consumption at the nth time step, $P_{EVC\_rt}[n]$ is the real-time measurement of the power consumption at the nth time step of the day, $P_{EVC\_his}[n]$ is the historical power consumption at the nth time step of a similar day, and k is the blending factor.

Statistical forecast model: The statistical forecast model predicts the random parameters of an EVC, such as turning ON/OFF times, based on the statistical analysis of the historical data of a particular EVC. Since the power consumption of an EVC during on time is approximately constant, i.e., its rated power, knowing the time stamps of ON and OFF instants are enough to reconstruct the load profile of an EVC. The EVC ON/OFF status and the duration time can be predicted with the current operating status and the statistics of that EWH in a similar situation, e.g., same hour in a day. Figure 24 shows the power usage profile of an EVC in a week. The x-axis unit is minute. The durations of the ON and OFF status within that particular day can be analyzed using statistical approach and are illustrated in Figure A16. Figure A16(a) shows the probability distribution of the duration when the EVC is on; and Figure A16(b) shows the probability distribution of the duration when the EVC is off.

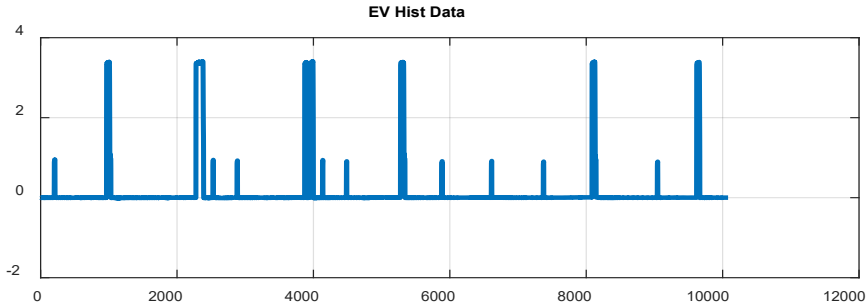

Figure 24. EVC power usage profile in a regular week.

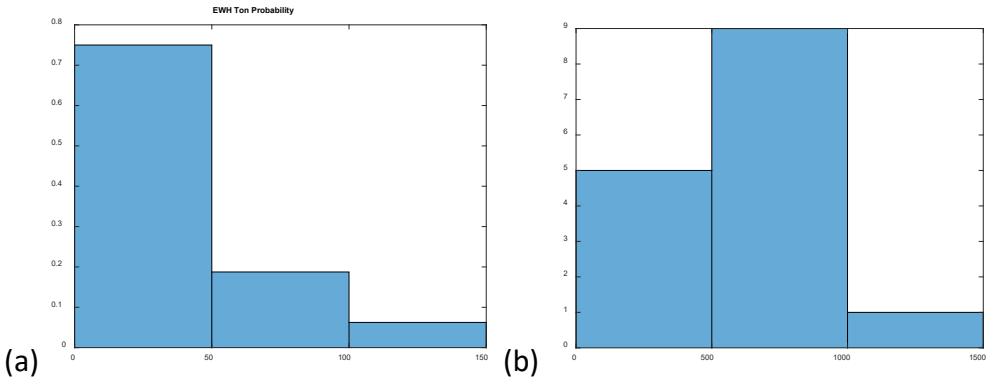

Figure 25. Probability distribution of EVC status duration: (a) on time; (b) off time

Results: Preliminary results of the two models are generated with the two weeks of the field data provided by Pecan Street. One week's data is used for learning purpose and the other is used for verification. The two weeks' data are plotted in Figure 26 as below.

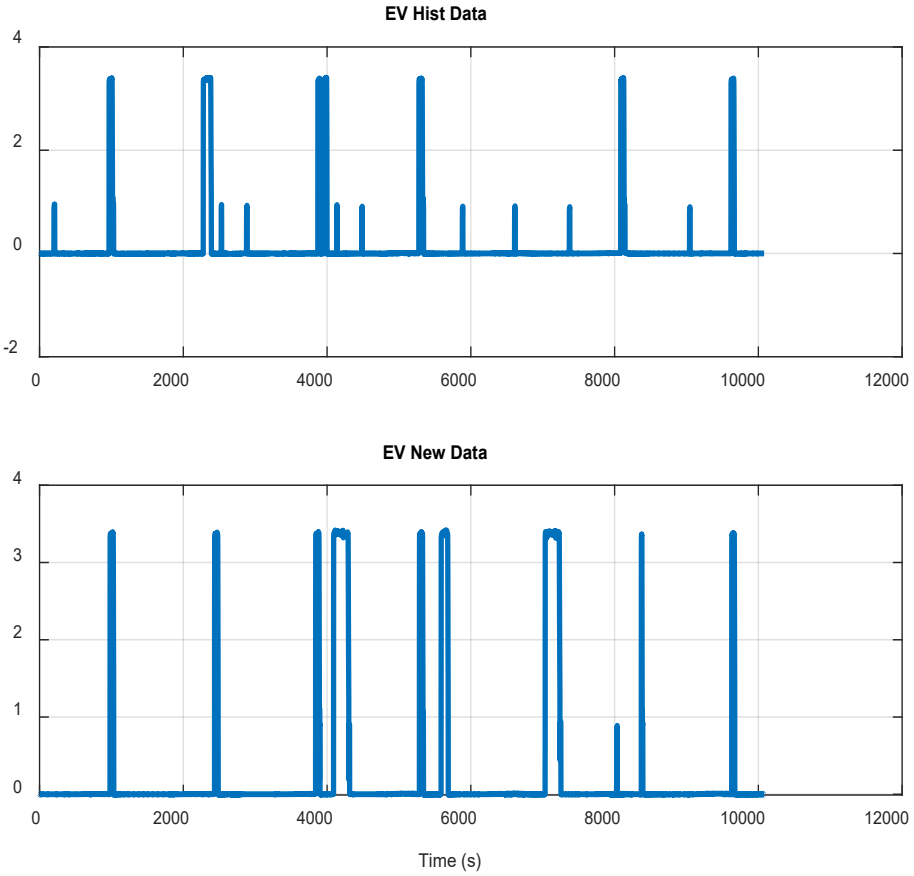

Figure 26. EVC weekly load profiles for model validation

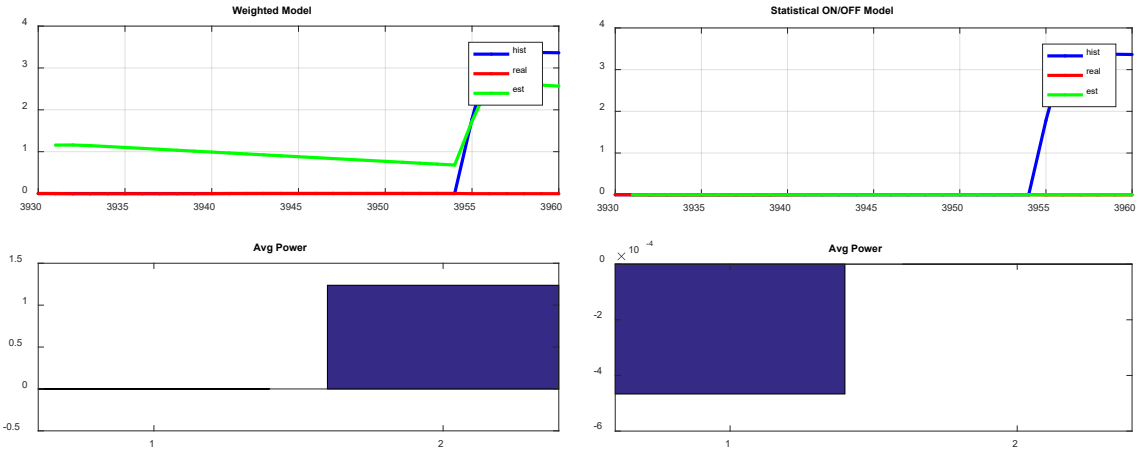

Figure 27.EVC prediction with the statistical model at 3930 minutes. Left: Time-series weight model; Right: Statistical ON/OFF model; Upper: time sequence plots; Lower: average power in 30-min time window

The results of the time-series weighted model and the statistical model in 3920 minutes are shown in Figure 27. The averaged power of the real measurements versus the estimated in the 30min window are also compared.

PV-Solar (PV) and Energy Storage: Simple calibration of a PV-gain calculated from historical solar-irradiance and solar-power generation are calculated, which is then used with forecasted solar-irradiance to forecast solar-power generation [23]. Other advanced techniques to forecast solar generation can also be used. However, since predicting weather is hard and advanced techniques have already been implemented to forecast solar-irradiance (SI) which can be readily accessed through weather services, a straightforward way to predict PV-solar generation is to estimate the home's PV panel sizing based on the generated power. Additionally, since PV is not being controlled and the development focus is on the edge-level controller and its coordination with the central-level controller, a simple yet effective way of forecasting PV-solar generation was utilized. Besides, many other information such as rating of the DERs and SOC are readily available using IEEE 2030.5 client-server through the inverter and meter-as-a-controller which reduces the burden of details modeling.

Modes of Operations: The edge-level control strategy is divided into two different modes. The first mode is called the Demand-Response (DR) mode, which occurs when a DR-event is triggered by the central-level control. During this mode, which lasts for a certain time duration, the central-level control will send a pseudo price signal to the edge-level control which is translated into a net-power requirement for the residential unit. The residential unit will then manage its DERs to achieve the net-power requirement from the central-level control. Figure 28 shows a depiction of the edge-level control during DR-mode.

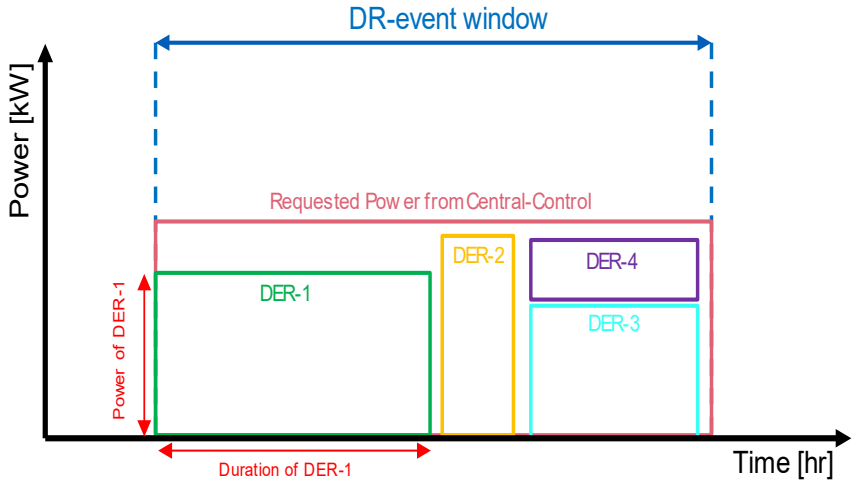

Figure 28. Edge-level Control during DR-mode.

The second mode is called the Idle-mode, which occurs when there are no DR event. In this mode, the edge-level control will manage its DERs to lower electricity cost for the homeowner.

DERs Scheduler Optimization Formulation: The DERs scheduler objective is to minimize the energy cost for homeowner while meeting several constraints to ensure grid-event objectives and homeowner's Quality-of-Service are met. First, only the air-conditioner (AC), solar-PV (PV) and residential energy storage system (RESS) are considered as controllable DERs. The dynamics of indoor air temperature and battery state of charge are modeled, and the parameters are

assumed to be known. Electric-water-heater (EWH) and electric vehicle (EV) are considered as uncontrollable DERs, where the power consumptions are forecasted using statistical methods. The problem is then formulated as an optimization problem, with the objective of minimizing the integral of the multiplication of electricity tariff with the net home power consumption from the grid. The net home power consumption is given by the summation of all controllable and uncontrollable DERs, which are constrained by an upper limit during a Grid-Event which is communicated by a central-level controller. Additionally, the net power of controllable DERs are constrained by the home's flexible power threshold outside of the Grid-Event, which is communicated by the edge-controller to the central-level controller. Two states dynamics considered from the controllable assets are the indoor air temperature which is controlled by AC power as input and RESS battery state-of-charge which is controlled by RESS power as input. The states are bounded by upper and lower limits. Parameters that define the dynamics of the indoor air temperature and battery state of charge are either calibrated or known. Additionally, the forecasted outdoor temperature and the solar irradiation are also assumed to be known. The objective of the optimization is to minimize the electricity cost for the user, where the tariff can either be constant or time-dependent, such as Time-of-Use tariff, as shown in the objective function. It will also ensure the Quality of Services are met while restricting the net home power during the grid event and the net controllable DERs power outside of grid event, as described in the inequality constraints. These requirements are formulated as a single mixed-integer optimization problem and solved using a generic solver, as shown below.

Objective Function:

$$\min \int_{t_i}^{t_f} C(t) \cdot P_{grid}(t)\, dt \tag{21}$$

where

$C(t)$ *= Known day-ahead electricity tariff.*

$P_{grid}(t)$ *= Power imported from grid =* $P_{AC}(t) + P_{ESS}(t) + P_{EWH}(t) + P_{EV}(t) + P_{UCT}(t) - P_{PV}(t)$.

$P_{AC}(t)$ *= Power consumption of Air-Conditioner (controlled)*

$P_{ESS}(t)$ *= Power consumption & generation of Energy Storage System (controlled)*

$P_{EWH}(t)$*= Predicted power consumption of Electric-Water-Heater (uncontrolled)*

$P_{EV}(t)$ *= Predicted power consumption of Electric-Vehicles (uncontrolled)*

$P_{UCT}(t)$ *= Predicted power consumption of other uncontrolled loads*

$P_{PV}(t)$ *= Predicted power generation of Solar-PV (uncontrolled)*

States:

1. Indoor Air Temperature (AC):

$$\dot{T}_{in} = f(P_{AC}(t),\, T_{out}(t), AC_{const}),\ where\ P_{AC}(t) = \left[P_{AC\_lo}, P_{AC\_hi}\right] \text{ discrete}$$

2. Battery State-of-Charge (ESS):

$$S\dot{O}C_{ESS} = f(P_{ESS}(t), ESS_{const}),\ where\ P_{ESS}(t) = \left[P_{ESS\_lo}, P_{ESS\_hi}\right] \text{ continuous}$$

Equality Constraints:

1. States initialization:

[i] $T_{in}(t_0) = T_{in\_initial}$ [ii] $SOC_{ESS}(t_0) = SOC_{ESS\_initial}$

Inequality Constraints:

1. Indoor Air Temperature (AC):
$$T_{in\_min} \leq T_{in}(t) \leq T_{in\_max} \quad \forall \quad t$$
2. Battery State-of-Charge (ESS) :
$$SOC_{ESS\_min} \leq SOC_{ESS}(t) \leq SOC_{ESS\_max} \quad \forall \quad t$$
3. Restrict power export to Grid (optional):
$$P_{grid}(t) \geq 0 \quad \forall \quad t$$
4. Restrict $P_{grid}(t)$ during grid event:
$$P_{grid}(t) \leq P_{GridEvent} \quad \forall \quad t = [t_{Start}, t_{End}]_{GridEvent}$$
5. Restrict net controlled DERs power outside of grid-event as communicated to central-control:
$$\sum P_{controlled}(t) \leq P_{Limit}(t) \quad \forall \quad t \neq [t_{Start}, t_{End}]_{GridEvent}$$

Knowns Inputs:

Forecasted outdoor temp:	$T_{out}(t)$
Forecasted solar irradiation & PV power:	$SI(t)$, $P_{PV}(t)$
DER's Parameters:	AC_{const}, PV_{const}, $RESS_{const}$
Forecasted uncontrollable loads:	$P_{UCT}(t)$
Known day-ahead electricity tariff:	$C(t)$

Coordination of Edge and Central-Controller: The third aspect is the coordination between the central-level and edge-level controls. This subtask aims to layout and finalize the overall architecture and coordination between the central-level and edge-level controllers. The overall system consists of a central-level controller and edge-level controllers. The edge-level controllers will send real-time information of disaggregated DERs loads and energy reserve estimates data to the central-level controller which are then stored centrally. Using historical DERs load and reserves data from the edge-level, together with potential renewable energy generation from weather forecast, the central-level controller will predict future grid load profile and potential grid energy/power reserves. Using the forecasted grid energy/power, along with real-time DERs loads and reserves estimates from the edge-level controller, the central-level controller will compute the DR energy/power reference. This DR reference is then converted into a pseudo-price that is sent to the edge-level controllers. A DR-event is initiated when a pseudo-price is sent to the edge-level controller. On the edge-level, this pseudo-price is the converted into an equivalent grid energy/power demand to be met by the edge-level controller. The edge-level controller will manage its local DERs to meet this grid demand, while also meeting the Quality-of-Service of the residential unit for user's comfort. Historical pseudo-pricing and aggregated local edge-level loads will be used by the edge-level controller as feedbacks to tune an aggressiveness coefficient to correct the participation level of the house to the grid service. A module on the edge-level controller will collect information on DERs operations and process the load information into disaggregated load data to be sent back to the central-level controller. Historical data inducing the responses of the house participation in the previous DR-events and

pseudo-prices will be utilized to train the central-level control module over times to improve its performance continuously. The overall architecture is shown in Figure 29.

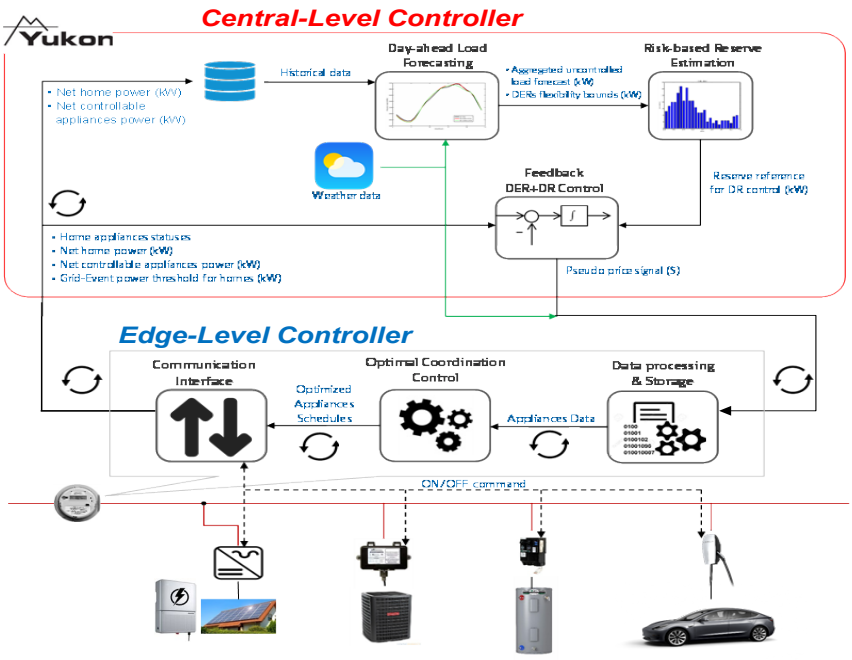

Figure 29. Overall Control Architecture

Through the design, development, and implementation of artificial intelligence and coordinated control between the central and edge layers, it is expected that the reliability, economy, and safety of the power distribution system during a DR event can be improved.

Task 3.0: Development of the risk-based DER dispatch bounds calculation framework

The NREL team made the following accomplishments within this task to develop risk-based DER dispatch bounds: (i) develop a sequence of problem formulations to solve for dispatch bounds from the ideal (deterministic) scenario to the practical realistic (data-driven, stochastic) scenario; (ii) design a new data-driven method for the dispatch bound problem to utilize historical data that can guarantee constraint satisfaction for a given probability and submit the results to a journal for publication; (iii) prototype the dispatch bounds on an IEEE test case under synthetic settings to understand what complications might be in the upcoming data-driven version, and to demonstrate the potential benefits of dispatch bounds; (iv) design an algorithm to turn historical forecast error data and controllable DER bounds into probabilistic profiles for an aggregation of homes.

The data we need at each node to solve for the dispatch bounds we define as the “Probabilistic Profile” of that node. It comes from the uncontrollable loads and controllable DERs of the homes aggregated at that node and has three parts that extend for 24 hours at 15-minute granularity: (i) forecasts of the uncontrollable loads, (ii) forecast error probability distributions, and (ii) control bounds for the controllable DERs. We obtained historical forecasts and their errors for an aggregation of four homes in Austin, TX from the Eaton team working on the forecasting task of

the project, and we obtained the control bounds of the controllable DERs at each of the same four homes from the Eaton team working on the Edge Controller.

Figure *30* shows the three parts of the probabilistic profile of the four homes on Dec 9th, 2020. The empirical forecast error distributions were built by taking the 28 days of previous and grouping them by the 15-min time of the day. In general, the error gets larger as we look further a head into the day until the end of the day which has less volatility. The control bounds come from summing together the upper bounds of the homes and summing together their lower bounds. The dip in the lower bound is from being able to curtail the PV power.

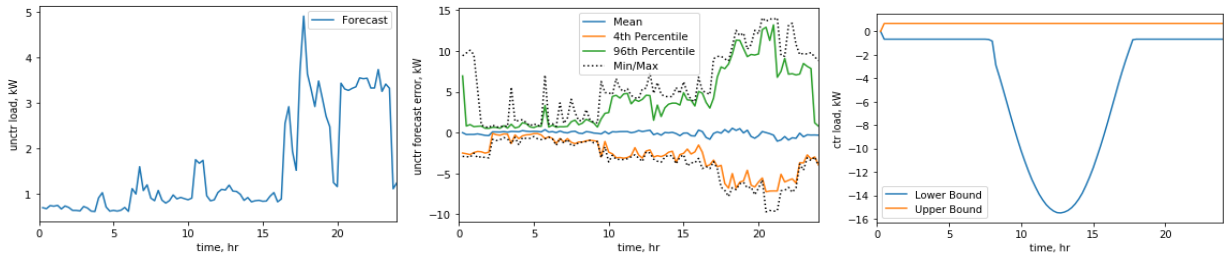

Figure 30. (a) Forecast of uncontrollable loads; (b) Empirical forecast error probability distributions; (c) Control bounds of controllable DERs

If we take the 24-hr forecasts, add on an error percentile, and add on the controllable region, we get

Figure *31* for the 4th and 96th error percentiles. Notice that where the two regions overlap, it means that it is possible for a setpoint to be made and complied with 92% probability. Extending this idea to all permutations of the spaces between lower and upper percentiles get different regions where a setpoint can be complied under a certain probability. Figure 33 shows this for the four aggregated homes. Compliance to a setpoint has the highest probability when the forecast errors are small (e.g., early in the day), or when the controllable region is large (e.g., middle of the day). With this method of probabilistic profile data visualization, it becomes easily apparent when and at what level an aggregation of loads is most controllable.

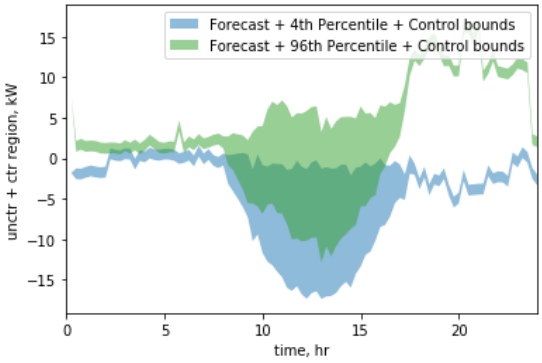

Figure 31. Controllable regions if the forecast error is at the 4th or 96th percentile

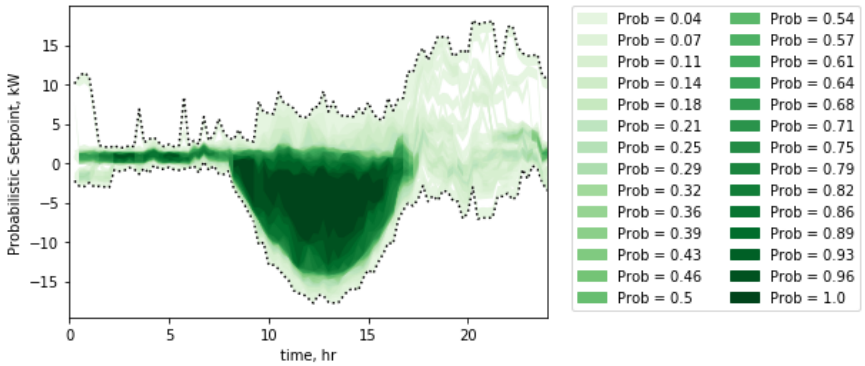

Figure 32. Probabilistic setpoints over 24 hours

From the Dispatch Bound optimization problem described in the project's proposal there were still many details that needed to be worked out about the problem and how the solved dispatch bounds would be utilized. At a basic level, dispatch bounds are meant to quantify the amount of future flexible load available for control at a node in a power system given that there are uncertainties in the whole system. In discussions with Eaton, it was decided that the dispatch bounds would be most useful as a day-ahead metric at 15-minute time granularity to size how much flexibility from controllable DERs could be sold into a day-ahead energy market. See Figure 33 for a detailed map of flow of data and information into and out of the Dispatch Bound Calculator.

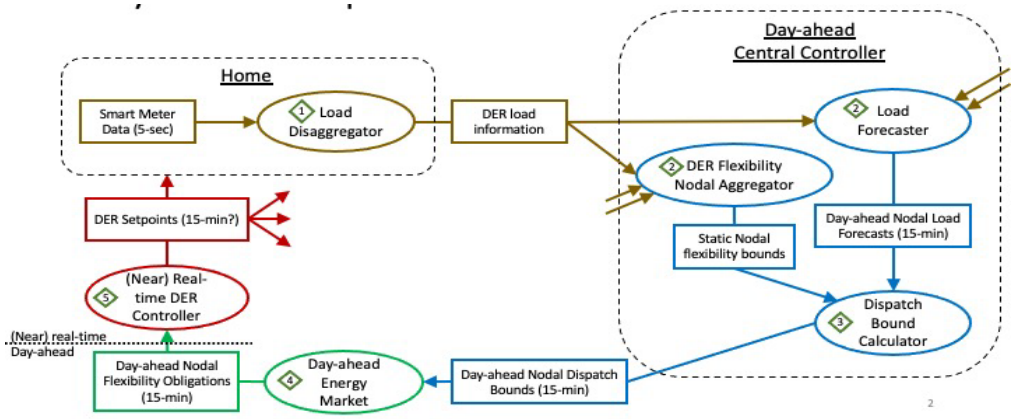

Figure 33. Flow Chart of the Day-ahead Dispatch Bounds

Thus, under this specific scenario, the task of the Dispatch Bound Calculator was to take (i) the day-ahead forecasts of the uncontrollable loads from an aggregation of homes, (ii) historical data of the forecast error, and (iii) the day-ahead controllable bounds of the controllable DERs, to find a subset of the day-ahead controllable (dispatch) bounds that will guarantee that the voltage magnitudes in a distribution system stay within their operational limits for a given probability. This type of guarantee is called a chance constraint, which has a long history in the Stochastic Optimization community. However, a challenge with chance constraints in this problem is that they are typically used to optimize a setpoint and not a (set-)interval as in our case. We reformulated the chance constraints on the interval into chance constraints on the upper and lower bounds of the interval so that we could use existing chance constraint solution methods.

Instead of making assumptions that the probability distribution of the forecast errors was of a certain convenient type (e.g., Gaussian), one of our goals was to use an empirical distribution built from historical data so that our solution could account for any problematic distribution that could arise. However, all the existing data-driven methods for chance constraints that we could find in the literature would add a significant amount computational runtime to solving the dispatch bound optimization problem; especially for high-dimensional data such as forecast errors for every node in a distribution network. Thus, we took a lightweight distributionally robust chance constraint method and modified it into a data-driven method. The original method assumed that the mean and covariance of the distribution were known a priori. Our adjustment allowed us to instead use the sample mean and sample covariance derived from data while making the same guarantees as the original method. Since we figured that other researchers may have run into similar issues in other application areas, we wrote a journal paper explaining our new method with its theoretical guarantees and submitted it to the INFORMS journal Mathematics of Operations Research.

To demonstrate the potential benefits of dispatch bounds and to discover any complicating factors we might run into, we prototyped a small numerical simulation under synthetic settings on an IEEE 33-bus distribution network. Specifically, we assumed that the forecast errors were Gaussian with known moments and that they were independent between nodes in the network. We also assumed that the controllable DERs were curtailable so that it would be possible to get a node's power injection to be within a static band. We recognize that these assumptions are very ideal which may not hold in reality but are being used as a placeholder until we obtain data or evidence to change them. Under these settings, we solve for the dispatch bounds, and display them (active and reactive power) for Bus 27 versus time for one day in

Figure 34 where positive bounds represent consumption and negative bounds represent generation. The dotted red and blue lines respectively are the upper and lower bounds of the available control region from the controllable DERs. The solid red and blue lines respectively are the upper and lower bounds of the dispatch bounds which are a subregion of the control region and are meant to guarantee voltage bound satisfaction with 95% probability. The grey region running along the bottom measures the distance between the upper and lower dispatch bounds.

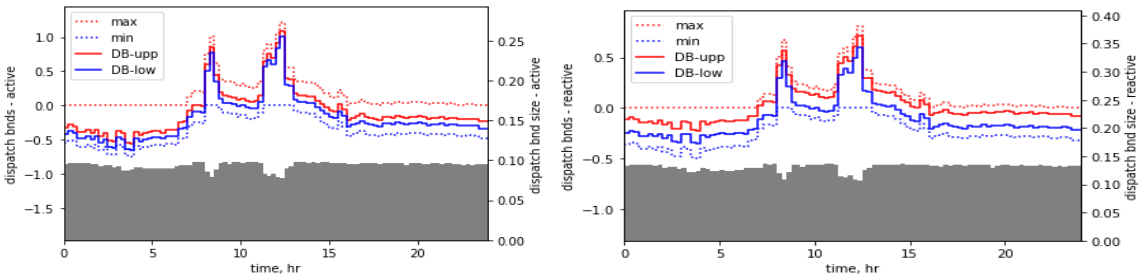

Figure 34. Dispatch bounds for Bus 27

Because these dispatch bounds are meant to guarantee voltage bound satisfaction if all the controllable DERs stay within the bounds, there are an infinite number of possible scenarios that

could be evaluated. We choose to evaluate four extreme scenarios to evaluate the efficacy of the dispatch bounds: (i) all controllable DERs are at their lower dispatch bounds; (ii) all controllable DERs are at their upper dispatch bounds and compare them against when: (iii) all controllable DERs are at their lower control bounds; (iv) all controllable DERs are at their upper control bounds. Figure 35 shows the voltage profiles under these four scenarios at Bus 27 where the voltage magnitude bounds were set to (0.95, 1.05) pu. We can see that the extreme dispatch bound scenarios (solid lines) are able to keep the voltages within or near the voltage bounds, while relying on only the control bounds (dotted lines) allow for extreme voltage violations. It is also interesting to note that the dispatch bounds were solved assuming linearized power flow equations, while the voltages shown in Figure 35 are from a nonlinear power flow solver.

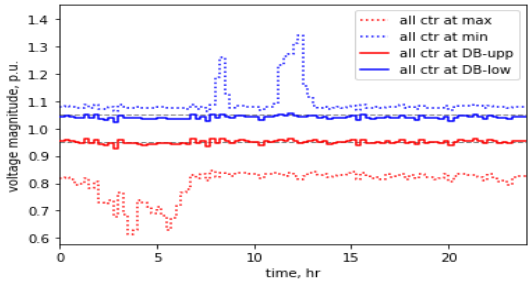

Figure 35. Voltage magnitude at Bus 27

From the Eaton team, we received: (i) the controllable load bounds of 14 (18) homes on Aug 17th 2020 (Dec 8th, 2020); (ii) the aggregated uncontrollable loads of the 14 (18) homes on Aug 17th 2020 (Dec 8th, 2020) and 30 days prior along with day-ahead forecasts for each of those days. All of the data was in 15-min granularity. The goal was to use this data in a power system simulation to find and evaluate the Dispatch Bounds. To expand the data both spatially and temporally, we used the bootstrapping method to generate random selections. Random selections of the 14 (18) homes were used to create the control bounds at different load buses in the IEEE 33-bus distribution network. Random selections of the 30 days were used to create a history of forecasting errors for each of the load buses.

One of the issues faced when solving for the Dispatch Bounds was that there were specific time intervals that no feasible Dispatch Bounds could be found because the space of the controllable loads was too small which causes the internal optimization problem solver to fail. To solve this issue, we added a dispatchable “slack” resource, analogous to a slack bus in a power flow solver, at each load and made them expensive so that the optimization problem would only use them when the control spaces were too small. One benefit to using the slack resources, especially in a day-ahead framework, is that it can give the utility a concrete signal of how much other resources need to be dispatched. A sample result of the new Dispatch Bounds at two buses is the following figure where the green dashed lines are the slack resources.

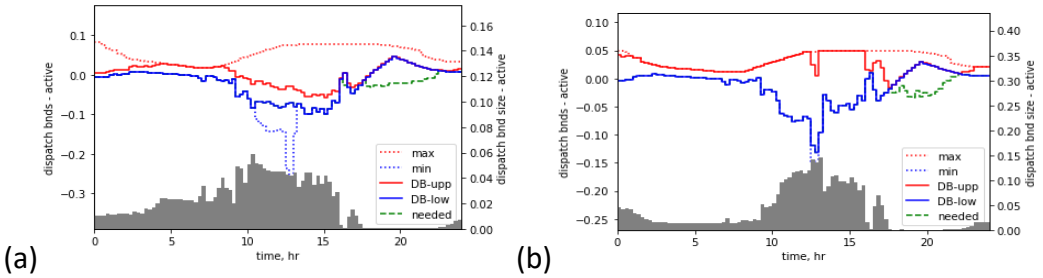

Figure 36. Dispatch bound and needed slack resources at (a)Bus 10; (b) Bus 2.

The resulting voltage profiles at the selected extreme scenarios are shown in the following figure, including when the slack resources are used to show the necessity of them with respect to keeping the voltage magnitudes within bounds, i.e., utilizing slack resources are needed to avoid under voltages between hours 18 and 21 due to the higher amount of load with smaller control space.

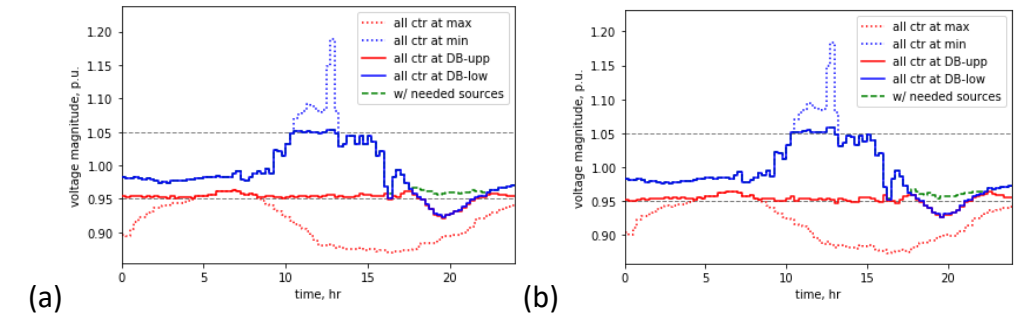

Figure 37. Voltage profiles at (a) Bus 10 and (b) Bus 27 under the extreme scenarios.

Task 4.0: Advanced metering hardware, firmware, and software development

The San Cloud Beagle bone Enhanced single-board computer was selected as the processing platform for the meter-as-a-controller. Off-the-shelf L&G meters are used to embed with meter-as-a-controller single board computer. The board integrates the necessary peripheral components such as GPS and WiFi to facilitate the meter-controller functions. The prototype physical meter adapter that included an enclosure for the SETO single-board computer and associated components were selected. The enclosure provides weather proofing and allows external access to the SETO meter controller without need to interrupt power supply or smart meter operation once installed. The mechanical and electrical layout were determined, and the detailed board layout and schematics produced to meet the system requirements.

An intercept board was designed to allow standard access to the meter from both the AMI smart meter node and the SETO meter-as-a-controller. See figure below:

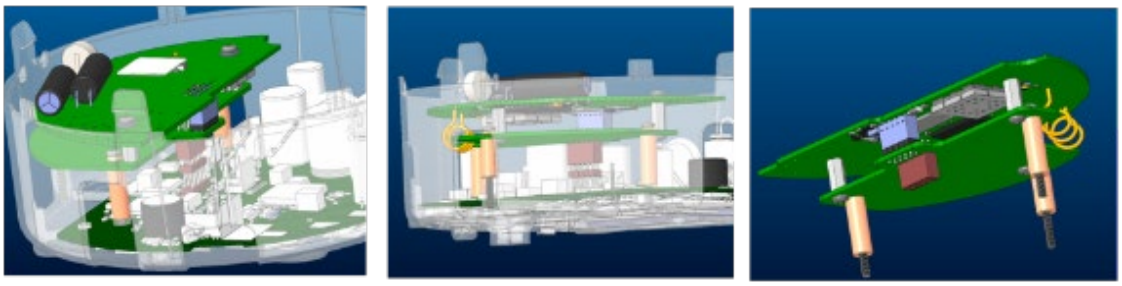

The design was completed for the low-level hardware (carrier) board that hosts the BBE and other peripherals for the meter-controller, to include its board layout and connectivity specifications. The hardware mechanical and electrical schematics were submitted to an external test certification company for design analysis.

Lastly, work was completed in the evaluation of the smart meter-reading interface and the development of the preliminary hardware-firmware design to allow meter-controller to transparently interoperate with the AMI node in accessing the smart meter over a single standard meter UART serial interface. This work included the ability to increase the meter-reading UART interface baud rate and configure the associated C12.18 interface protocol to allow the meter-controller to perform high-frequency load disaggregation meter-reading while minimizing impact to existing AMI node standard meter reading operations.

Smart meter application design: The end-to-end system communications control and security architecture for the SETO hierarchical control system was completed.

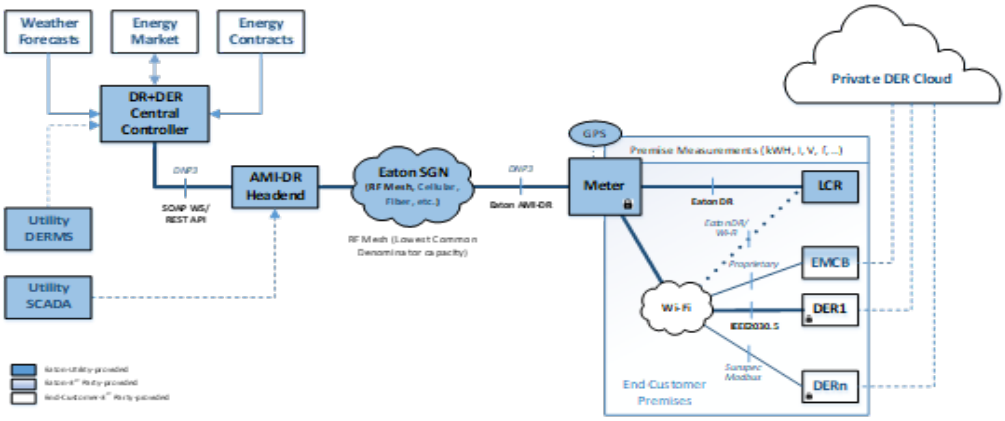

Figure 38. Interworking between the DR+DER Central Controller and Utility DER Management Systems (DERMS)

The figure above illustrates the high-level system architecture including the potential interworking between the DR+DER Central Controller and Utility DER Management Systems (DERMS) as well as the potential for Utility SCADA system interworking for access to behind-te-meter (BTM) DERs.

Communications, control and security protocol requirements for implementation of the end-to-end system were defined and evaluated. Regard qwas given to the requirement for supporting

heterogenous network technologies as part of utility AMI smart grid communications networks. This not only reflects the reality of the current utility landscape but is also important in the transition to different next generation networks. The figure below illustrates a combined RF mesh and cellular network-based utility infrastructure connecting the utility headend to different customer premise sites.

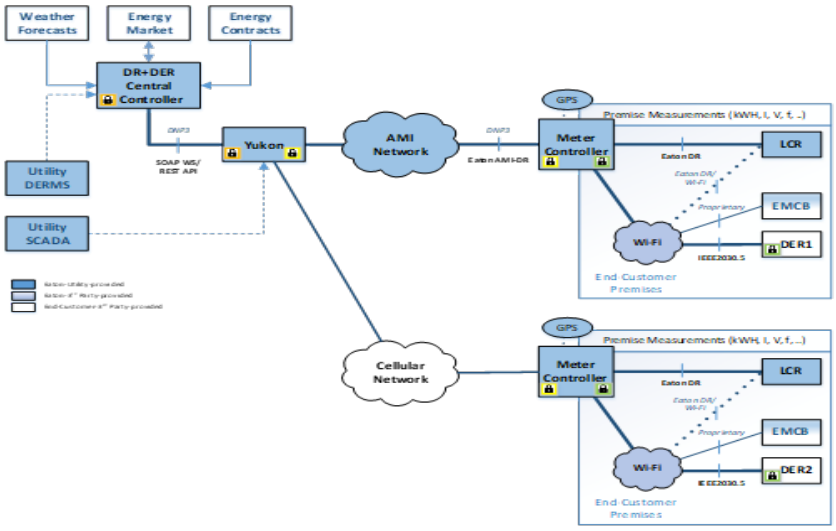

Figure 39. Combined RF mesh and cellular network-based utility infrastructure

The system architecture model is based on the use of public key infrastructure standard C.509 certificate-based security in each of the interlocking security domains from the utility headend enterprise network to the utility field area network. The three connectivity specified domains are: the Utility Enterprise Network Application Server connectivity domain, the Utility Headend-to-Meter wide area Field Network connectivity domain, and the Premise Network Meter-to-DER connectivity domain. DER control shall be delivered through an integrated, end-to-end system of standardized application layer and transport layer security with standard public key infrastructure (PKI)-based security applied in each of the linked domains. While introducing additional PKI management requirements, certificate-based PKI security provides the most robust mechanisms for securing end-to-end DER control while supporting standardized and interoperable security.

IEEE 2030.5 server: EPRI developed an IEEE 2030.5 server software that is a part of the meter controller used in this project. The server can communicate with a DER gateway, which includes an IEEE 2030.5 client. The gateway is connected to a Fronius inverter that is used in this project. The server is used to control the DER by issuing several control commands such as the active power limit setpoint. EPRI's IEEE 2030.5 server supports DER operations defined in the Common Smart Inverter Profile (CSIP) standard. The server integrates with the meter edge controller application that manages the premise DERs and can serve up to 16 DER clients. The server is built from SEP schema 2.1.0 from IEEE 2030.5 standard and is extended to add advanced grid-edge functions such as loss of master & reversion to defaults and advanced scheduling features. Table 8 below shows the technology stack of the server built by the EPRI team.

Table 8. Technology Stack of IEEE 2030.5 Server

Role	Facility DER Server
Profile	Common Smart Inverter Profile (CSIP) – 2018 – Version 2.1
Schema	SEP 2.1.0+
Programming Language	C
Operating System	Linux
Target Hardware	Embedded Platforms (Ex: Raspberry Pi)
Compiler	GCC
Format	Static library (.a) or Dynamic library (.so)
Dependencies	Microhttpd, GNU TLS (Only for Standalone version)
Security	TLS v1.2/1.3 (Only for Standalone version)

Releases: Table 9 shows the various releases of the server library and the associated features that EPRI team has been working on.

Table 9. IEEE 2030.5 server releases

Release	Description	Capabilities
Initial version	Basic server Integrated with microhttpd, Server control and HTTP object APIs	Start/Stop Server Open/Close/Write HTTP client
Release 2	Object Handling APIs, List Handling APIs, Scheduling APIs	Create, update and get basic smart energy (SE) objects like DeviceCapability, EndDevice, DERProgram, DERControl etc
Release 3	Device Data APIs, Access Management APIs, utility/helper APIs	Get end device availability, status, settings, log events and meter data
Release 4	Final Release with API documentation and source code	

CSIP Testing: As part of the CSIP compliance testing, EPRI carried out a number of informal tests following the official SunSpec Common Smart Inverter Profile (CSIP) Conformance Test Procedures. We performed a subset of the tests listed in the CSIP test procedures document. The subset of tests is chosen based on the most common interactions between an IEEE 2030.5 server and a client. These tests verify the interoperability of DERs using the 2030.5 protocol. They make

sure that the 2030.5 functional subset that must be supported are present in the server and client used for this project. The tests were selected based on the applicability of the 2030.5 protocol to this project and on the functionality of the client. The 2030.5 client used in this project works with one single DER; in other words, it is not an aggregator type client. Hence, all the tests related to aggregator clients were out-of-scope of this testing.
The test setup included the 2030.5 server software running on a Linux OS computer. The server is connected to a DER gateway software which includes the 2030.5 client. The gateway runs on a Linux OS, as well. The gateway is also connected to a DER simulator software running on a Windows OS computer. The test setup is depicted in Figure 40.

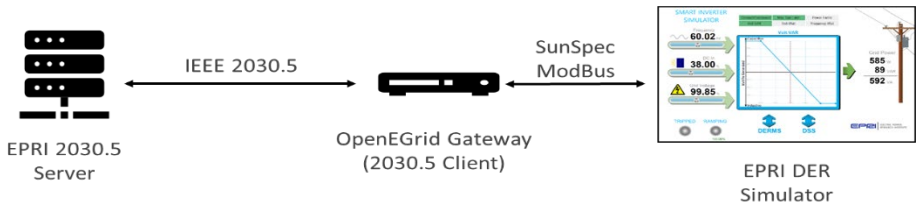

Figure 40. Test setup for CSIP compliance of 2030.5 server and client

The 2030.5 server is used for sending control commands to the DER gateway. The DER gateway incorporates a 2030.5 client. All messages between the client and the server follow the standard 2030.5 protocol. The gateway is responsible for translating the 2030.5 messages into SunSpec Modbus messages. The DER simulator has a SunSpec Modbus interface where it can communicate with the gateway. The DER simulator receives control commands coming from the gateway, as well as it makes the DER status (measurements) available to be read by the gateway. The gateway can also send the DER status to the 2030.5 server using the 2030.5 protocol.

Task 5.0: Stakeholder engagement (Budget Period 1)

Task Activities:
In the budget period 1, the Eaton team had formed an industry advisory board combining multiple utilities that includes investor-owned utilities, co-operatives, and municipalities. ComEd, Southern California Edison, San Diego Gas and Electric, Provo power, Loveland water and power, Grand Valley Power, Jo-Carroll Energy, Sterling Municipal light department, and Delaware Electric co-op have been the part of industry advisory board. Two things were focused for engaging the stakeholders in the first year:

1) The usecases and corresponding elements for DERs and flexible loads were discussed to develop the coordinated control strategy in different layers
2) A letter of commitment from a utility partner who is willing to host the demo for the developed technology

Task 6.0: Hierarchical grid services control algorithm development

In general, coordination between central-level and edge-level involves information exchange between both levels as shown in Figure 41 This information exchange is divided into three categories. First, multiple SETO homes and non-SETO homes are grouped together as a node point, where the net load among these homes can be communicated to the central control. The nodal location is a common point for the homes in the grid network where the net load can be measured and communicated by the utility operator, such as a distribution transformer. Secondly, all SETO homes communicate directly to the central control. The information sent by the homes are related to DERs load flexibility forecast and actual loads in SETO homes, which are used as feedback for the central control to make group-level decisions. Finally, central control also broadcasts a common message to all edge controllers in SETO homes related to the ancillary grid service. The framework and subfunctions within the blocks in Figure 41 will be discussed in more detailed next.

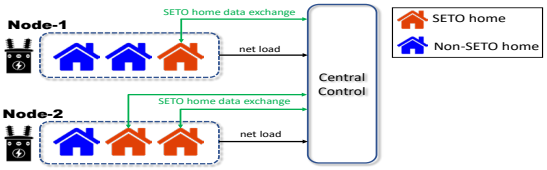

Figure 41. Overview of Information Exchange Between Edge-Level and Central-Level

First, detailed functional blocks within the edge-level and the central-level controllers are discussed. Next, the integration phases, from a simple to the final simulation scenario are elaborated. The edge control contains two functions; first is a data repository function that automate load data cleaning, disaggregation and combining that the controller receive updates periodically and by query from multiple sources.

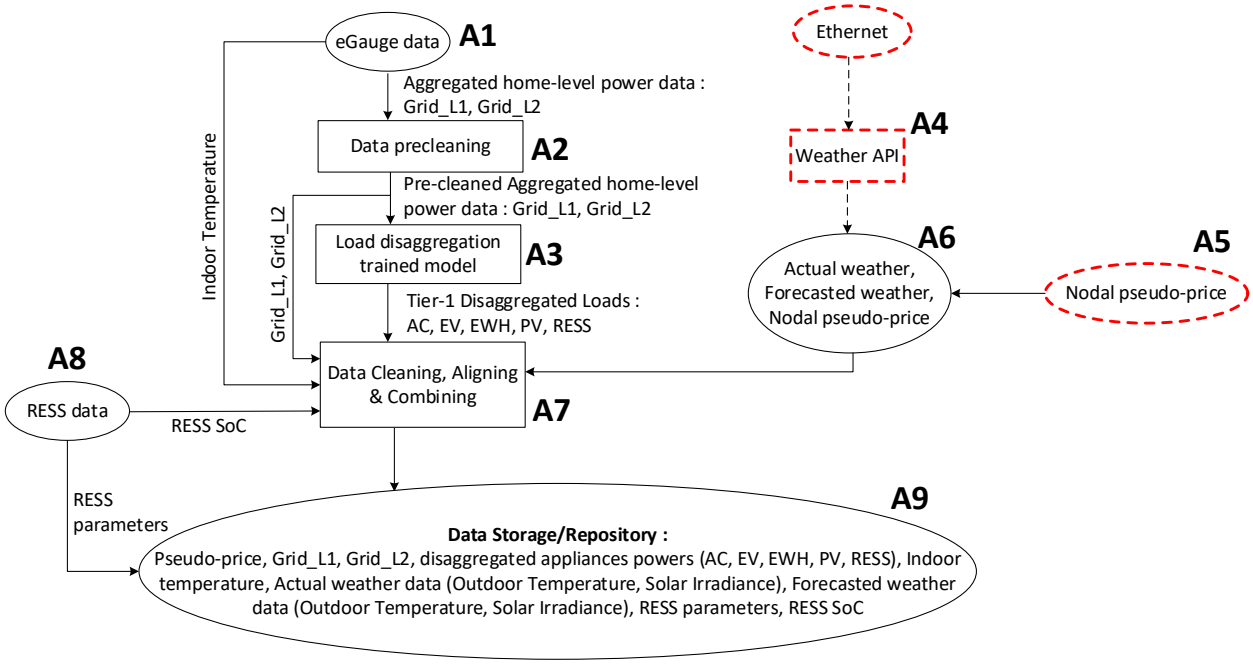

Figure 42. Functional Blocks in Edge-Level Data Repository

Data Repository for Edge Controller: Blocks A1-A9 in Figure 42 represents the different inputs, outputs, and processes in related to the data repository on edge-level. A1 represents the home aggregated load data, given by Grid_L1 and Grid_L2, as measured by an eGauge sensor from the two legs of a home's power supply. A2 represents precleaning of this data in the event of missing data or irregularity readings before data is fed into the trained load disaggregation model shown in block A3. The output of A3 are the disaggregated loads for Tier-1 appliances such as air conditioner (AC), electric vehicle (EV), electric water heater (EWH), PV-solar (PV) and battery (RESS) powers. A4 represents the weather API to query actual and forecasted weather information from a weather data server via ethernet. A5 represents the nodal pseudo-price data that is received from the central level. Ideally weather API A4 is located in central level to have a single and reliable ethernet source. However, for the purpose of simulating the edge-control only, A4 and A5 can be assumed to reside in edge-level as shown in A4-A6. Constant DERs parameters can be queried from DERs controller and sent to the data repository A9, while time-varying dynamic states of the DERs (if available), such as battery SoC are combined with other time-varying data in A7. In A7, data from A3, A6 and A8 are further cleaned, aligned and combined in the edge data repository A9. Time-series historical power consumption data, constant DERs parameters and time-series weather data are used to calibrate DERs models and forecast DERs states and powers in the edge-level DERs controller, shown in Figure 43.

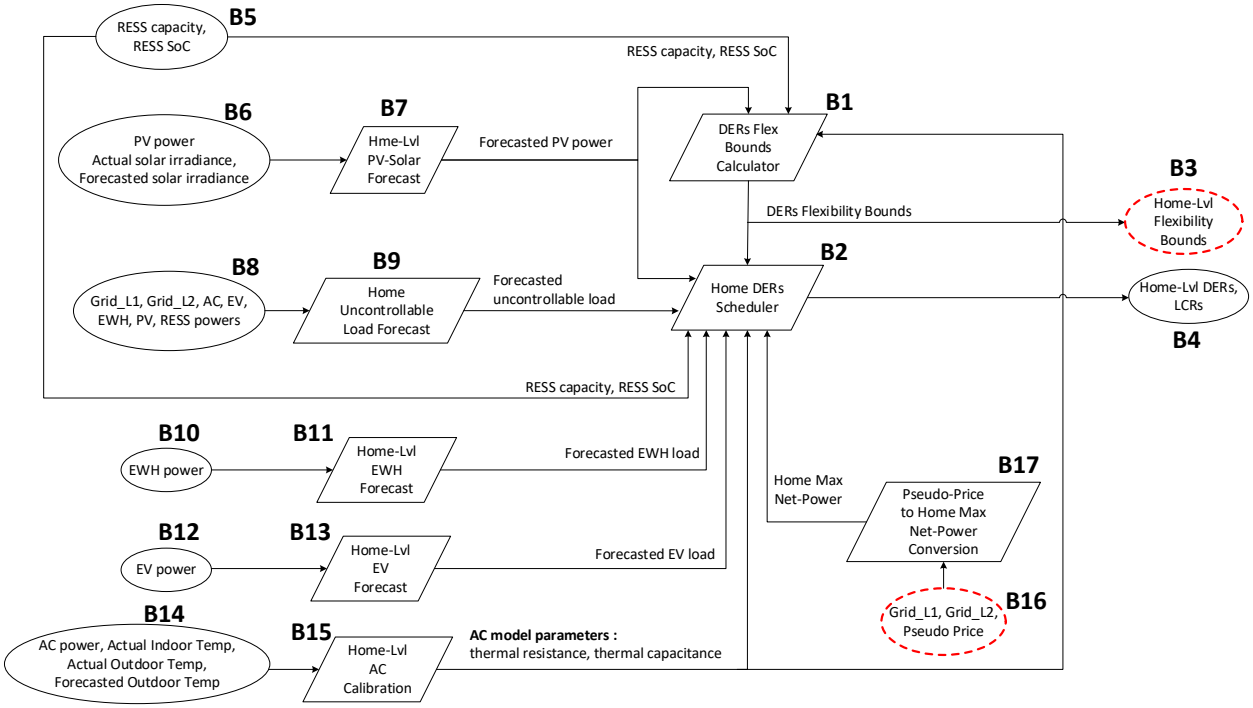

Figure 43. Functional Blocks in Edge-Level DERs Controller

DERs Controller: The edge-level DERs controller consists of two primary functions; first is to calculate DERs flexibility bounds shown in B1 and secondly to schedule DERs inside of home shown in B2. B1 calculates the maximum net home minimum and maximum power flexibility

bounds through an optimization, which are sent to B2 as the net power constraints when scheduling DERs and communicated to the central level controller via B3 to calculate the grid-level dispatch bounds. B2 optimizes the scheduling of the DERs in the home to meet an economic or grid-level objectives while meting the quality of service (QoS) of the home. B5 represents the initial state of charge and capacity of the battery from the data repository that are extracted by B1 and B2 to estimate battery flexibility. B6 represents the historical PV-solar power, historical actual solar irradiance and forecast solar irradiance from the data repository. B7 utilizes the information to forecast availability of PV power for B1 and B2. B8 represents the net home power consumption and the Tier-1 DERs powers from the data repository, where the difference of these two loads is used to forecast the home uncontrollable load via B9 and sent to B1 and B2. B10 and B12 are EWH and EV historical power consumptions that are used to forecast consumptions of EWH and EV through B11 and B13 for B1 and B2. Historical AC power consumption, indoor temperature and outdoor temperatures from data repository are represented by B14 and are used to calibrate the AC model parameters in B15. The parameters are used to estimate indoor temperature forecast using forecasted outdoor temperature in B14, along with the optimized AC power in B1 and B2. B16 represents the historical home net power consumption and historical pseudo price signal from data repository that are used to estimate the home maximum power threshold in B17 during a grid-event for B2.

Integration & Process Flow: The different functions in edge-controller are integrated and a process flow is established across different edge-control functions shown in Figure 44 and explained in Table 10.

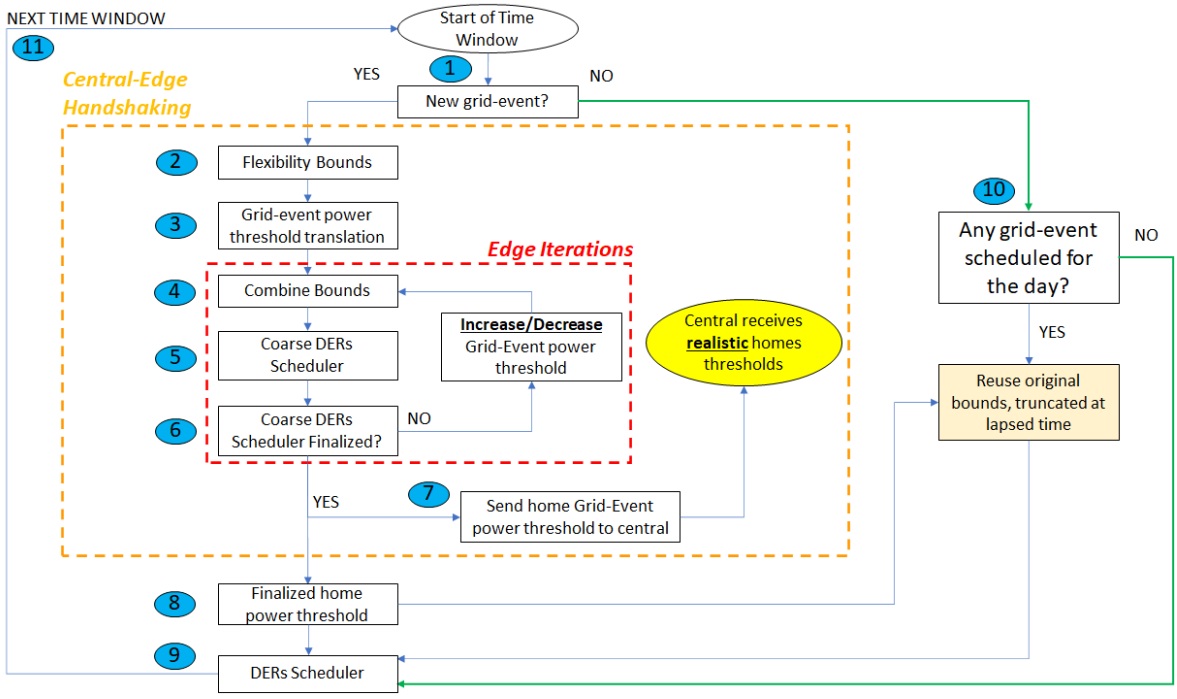

Figure 44. Edge-Level Controller Process Flow Diagram

Table 10. Edge-Control Process Flow Descriptions

Steps	Descriptions
Step-1	At start of simulation, edge-control checks if there is pseudo-price sent from central-control to indicate a grid-event (or not).
Step-2	If there is a pseudo-price from central, edge-control proceeds to calculate DERs flex bounds.
Step-3	Pseudo-price received from central-control is translated into power threshold during grid-event.
Step-4	Upper bounds from DERs flex bounds (from Step-2) & grid-event power threshold (from Step-3) are combined as optimization constraints for DERs Scheduler (in Step-5 and 9): • Upper bound from DERs flex bounds represents the constraint for net controllable DERs power, outside of grid-event. • Grid-event power threshold represents net power threshold for combined uncontrolled loads & controllable DERs during grid-event. The constraints represent home power threshold commitments communicated to central-control.
Step-5	Using constraints in Step-4, DERs schedules are optimized using coarse 1-hour time-steps to allow faster solving time, for multi-iterations to adjust grid-event power threshold to a feasible value, to account for the home's DERs availabilities & capacities.
Step-6	Grid-event power threshold is increased or decreased iteratively until the home's lowest feasible power threshold is found: • If solution is not found, power threshold is increased. • If solution is found in first trial, power threshold is decreased.
Step-7	Once a solution with the lowest threshold limit is found, this feasible grid-event power threshold is sent to central-control.
Step-8	Time-series home power thresholds are finalized as input to DERs Scheduler in Step-9.
Step-9	DERs schedules are optimized using finer 15-minute time-steps & implemented on the DERs in current execution window.
Step-10	With repeating receding-horizon executions, edge-control will check if it received NEW message from central-control, indicating a new grid-event: • If there is no NEW message but there is grid-event scheduled in previous receding-window, it will utilize the original power threshold (from Step-4) & re-schedule DERs (Step-9). • If there is no NEW message & no grid-event scheduled in previous receding-window, it will schedule DERs without power constraints (Step-9). This is the idling/economic mode.
Step-11	Edge-control is executed in a receding window manner at fixed time intervals (4-6 hour intervals).

General Architecture of central Controller: Central-level functional blocks are shown in Figure 45. C1 represents both the nodal-1 aggregated data consisting of both SETO and non-SETO homes that are measured and sent from a nodal point in the grid (e.g., distribution transformer) to central-level (green arrows) and the edge-level data that are directly sent by SETO homes controllers to central-level (red arrows). Similarly, C2 represents the nodal-2 aggregated data and nodal-2 SETO homes data sent to the central-level.

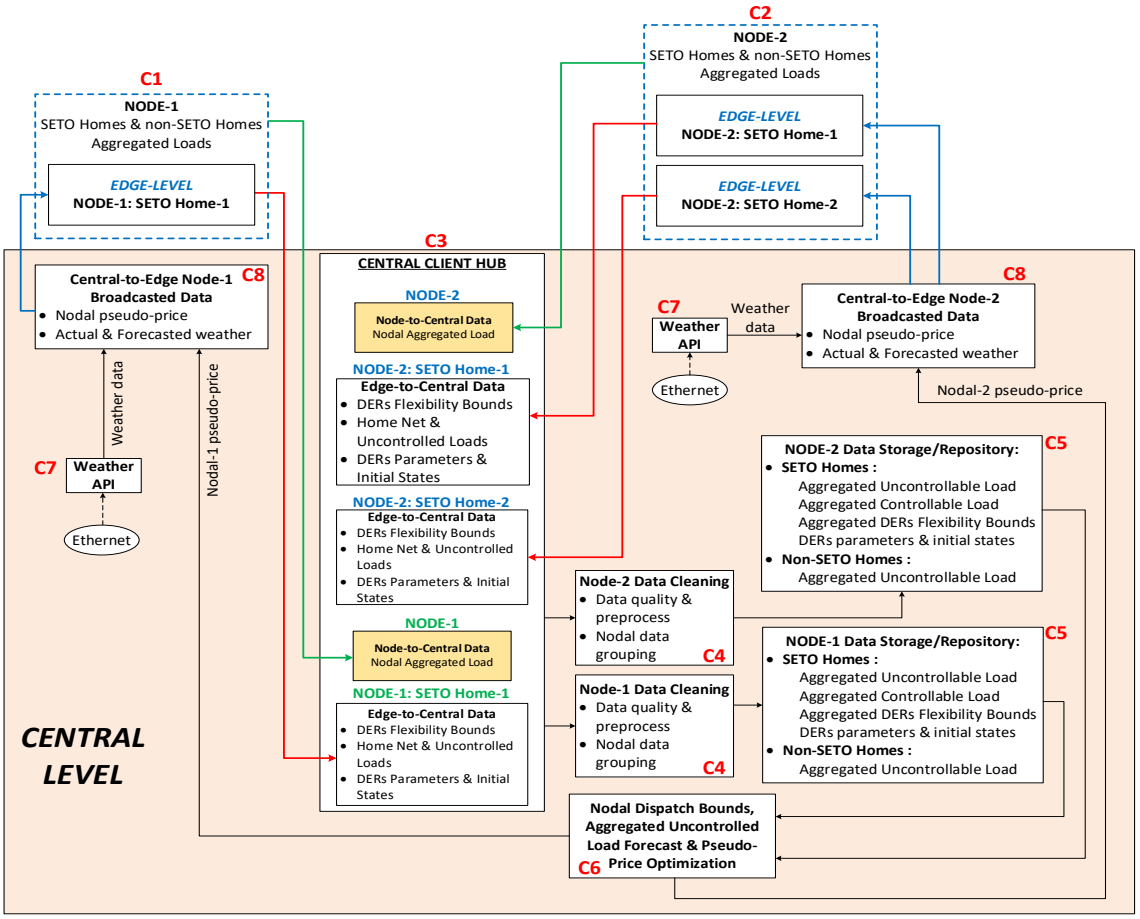

Figure 45. General Central-Level Functional Blocks

At central-level, a Central Client Hub C3 receives the nodal -aggregated load data from all individual nodes and DERs flexibility bounds, net loads, uncontrolled loads, DERs parameters and DER initial states from each SETO home in multiple nodes. C3 will pass the received data to the nodal data cleaning block C4 for data sorting, aggregation, quality check and preprocessing. Outputs from C4 are sorted according to their respective nodal locations, and consist of SETO homes aggregated uncontrollable load, SETO homes aggregated controllable load, SETO homes aggregated DERs flexibility bounds, SETO homes DERs parameters, SETO homes initial states and non-SETO homes aggregated uncontrollable load. These data are stored in nodal data storage C5. The historical loads and DERs data on central-level are used as inputs for nodal dispatch bounds calculation, aggregated uncontrolled load forecast and pseudo-price optimization in C6. The nodal pseudo-price and weather data from C7 are sent to the nodal broadcaster in C8. C8 broadcasts nodal pseudo-price, actual weather data and forecasted weather data to the SETO homes, shown by the blue arrows.

Edge-Controller & Central-Controller: Client-Server: Figure 42 and Figure 43 represent the integration between multiple functional blocks that can be used to simulate a simple edge-level simulation without considering the central-level control, where data in A4, A5, B3 and B16 which

requires interactions with central-level controller, can be artificially moved to edge-level blocks. A complete interaction would require a server-client functions both on the edge-level and central-level to facilitate data transfer between the controllers. Figure 46 shows the server-client functions that resides in the edge-level. The edge-level would require the nodal pseudo-price and weather information from the central-level, while the central-level would require the DERs flexibility bounds, home net & uncontrolled loads, DERs parameters and DERs initial states from the edge-level.

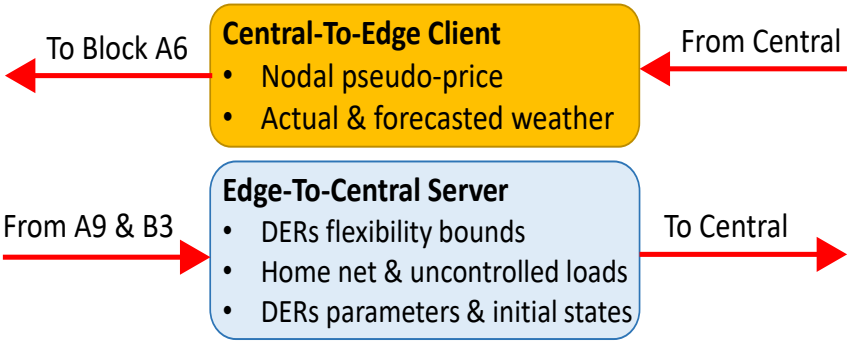

Figure 46. Edge-Level Server-Client Functions

Edge-Controller & Central-Controller: Pseudo-Price Correction Mechanism: The framework for the pseudo price feedback mechanism is given in Figure 47. The pseudo prices are sent from the central controller to the edge controller during grid service events to modify the customer usage for the desired peak reduction.

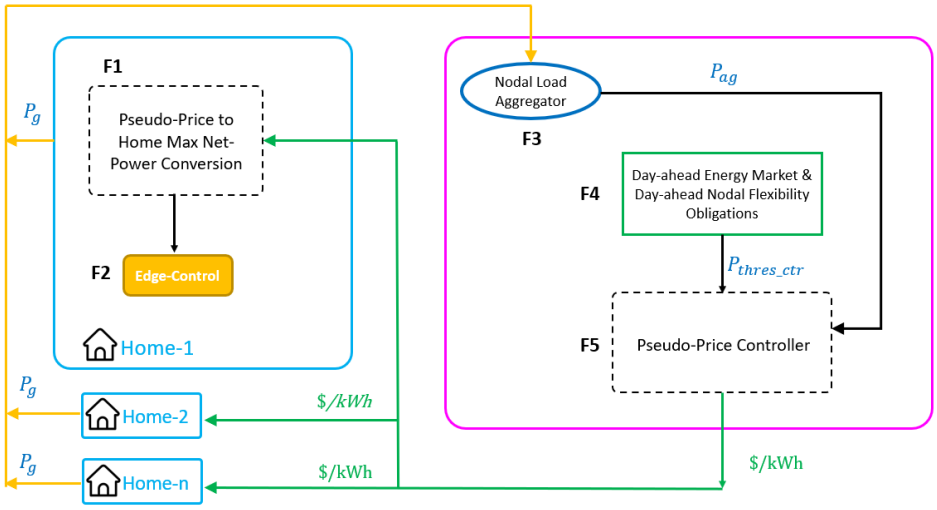

Figure 47. Pseudo-Price Feedback Mechanism

This is not the energy price customer pays for the demand usage, but it is a form of control signal generated by the central controller. The central controller sends the same pseudo price to all the homes connected to a node and is not individualized to each home. This helps in maintaining

user privacy and safety against cyber-attacks since information is not tagged to a specific household. This approach also helps in lowering the communication bandwidth since we can broadcast the message instead of sending unique message to each household.

F4 in Figure 47 represents the information from the day-ahead energy market and nodal flexibility bounds based on which the central controller will decide the reference threshold power or power reduction for the upcoming grid service event. The pseudo-price controller F5 generates the pseudo price based on the reference power threshold, historical aggregate power consumption, and energy price. The pseudo prices are broadcasted to the residential smart meters which are received by the pseudo price to home power threshold converter F1. F1 converts the received pseudo price to a household level threshold based on the historical power consumption of the household and energy price. The generated household level power threshold is used by the edge-controller to modify the user's power consumption. The residential power consumption P_g feedbacks to the central controller where the nodal load aggregator F3 combines the power consumption from multiple households to generate the net-power consumption P_{ag}. The pseudo price controller uses this information to update the pseudo price to reach the desired aggregated reference threshold power.

Simulation Results: Simulation results are shown in Figure 48. In this exercise, a mock central-control is utilized to send a price signal to the edge-control in Home-1. The grid-event occurs at 18-20hrs, with the central-control sending a pseudo price of $0.10 per kWh. The edge-control receives this and translated it into a grid-event threshold of 1.5kW. However, through Step 4-6 iterations, edge-control had to increase the limit to 3kW, as 1.5kW was too low for the load consumptions and DERs availability for Home-1, as shown in Table 11. The objective of DERs scheduler is to minimize the energy costs for the homeowner based on the ToU rate, while at the same time limit the net power consumptions based on the power thresholds. Note in Figure 48 column-[1] row-[2], net power imported from grid (dark-blue shade) between 18-20hrs is limited to the threshold of 3kW (black dotted line). Imported power from grid is also minimized between 9-21hrs by utilizing more battery energy (light-blue shade) when the TOU rate was high, especially during grid-event between 18-20hrs. These are accomplished while keeping the indoor temperature and battery SoC within its upper and lower limits, as shown in Figure 48 , column-[2], rows-[2,3] and maintaining net home power below the committed thresholds to central-control in Figure 48, column-[1], row-[3]. More results will be discussed in the next multi-homes simulations section, especially for homes without battery storage.

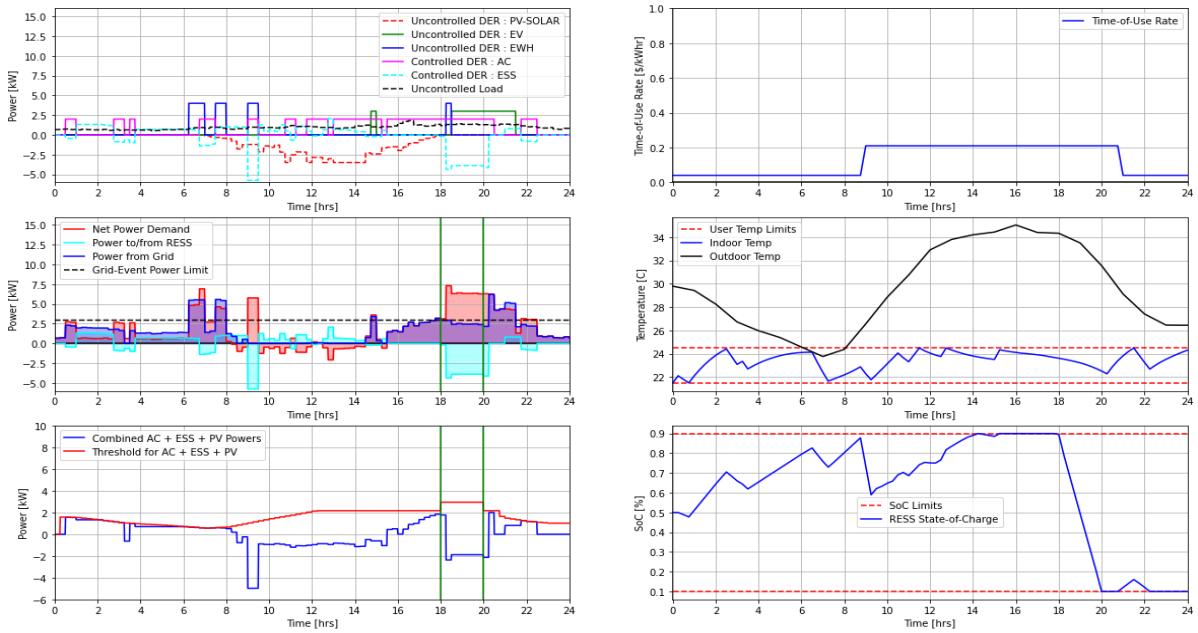

Figure 48. Single-Home Integration Simulation Results for Home-1

Simulator for Multi-Homes Edge-to-Central Integration & Multi-Nodes Edge-to-Central Integration: In multi-home simulations, a group of 13-homes with different sets of DERs assets were selected as home candidates to implement multi-homes simulation shown in Table 11. Based on edge-control architecture explained before, each SETO home that receives central-control's pseudo-signal will adjust its net power threshold during the grid-event to the lowest it can manage, based on the load behavior and DERs availability of the home. Hence, some homes may not be able to meet the requested threshold, but homes may reduce it beyond its threshold. As an aggregation however, the group of homes at each nodal location will strive to minimize power consumption during a grid-event.

Table 11. Home Candidates DERs Compositions

Home	Air Cond [kW]	Solar-PV [kW]	EV Charger [kW]	Battery [kWh]	Electric Water Heater [kW]
Home-1	**2**	**3.5**	**3**	**10**	**4**
Home-2	**2**	**4.5**	**N/A**	**10**	**N/A**
Home-3	**3.5**	**3.5**	**N/A**	**10**	**N/A**
Home-4	**1**	**3.5**	**N/A**	**10**	**N/A**
Home-5	**2**	**3.5**	**N/A**	**10**	**N/A**
Home-6	**3**	**3.5**	**N/A**	**10**	**N/A**
Home-7	**2**	**5**	**N/A**	**10**	**N/A**
Home-8	**2.5**	**3.5**	**3.5**	**10**	**N/A**
Home-9	**3.5**	**4**	**3**	**10**	**N/A**
Home-10	**2.5**	**7**	**11.5**	**10**	**N/A**
Home-11	**2**	**5**	**N/A**	**N/A**	**N/A**
Home-12	**2.5**	**3.5**	**3.5**	**N/A**	**N/A**
Home-13	**3.5**	**4**	**3**	**N/A**	**N/A**

As shown in Figure 48, the load threshold during grid event must be increased due to high load consumption at the home, despite having a 10kWh battery, PV solar and controllable air-conditioner. Conversely, for Home-4, a pseudo-price signal of $0.10 per kWh is translated into a power threshold of 1kW during a grid-event between 18-20hrs. However, through Step 4-6 iterations, the edge-controller calculated that the home can accommodate 0kW during the grid-event as shown in Figure 49, column-[1], row-[2,3]. Looking at DERs compositions of Home-4, it has a small 1kW AC, a 3.5kW solar-PV and a 10kWh battery. Home-4 also consumes around 1-1.5kW of net uncontrolled loads throughout the day. Due to battery storage, PV-generation and low consumptions, Home-4 can produce net-zero grid consumption during the grid event, while maintaining the quality-of-services for indoor air temperature and battery state-of-charge. Subplot top-left shows the appliances load profiles & power ratings. Subplot mid-left and bottom-left shows a net-zero grid consumption during grid event by offsetting home loads using home battery. Subplot top-right shows the Time-of-Use tariff. Subplot mid-right and bottom-right show the Quality-of-Service being met for AC and Home Battery.

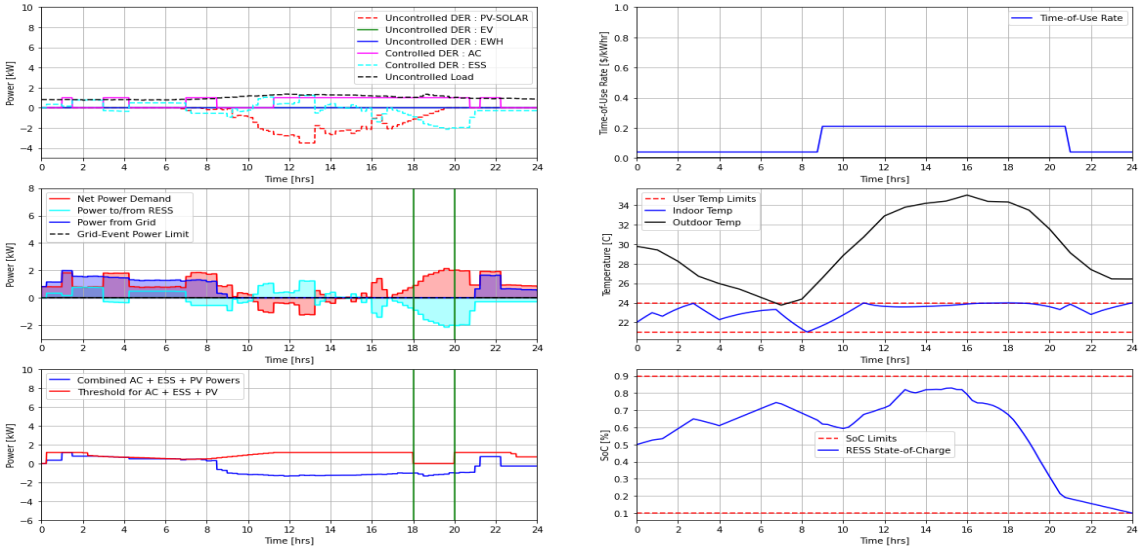

Figure 49. Simulation Results for Home-4

Homes 11-13 in Table 11 do not have batteries for storing energy from either excess solar-PV power or the grid to minimize grid power-import during a grid-event. However, the home can store thermal energy in the form of lowering its indoor temperature, which represents the home thermal energy capacity. Therefore, for homes without energy storage, indoor temperature range plays a big role in determining whether the home can participate in a grid-event or not. Home-11 simulation results in Figure 50 shows such behavior. The indoor temperature range is increased to between 19-25°C in Figure 50, column-[2], row-[2], to allow Home-11 to be cooled down enough to avoid AC from turning on during a grid-event between 18-20hrs as shown in Figure 50, column-[1], row-[1,2,3].

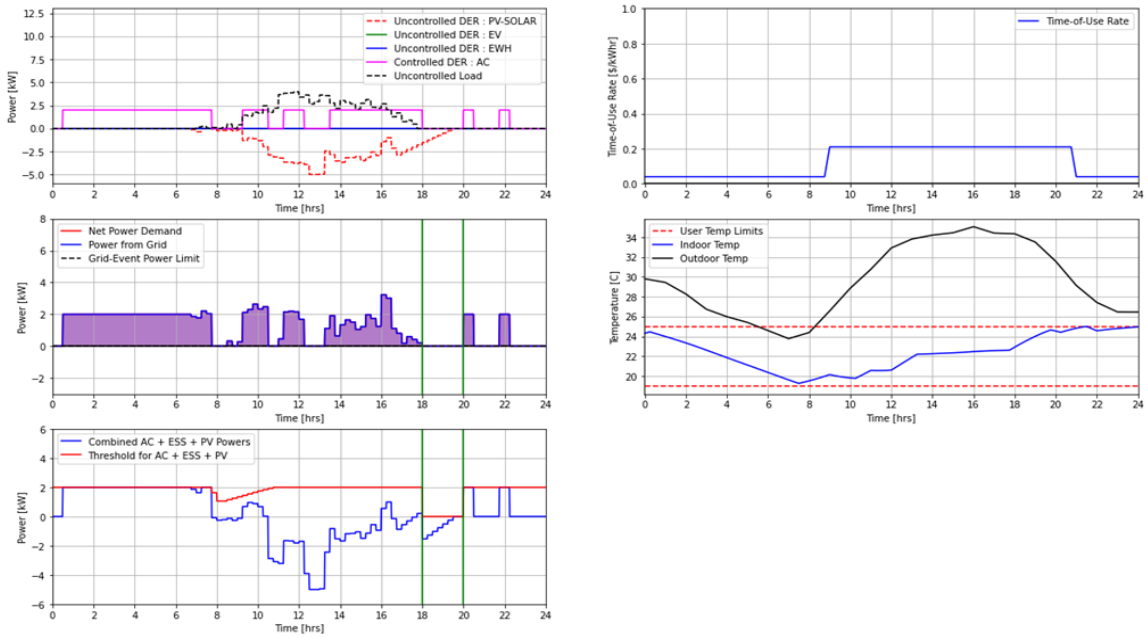

Figure 50. Simulation Results for Home-11

Different combinations of multi-homes simulations can be created using homes listed in Table 11 to analyze potential peak power reductions during a grid event. Figure 51 shows the net power imported from grid for Homes 1-13. In general, edge-control reduces power imported from grid during grid-event between 18-20hrs. Additionally, power consumptions during high ToU between 9-21hrs are also reduced.

Table 12 shows the different combinations of homes with its peak net power during a grid-event with edge-to-central coordination, compared to its worst-case scenario where uncontrolled loads with controlled DERs coinciding during the grid-event. The first scenario where all homes have battery resulted in the highest power reduction during grid event at 88.2%, while the lowest is when all homes do not have battery at 63.5%. The case where half of the homes have battery while the other half does not have battery resulted in 81.3% of power reduction, which is higher than the case with 80% of homes have battery. Home with no battery however may still be able to reduce its consumption during a grid-event, as shown in Home-11 in Figure 50. However, a home without battery may still unable to displace high uncontrolled load if it occurs during a grid event. Therefore, the percentages of homes with battery may still play significant role in reducing grid-event average power at the nodal level. Scenario with 20% of homes with battery resulted in 70.5% power reduction during grid event.

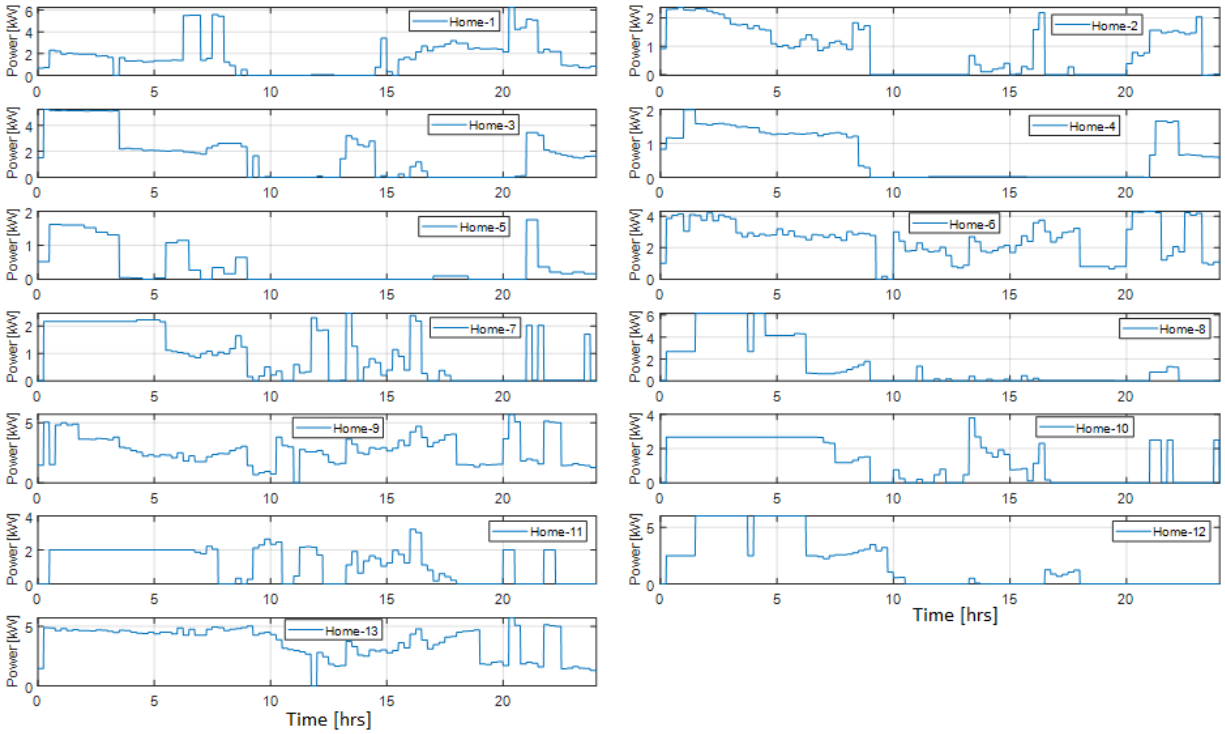

Figure 51. Net Power Imported From Grid for Candidates Homes 1-13

Table 12. Multi-Homes Scenarios Power Reductions during Grid Event

Scenario Descriptions & [Homes List]	Average Nodal Power, with Controls [kW]	Average Nodal Power, Worst-Case [kW]	Power Reduction [%]
All Homes Have Battery [Home-1 to Home-10]	4.97 kW	42.20 kW	88.2%
All Homes Does Not Have Battery [3 x Home-11, 3 x Home-12, 4 x Home-13]	13 kW	35.62 kW	63.5%
50% Homes Have Battery 50% Homes Does Not Have Battery [Home-1 to Home-5, 2 x Home-11, 2 x Home-12, 1 x Home-13]	5.88 kW	31.48 kW	81.3%
80% Homes Have Battery 20% Homes Does Not Have Battery [Home-1 to Home-8, Home-12, Home-13]	6.69 kW	34.20 kW	80.4%
20% Homes Have Battery 80% Homes Does Not Have Battery [Home-1, Home-2, 3 x Home-11, 3 x Home-12, 2 x Home-13]	9.10 kW	30.88 kW	70.5%

Delaware Electric Cooperative Service Area Batch Simulations: Power consumptions data for 19 volunteer homes with valid data in Delaware Electric Cooperative (DEC) service area were collected for the month of July 2023 and simulations were performed using the data to analyze the potential savings from implementing the proposed control methods.

First, the benefits for utilities are calculated during Coincidental-Peak (CP) days. Simulations were performed for the 19 homes based on actual CP days in July 2023 to get the kW reductions from the 19 homes using the proposed controls methods. There were 5 actual CP days in July 2023 - July 5th, 6th, 12th, 13th and 14th with each day having a 1-hour CP duration starting at either 5PM or 6PM. Then, the cost-saving multiplier (dollars per kW saved) is calculated based on actual CP events in 2021 and 2022, which are then averaged and inflation-adjusted to be $21.75 per kW saved for 2023. Finally, the potential savings from CP reduction in July 2023 is projected for the 102,000 homes in DEC service area. As shown in Figure 52, based on simulation analysis there is a potential to save between $115K-$1.15M if the proposed controls are deployed in 10%-100% of the homes in DEC territory during coincident peaking (5 days per year & 5 hours total).

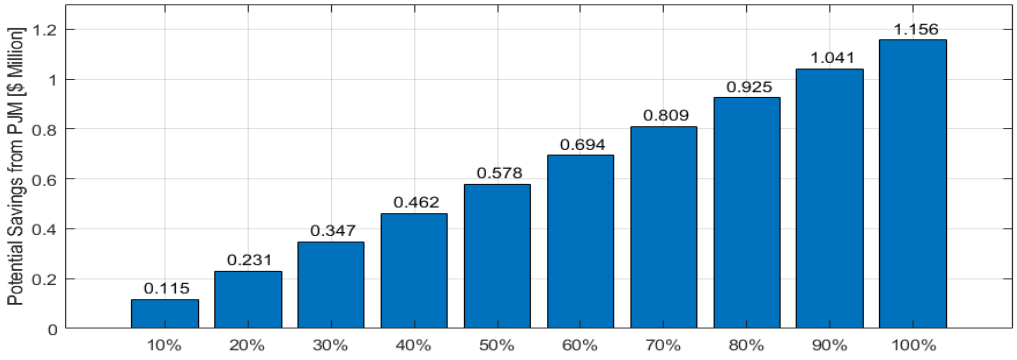

Figure 52. Potential Savings for Utility during Coincidental-Peak Days in July 2023

Secondly, the benefits for homeowners are calculated during non-Coincidental-Peak (non-CP) days. As proposed, the home-controller will perform energy saving functions in the homes without impacting the quality-of-services (QoS) for the homeowners. As shown in Figure 53, simulation results show there is a potential to save DEC homeowners between 15%-45% energy in the month of July 2023 if the proposed controls were implemented. Note the varying savings are based on the home's appliances and ratings - for example, home with higher PV and lower AC power-ratings tends to benefit more.

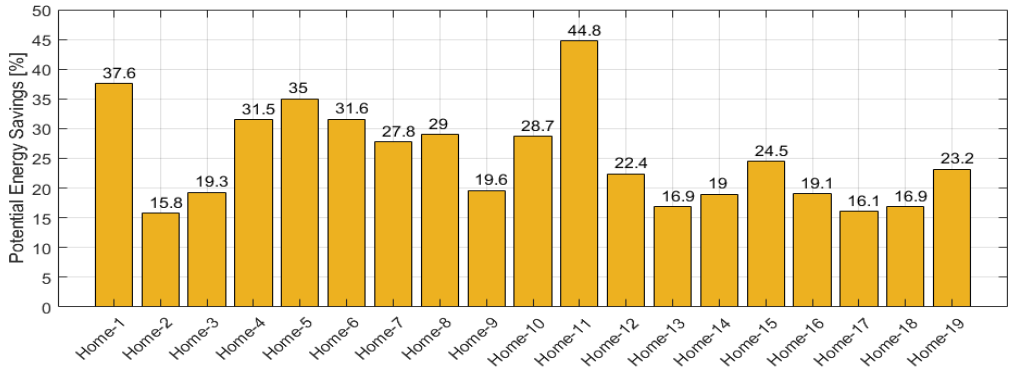

Figure 53. Potential Savings for Homeowners during non-Coincidental-Peak Days in July 2023

Key takeaway on this section is that the coordination between edge-level and central-controller is defined and batch simulations are performed to shows benefits in terms of energy savings and

peak load reduction during grid-event; all while maintaining comfort bounds for the homeowners.

Task 7.0: Development of the risk-based DER dispatch bounds calculation framework

Task Activities:

Central controller formulation and simulation: Previously, the central-controller code was tested with simulations using feeder models from PandaPower and only a small (5-bus) feeder model from OpenDSS. Because the real-world demonstration will use the J1 feeder model from OpenDSS, we needed to make sure that the code would work with that model and the new data from DEC. The J1 feeder model in OpenDSS is a three-phase model and was modified into an equivalent single-phase model for the central-controller. Because the J1 feeder has transformers that affect admittance matrix and some of the nodes have different nominal voltages (e.g., the nodes near the head of the feeder containing voltage regulators), the central-controller code had to be modified to allow for a heterogeneity of nominal voltages across the nodes.
Using the load data, flexibility bounds, and bootstrapping method from the numerical simulations from the work done in Task 3.0, we tested the central controller on the reduced J1 feeder. 23 of the 223 nodes with loads were chosen among 3 different branches of the feeder to be controllable with pseudo-prices. One noticeable difference between using the J1 feeder and the previous distribution networks is that the voltages in the J1 feeder are more sensitive to changes in the load. For example, at node x_6009029653-a, near the end of the feeder, the target load for control is larger than the control region (forecasted load) at the beginning of the day, whereas the targeted load goes below the control region in the later afternoon and evening as shown in the figure below.

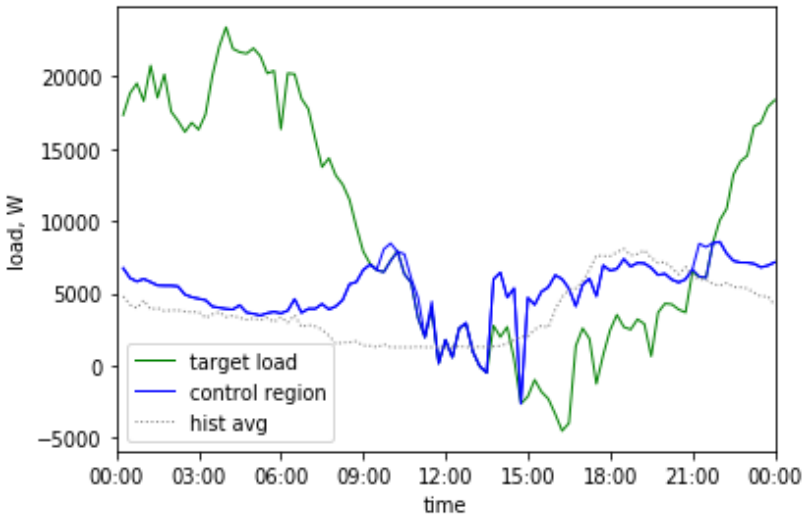

Figure 54. Load reduction response for J1 feeder

Consequently, the pseudo-prices reflect this by being very low in the morning and high in the late afternoon and evening as demonstrated in Figure 55.

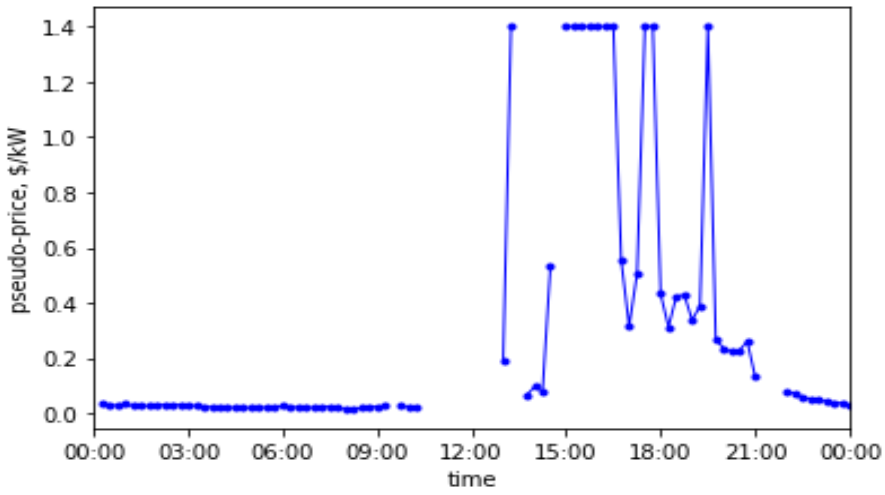

Figure 55. Pseudo price response

Intuitively, this means that a seto-home or meter-controlled home with controllable energy storage would be signaled to store energy early in the day to be used later in the day.

The bootstrapping module was changed to fit the data availability from DEC, specifically for the uncontrolled nodes; 20 aggregations of uncontrolled homes were randomly placed among the uncontrolled nodes for the J1 feeder. One node near the end of the feeder was picked to be the SETO-node with 5 SETO-homes aggregated at that node.
The main challenge with the J1 feeder and the DEC data was that optimization solver in the central-controller would fail at certain time intervals by saying that the problem was infeasible and not output a pseudo-price for those time intervals. To avoid these issues, we made the following changes to the code:

1. Added the option to add auxiliary nodes that can inject reactive power with a high penalty to the optimization objective function. For the J1 feeder, these auxiliary nodes were added to the same location as the voltage regulators.
2. Added in contingency rules for when the optimization solver says that the problem is infeasible; it uses the latest feasible solution that was previously solved.

The modified central-controller code was tested under various forecasting error sizes and loading factors.

Task 8.0: Advanced metering hardware, firmware, and software development

Smart Meter: Prototype hardware was received, and hardware functionality was verified.

Figure 56. Smart-meter hardware prototype

The Figure above show different views of the integrated hardware components on which the current end-to-end communications firmware and controller algorithms were being developed and tested. The pictures show (from left to right): 1) the new field demo hardware carrier board integrated into the external meter adaptor enclosure, without the main BeagleBone processor board installed, 2) the carrier board with the BeagleBone processor board installed (mounted), and 3) the complete hardware setup including the partially visible attached smart meter (with enclosed intercept board) and the ribbon cable-connected, door-mounted AMI RF communications module for SETO data communications across the RF mesh AMI network.

Node controller Firmware: The functionality allowing meter-based Premise Controller to be a local controller for Load Control Relay (LCR) switches was developed. Unlike typical AMI-Demand Response (DR) in which DR controls originate at the headend system, in the SETO hierarchical control design, the Premise Controller is also a controller for premise DR assets. Firmware was developed and successfully tested in allowing the Premise Controller to activate DR controls in conjunction with the overall premise edge control algorithm. Work was completed on the firmware that allows the premise LCR to accept local premise controller commands that take precedence while the LCR devices remain also utility system-controllable from the Headend System. The Figure below provides an overview of the two-level broadcast communications that has now been implemented and tested.

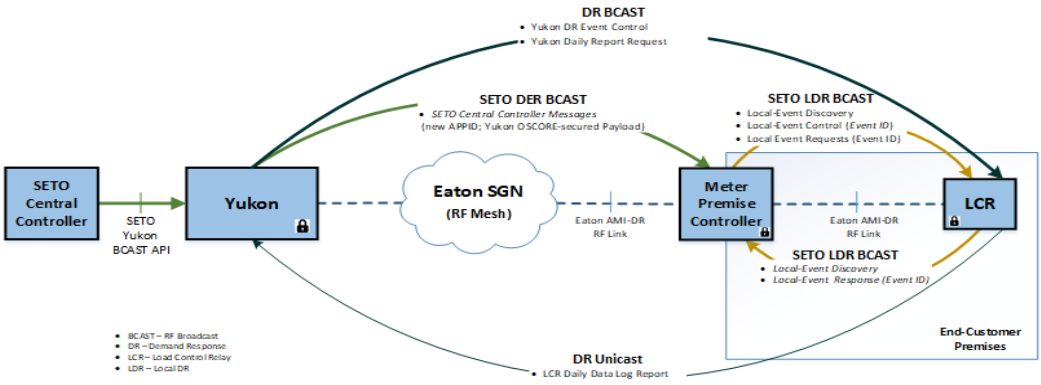

Figure 57. Message broadcasting between Yukon and Meter-controller.

System-wide broadcasts allow the Central Controller to broadcast control commands and other

DER+DR application data to groups or to all Premise Controllers using a modified AMI system broadcast mechanism. Local premise-level broadcasts were further implemented for the local Premise Controller DR control and device management. It should be noted that a feature of the local premise broadcast is that while it does use an RF broadcast mechanism to increase the reliability of communications between a Premise Controller and the local LCR(s), that number of RF mesh network transmission hops is limited and controlled. This allows Premise-originated broadcasts to be sent frequently, if needed, without unduly adding to the AMI network RF mesh background traffic.

Headend system communication interworking testing- SETO node to Central and vice versa: SETO project applies smart meter as the edge controller for distributed energy resources on premises. The communication infrastructure block diagram is shown below.

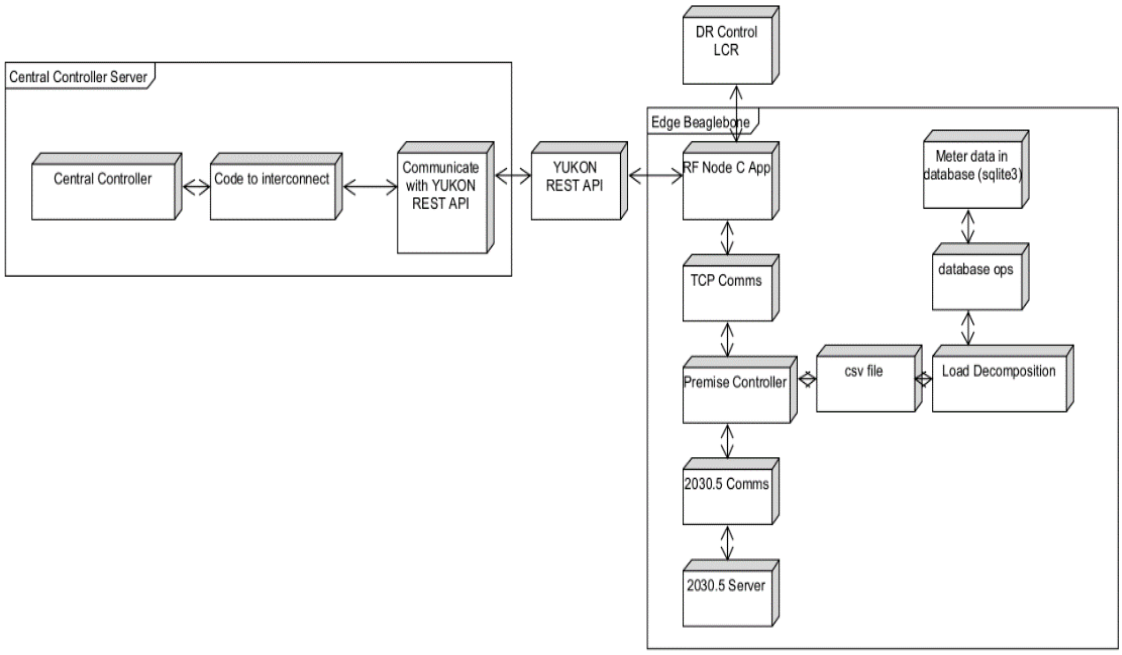

Figure 58. SETO Communication Infrastructure

The project deploys a central controller at the utility headend system to allow for grid services on the distribution network or for user-centered premise energy management services control. As a result, the project requires solid data exchange between the edge and central controllers to share information and commands. The project utilizes the Eaton YUKON system for data exchange through the AMI.

Central controller resides in Central controller server, which communicates to Eaton YUKON system through REST APIs. YUKON would transfer the data between the central controller and the specified premise node or group of premise nodes. RF node C App on the premise node receives/sends the data on the node side for end-to-end communication, interacts with the

premise controller algorithm through TCP communication process, and take care of LCR DR control. Meter data is stored in sqlite3 database and input to load decomposition for processing through database operation module. 2030.5 Server controls the DERs in the house and communicates with premise controller.

The team utilized the TCP communication module for edge-control to facilitate message sending and receiving through local socket port. The local port is the point where messages are exchanged with the edge device RF Node that sends/receives messages to/from central control. Messaging formats were specified to standardize the information exchanges between edge-control and central-control. These messages are then embedded in JSON format and echoed though the TCP communication module to ensure the format is transmittable and receivable.

Task 9.0: Lab testing and end-to-end integration testing

NREL Lab Setup: In this task, Eaton team has established an architecture for end-to-end system integration testing & validation in lab environment.

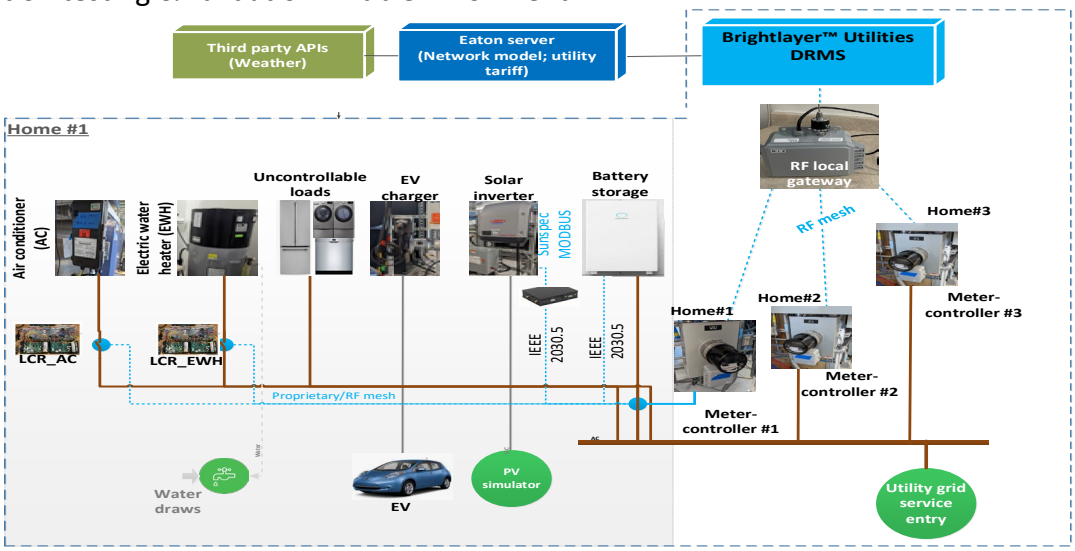

Figure 59. Testbed integrating SETO Smart Meter/Controller and Hierarchical Grid-Service Control System.

The objective was to leverage NREL's Smart Home hardware in loop (HIL) setup to test and validate three SETO AMI meter/controller prototypes (unit-level) for three virtual smart homes; and also integrate with Eaton's Yukon AMI DR headend device and DR+DER Central Controller. *Figure 59* shows the testbed integrating SETO Smart Meter/Controller and Hierarchical Grid-Service Control System. This lab setup also targets to help identify and mitigate risks prior to the field demonstration in BP3.

A description of how the load models were mimicked are provided below. Uncontrolled loads are considered based on inflexibility or if there is not much to gain from them while controlling the whole house consumption. For example, washer/dryer are running occasionally, adding another

layer of control through a relay or breaker installation and commissioning may not provide enough justification for benefit to cost ratio; therefore, they are not considered in this test.

- **HVAC:** Pair hardware, including thermostat, with building simulation running in real-time using weather file from Austin, TX. The building simulations should match properties of buildings from Pecan Street.
- **Water Heater:** Create draw profiles for different homes in Austin, TX. The draw profiles will run on a schedule that can easily be repeated.
- **PV:** DC power from panels is simulated using DC power supplies that follows insolation data from historical Austin weather.
- **EV:** Load data from Pecan Street will be used to determine start time, duration of charging.
- **Uncontrolled loads:** This will include refrigerators, washer, dryer in each home and lights on timers in each home. Lights are a good load since that can be tailored by the number of lights to get the wattage need to be consumed.

For the purpose of control, HVAC and electric water heaters are controlled via Eaton's load control relay over RF mesh and PV and Battery are controlled over WiFi using IEEE 2030.5 protocol. This is shown in *Figure* 59 as well.

Testing the developed load disaggregation and controller code on BBB : The developed edge-controller modules are tested independently and as an integrated system on an open-source embedded platform, BeagleBone Black (BBB). BBB is a low-power, open hardware with a Linux based system with a small footprint, the size of a credit card. For the software integration testing, an upgraded version of Beagle board called SanCloud BeagleBone Enhanced is used. It has upgraded RAM, ethernet speeds, and Wi-Fi/Bluetooth facility. The system uses AM3358 Sitara processor and Debian based operating system. The following tasks were completed on the BBB platform.

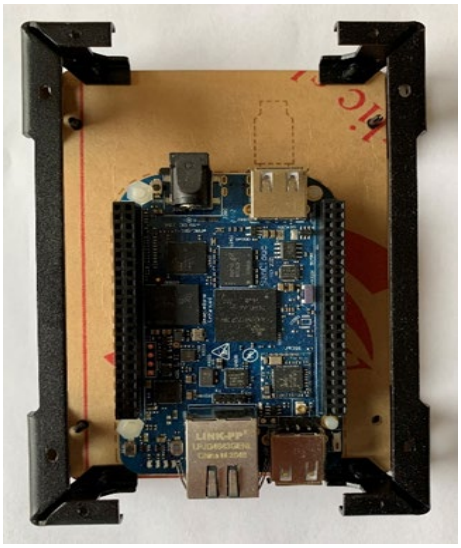

Figure 60. SanCloud BeagleBone Enhanced

- An initial testing was conducted on the BBB to learn its development tools and functions.
- The developed modified persistence forecasting model was successfully tested on the BBB. The aggregate of 14 residential households generated from the disaggregated load profiles was loaded into the BBB as input to the forecast model to generate day-ahead forecasts (24-hour ahead with 15-minute resolution)
- Tested the modeling and calibration of DERs (AC, PV, EWH, & EV) for the edge analytics with preloaded data.
- Ensured the execution of the load disaggregation module on the BBB platform
- Created a common database for the load disaggregation module to write the results and the edge-control algorithm to read.

- Executed the edge-control algorithm on the BBB, using the load disaggregation output read from the common database.

The BBB used for the software integration testing is shown in Figure 60. The board is enclosed in an open hardware facilitator to protect from short circuits. The edge controller framework uses an optimization suite, Gekko, to find the optimal schedule for the appliances. Gekko is a python package for solving mixed-integer and differential algebraic equations and can be used for machine learning and optimization problems. As a step prior to running the edge controller code, the optimization suite was installed on the BBB. The BBB is connected to the Wi-Fi to receive code and commands. The edge controller eco-optimization codes and input data files are transferred to the BeagleBone and tested the functionality to ensure accuracy and same results as with running on PC. The eco-optimization code for a simulation period of 18 hours was executed with a run time of 3 hours on the BBB. The team will work reducing the computational time by changing the simulation time horizon or time step/time resolution.
The final solution for the integrated edge controller–load disaggregation module is shown in the Figure 61 below.

```
 ----------------------------------------------------
 Solver         :  APOPT (v1.0)
 Solution time  :  204.4613 sec
 Objective      :  5078.579556677797
 Successful solution
 ----------------------------------------------------
```

Figure 61. Results from executing the integrated edge-controller on PC

The final objective value for both code runs was found to be matching and the execution time for the final optimization module as shown in the figure below.

```
 ----------------------------------------------------
 Solver         :  APOPT (v1.0)
 Solution time  :    3960.2639999999956      sec
 Objective      :    5078.5795567873593
 Successful solution
 ----------------------------------------------------
```

Figure 62. Results from executing the integrated edge-controller on BBB

The run-time for the different modules within the edge-controller code are shown in the table below. The edge-controller program executed in around 55 minutes for finding the set points for a 24 hour ahead period with 15-minute resolution. This runtime is reasonable for a day-ahead planning given the complexity of the optimization problem of handling multiple DERs with upper and lower constraints for the states to maintain Quality-of-Service and for the inputs to adhere within the operation limits of the DERs. The optimization can be executed by the firmware 1 or 2 hours before the start of the next day as a planning tool. Additionally, the low-cost for a single

board computer such as BBB for around $50 is an attractive price-point for broader deployment of the meter controllers in multiple homes.

Table 13. Run-time Analysis

	Time (Secs)
DER Flex bound calculation	93.56
Coarse time (1-hour) DER-scheduler	438.84
Finer time-step (15-minutes) DER-scheduler	2794.2
Total	**3326.6**

Task 10.0: Field deployment and demonstration

Pecan Street worked in tandem with DEC to identify communities that had a feeder with a high penetration of rooftop PV. DEC reviewed the individual circuits on their maps and narrowed it down to three that could be targeted for participant recruitment. The three target communities were in Lewes, Delaware.

Pecan Street developed recruitment materials for DECs marketing team to distribute, including a 1-pager about the project, newsletter language, and examples of social media posts that proved successful with previous recruitment. DEC conducted targeted outreach to solar homes in the community with the most solar homes. After a few rounds of newsletters, Facebook posts, and attendance at the neighborhood HOA meeting it became clear that recruiting all 25 homes in the one neighborhood was not achievable. After 3 months of targeting the first neighborhood, DEC broadened the participant outreach by sending out digital newsletters and mailers to the homes on the circuit with the second highest number of solar homes.

Thirty-four households expressed interest in the program and Pecan Street was able to secure participant agreements and get completed enrollment form questionnaires from 23 households. The enrollment form was developed to determine if homes had rooftop PV, an electric vehicle that is charged on site, a smart thermostat, an electric water heater, and/or interest to install an energy storage system at their home. The table below displays a snapshot of some of the data collected from the enrollment form.

Table 14. Participants list with End-User Asset.

Circuit	Rooftop Solar	EV on premise	Smart thermostat	Interest in BESS	Electric water heater
1	No	Yes	Yes	Yes	No
1	Yes	Yes	Yes	Yes	No
1	Yes	No	Yes	No	No
1	Yes	Yes	Yes	Yes	No
1	Yes	No	Yes	No	No
1	Yes	No	Yes	Yes	No
1	Yes	No	Yes	Yes	No
1	Yes	No	Yes	Yes	No
1	Yes	Yes	No	No	No
1	No	No	Yes	No	No
1	Yes	Yes	Yes	Has Powerwall	No
1	Yes	No	Yes	Yes	No
1	Yes	No	Yes	Yes	No
1	Yes	No	Yes	Yes	No
1	Yes	No	Yes	No	No
2	Yes	Yes	Yes	Yes	No
2	Yes	No	No	No	No
2	Yes	No	Yes	Yes	No
2	Yes	Yes	Yes	Yes	No
2	Yes	No	Yes	Yes	No
2	Yes	No	Yes	Yes	No
2	Yes	No	Yes	Yes	No
2	Yes	No	Yes	Yes	No

Pecan Street trained a local electrical contractor to perform the eGauge installations and installations began in July 2022. All eGauge installations underwent a quality control process to check the data reporting from all installed systems and coordinated troubleshooting site visits with households and the local electrical contractor where system installation checks were deemed necessary. Pecan Street's data team also set up server access for project team members to access the data for all Delaware households. A script was written to automate delivery of the previous month's data on the 3rd of each month.

Beginning in the second quarter of 2022 Pecan Street began development of the temperature sensors. Procurement of the Raspberry Pi hardware was delayed due to a shortage of available Raspberry Pi's as a result of supply chain issues. The temperature sensors were designed to allow the homeowners to self-install without having an electrician or other specially trained individual install the device. To obtain information on participant's preferred thermostat settings, comfort bounds for the filed demonstration and other information that the team anticipated may be needed for a successful demonstration Pecan Street created a short questionnaire to share with participants.

Initial test plan: As a draft test plan, Eaton team along with Pecan St And Delaware Electric discussed the following items to be tested:

- End-to-end RF system inter-working between live Yukon network and installed meter-controllers in the field
- Communication and data exchange between central controller and Yukon network
- Inter-connectivity between meter-controllers and load control relays controlling the HVAC and electric water heater
- Selected control use cases in the NREL testbed and volunteer homes

Task 11.0: Stakeholder engagement (Budget Period 2)

In BP2, Eaton team along with partners mainly focused on the use cases that need to be validated and the test plan that will occur in the field trial. Both use cases and test plan were disseminated to the stakeholders in the industry advisory board.

Task 12.0: Lab testing and end-to-end integration testing

IEEE 2030.5 testing: The IEEE 2030.5 protocol specifies the application layer protocol that is used for communication between devices in a smart grid environment. It is designed to enable a variety of use cases, including demand response, energy management, and grid optimization. The protocol provides a standardized interface for exchanging information between different types of devices, such as smart meters, thermostats, and energy management systems. IEEE 2030.5 uses a RESTful (Representational State Transfer) architecture, which is a common approach for building web services. This makes it easy to integrate with existing web technologies and simplifies the development of new applications.
In this project, the team utilized 2030.5 protocol to control behind-the-meter DERs. The team designed and implemented the communication architecture in the past reporting quarters. During this quarter, the team focused on testing the implemented communication architecture. In the NREL testbed, there are 3 homes, each of which comes with a PV inverter. The team connected the inverter with the meter-based controller through a gateway via Wi-Fi. Below are the screenshots that the team successfully conducted the testing. Screenshots cover sending command from the meter controller, the feedback from 2030.5 server, and the inverter curtailing generation according to the command.

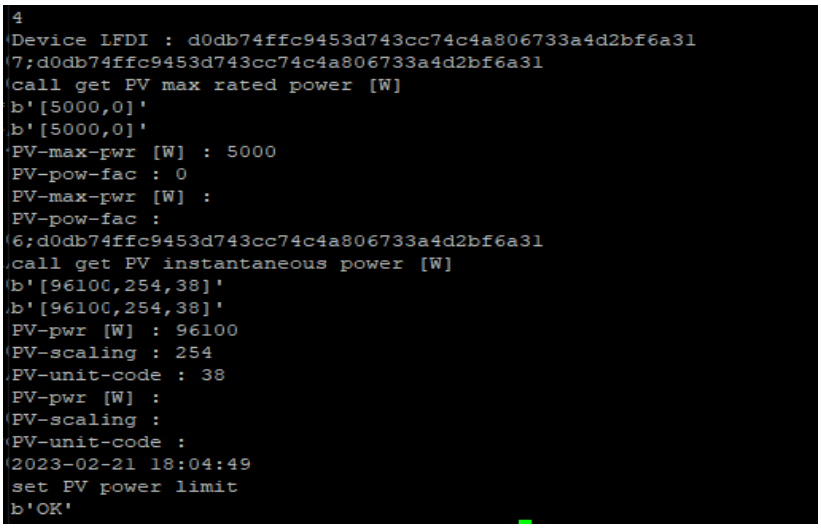

Figure 63. Standalone python script to obtain PV status and setpoint

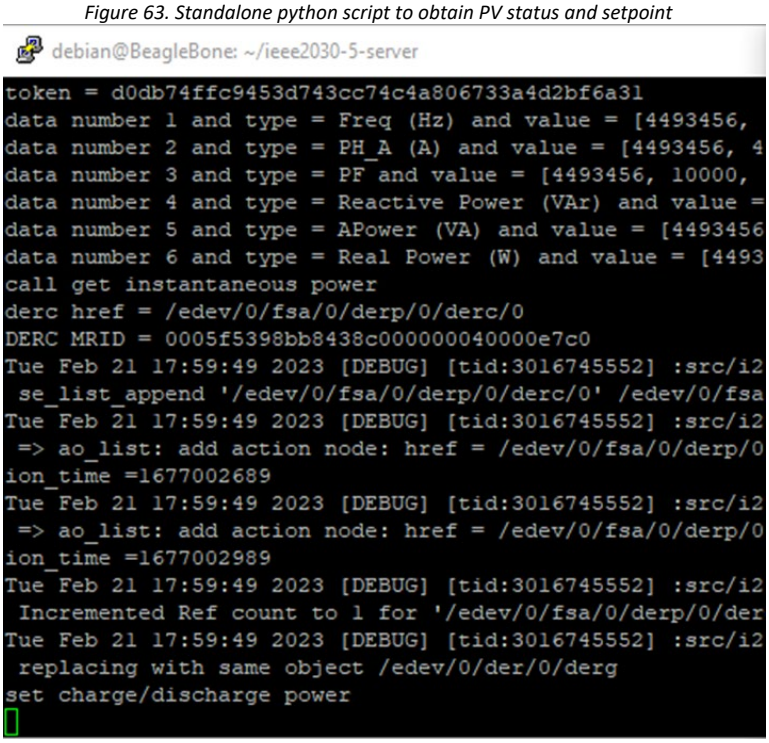

Figure 64. *2030.5 Server to transfer information between meter controller and gateway*

```
Tue Feb 21 18:03:43 2023 [INFO ] [tid:3064951904] : POST https://192.168.8.1:5556/rsps/0/rsp 201 /rsps/0/rsp/0
Tue Feb 21 18:04:49 2023 [INFO ] [tid:3052401760] : GET https://192.168.8.1:5556/edev/0/fsa/0/derp/0/derc/0 200
<DERControl xmlns="urn:ieee:std:2030.5:ns" href="/edev/0/fsa/0/derp/0/derc/0" replyTo="/rsps/0/rsp" responseRequired="07">
  <mRID>05f5398bb8438c000000040000e7c0</mRID>
  <description>charge/discharge power</description>
  <version>1</version>
  <creationTime>1677002389</creationTime>
  <EventStatus>
    <currentStatus>1</currentStatus>
    <dateTime>1677002688</dateTime>
    <potentiallySuperseded>false</potentiallySuperseded>
    <potentiallySupersededTime>0</potentiallySupersededTime>
    <reason>Active</reason>
  </EventStatus>
  <interval>
    <duration>300</duration>
    <start>1677002689</start>
  </interval>
  <randomizeDuration>0</randomizeDuration>
  <randomizeStart>0</randomizeStart>
  <DERControlBase>
    <opModConnect>true</opModConnect>
    <opModMaxLimW>1000</opModMaxLimW>
  </DERControlBase>
</DERControl>

<DERControlResponse xmlns="urn:ieee:std:2030.5:ns">
  <createdDateTime>1677002691</createdDateTime>
  <endDeviceLFDI>d0db74ffc9453d743cc74c4a806733a4d2bf6a31</endDeviceLFDI>
  <status>2</status>
  <subject>05f5398bb8438c000000040000e7c0</subject>
```

Figure 65. 2030.5 Gateway log showing event activated

Figure 66.PV inverter follows the command and curtail PV generation

The final step is to integrate the standalone code with the meter controller firmware and run the control every 5 minutes, with 4-minute curtailment and 1-minute off. The Figure 67 below gives the control curve. The PV simulator originally stay steady around 4kW, then with the control

issued, it reduces generation to given setpoints for 4 minutes and then restore to 4kW for 1 minute.

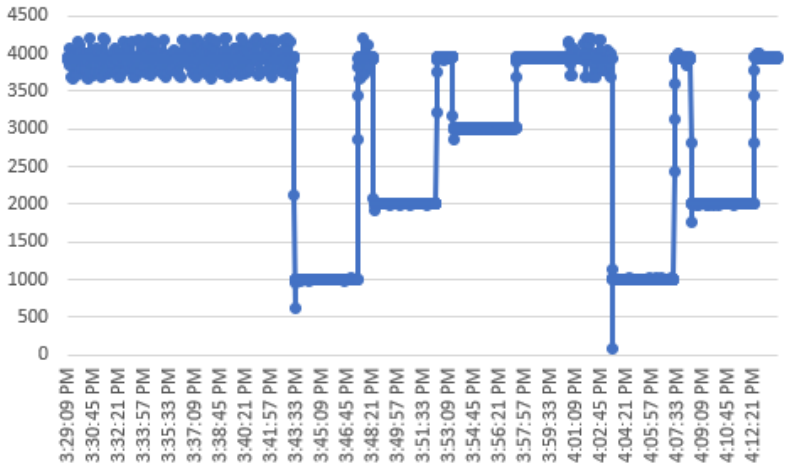

Figure 67. PV control runs with a schedule

Load Control Relay (LCR) Commissioning: In this project, on top of controlling smart home appliances which supports IEEE2030.5 protocols, the smart meter will also control home appliances that have not widely adopted IEEE2030.5 standards, such as the air conditioner (AC) and electrical water heater (EWH). These appliances will follow a schedule that is prepared by the smart meter by considering user comfort bounds, home economic objective, and power curtailment objective. In order to switch on and off the appliances that are non-IEEE2030.5 compliant, controllable Eaton Load-Control-Relays (LCR) are installed between the appliances and their electrical power sources. LCRs communicates to the smart meter via Eaton's proprietary radio frequency (RF) mesh network. In this work, the communication to the LCR is handled by a subroutine called the Node-Controller. The home intelligence is hosted in a separate subroutine called the Premise-Controller which among all intelligence tasks include the preparation of the appliance's schedules. Premise-Controller communicates to the Node-Controller through a local TCP channel within the smart-meter. The communications are mainly divided into two categories: LCR discovery and LCR Command Sending, before conducting the control test.

LCR Control Lab Test

Repeated LCR-OPEN (device off) and LCR-RESET (device on) commands were sent to control the air conditioner (Figure 68) and electric water heater (Figure 69) in a laboratory environment. For AC, the thermostat was set to be controlled at a low temperature to ensure it is always on, so that when LCR-OPEN and LCR-RESET commands are sent, the AC will turn on and off immediately.

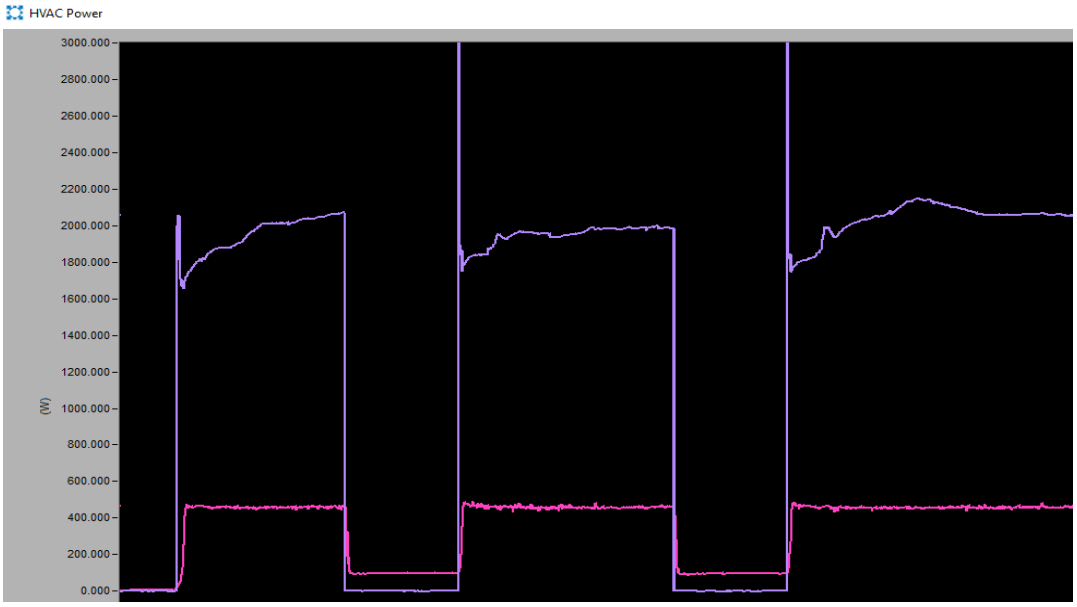

Figure 68. LCR-OPEN and LCR-RESET Commands Test on Air-Conditioner

For EWH, whenever an LCR-OPEN command is sent, the device will turn off immediately as shown in. However, whenever an LCR-RESET command is sent, the device will perform a safety check before turning on. This is because during a prior LCR-OPEN (device off), the power to the EWH was abruptly cut off, therefore the (smart) EWH assumes that there was a power outage. Due to this, the EWH will perform a safety check by sending pulses of power to the heating element while measuring temperatures in the EWH to ensure there is enough water in the tank before the electrical heating element is being turned on, as shown in Figure 69.

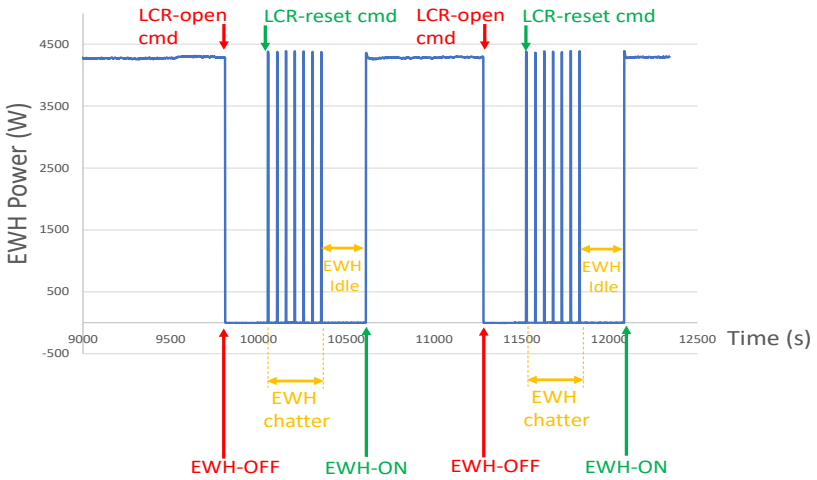

Figure 69. LCR-OPEN and LCR-RESET Commands Test on Air-Conditioner Electric Water Heater

Edge-Firmware Integration

Figure 70 shows the overall diagram of the edge-firmware. The objective of this task is to map out the data exchanges and the coordination of the different functions within the edge-firmware. First, *crontab* within the Linux system is utilized to boot-up the main edge-firmware. Within the main edger-firmware, different functions are then scheduled periodically, at different cadences depending on the needs of every function, using a non-blocking background routine called the *apscheduler*. The tasks within edge-firmware are categorized into three main groups; Edge-Execution, Edge-Databases and Edge-Control Functions.

Edge-Executions contains three main functions; Database-Ops, Signal-Listen and Signal-Send. The objective of the Edge-Executions is to coordinate data flow (listen, write, read, send and format) between multiple edge functions and databases. **Database Ops** receives home-aggregated data from the actual home meter and sends it to the Load-Disaggregation module. **Signal-Listen** listens for messages from three sources; central-control (actual and forecasted weather data), local-LCR and local-2030.5 devices (discovery and acknowledgement messages) via two intermediaries; TCP-Comm (that communicates to both the LCR and central-control) and 2030.5 API (that communicates to 2030.5 devices). Once received, the data will be erased from the buffers within the TCP-Comm and 2030.5 API, which is why they need to be formatted and written in their respective databases, specified by the tags within the messages. **Signal-Send** reads specific data from the different databases, formats and sends them to three sources; central-control (edge data for grid-event planning), local-LCR (LCR commands) and 2030.5 devices (2030.5 devices commands), also through the two intermediaries; TCP-Comm and 2030.5 API, as shown in Figure 70.

Edge-Databases contains historical data (*Home_Database*) to be used by the Edge-Control function and to be sent to Central-Control, temporary storages (*GridEvent_Pseudo*, *GridEvent_PwrThr*, *DERs_Flexbounds*) for data coordinations between different functions and storage for reference DERs schedules (*Schedule_PowerRef*, *Schedule_StateRef*) from the Edge-Control to Signal-Send.

Edge-Control Functions contains two main functions: Load Disaggregation (LD) and Edge-Control. **Load Disaggregation** module receives aggregated load profile from the meter at specific time-intervals and utilizes classifications and machine learning algorithms to disaggregate it into individual DER load profiles, which are then stored in *Home_Database* for Edge-Control. Within the **Edge-Control** module, there are several submodules that perform separate tasks depending on the daily scenarios; either a day without a grid-event, or a day with a grid-event. During a day without grid-event, the Edge-Control perform DERs models calibrations and scheduled the DERs operations with the objective to minimize the electricity cost for homeowners. During a day with grid-event, the Edge-Control perform DERs models calibrations, DERs Flexibility Bounds calculations (which is sent to the central-control), Pseudo-Price conversion and DERs Scheduling by considering additional constraints for the grid-event. Note that the scheduling are done in a day-ahead manner which provides the operating-points references for the DERs.

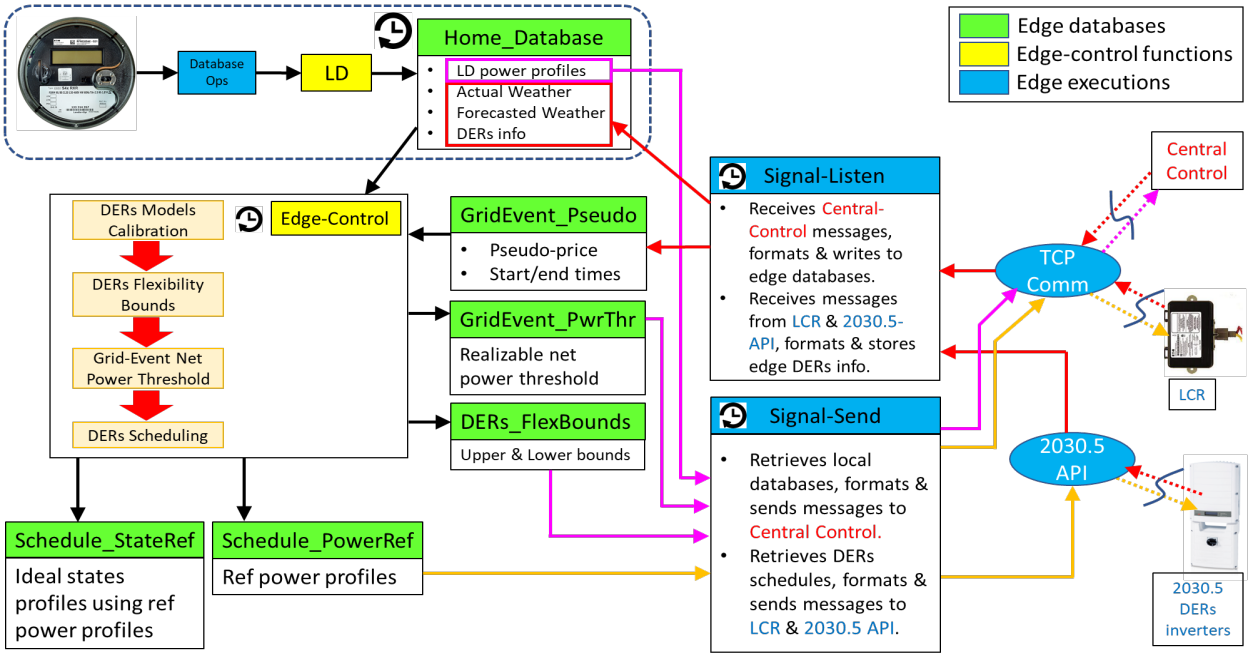

Figure 70. Edge-Controller Firmware Diagram

Premise-Controller Validation in Meter Controller: Premise controller validation involves testing the logics to executes three main events that is programmed to be handle by the smart meter, which are the Idle, Grid-Event mode and Coincidental-Peak modes, shown in Figure 71. These events are governed by the event message received (or not) from the Central-Controller. When an event information is received by the Premise-Controller from Central-Controller, it will store the event information in the meter, which includes the start/end time of the event and the pseudo-price. In the meter, two subroutines are executed every two hours and at every 10PM to check this event information. During the two-hours check, if (1) the start/end time of the event is on the same day, (2) the event start-time is within 2 hours lookahead from current-time and (3) the event start-time is before 8PM on current day, then a Coincidental-Peak event is assumed and all routines related to preparing the home end-devices schedule will be executed (mainly are future states forecast, DERs flexibility bound calculation, Optimal DERs/DR scheduling, as discussed in previous reports). If the event start/end time occurs the next day, the controller will not execute anything. However, at 10PM the same day, it will perform the same check for either Day-Ahead Grid-Event mode or Idle mode. If there is an event message from Central-Controller with a start/end time on the next day, a Day-Ahead Grid-Event is assumed and again all routines related to preparing the home end-devices schedule for the a Grid-Event for the next day will be executed. If at 10PM there are no messages from the central controller, then a next-day Idle mode end-devices schedule will be prepared. The logics were tested in the smart-meter and it was able to produce the end-devices schedules in preparation for the said events.

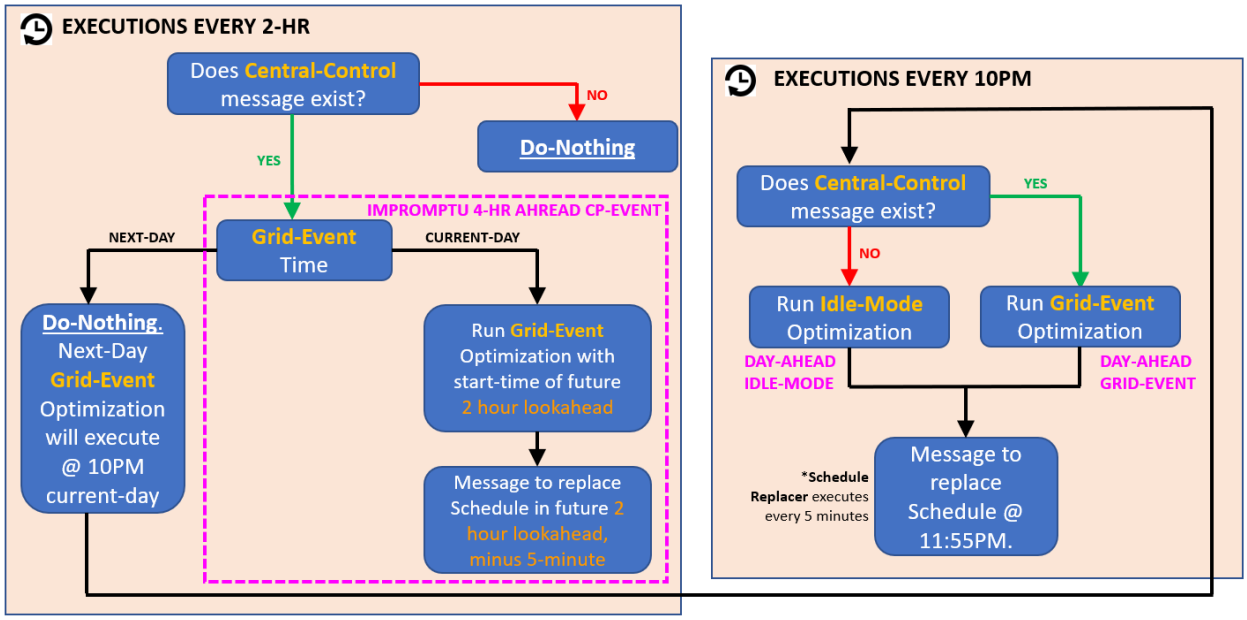

Figure 71. Premise-Controller Logics for Grid-Event, Idle-Mode and Coincidental-Peak Implementations

Central Controller Integration: This task involved the integration of different modules of the central controller. The components which were previously developed and tested individually are brought together to work as a single entity. The different modules include data storage, data aggregation, day-ahead forecasting, forecasting error, weather API, feeder level information, data sorting, file creation, scheduler, and central controller algorithm. The incoming data from controlled homes (disaggregated power profiles, DER flexibility bounds) and the nodal level information which provides an insight into the net nodal level load values are accepted and stored in the central controller database. The data aggregation module combines the values from individual homes to get the nodal level values. The generated nodal level uncontrolled load values are used by the forecast module to generate the day-ahead forecast and the forecast errors for a month prior to the forecast day.

The weather API captures the weather information in a day-ahead time horizon and pulls the actual weather information of the location every 2 hours. All these information is stored in the central controller database. SQLite3 is used as the database system for the central controller. The feeder level information includes the admittance matrix and load sizes and is stored as csv files. The next step in the process includes data sorting and file creation. All the required data for the central controller are queried from the database tables and are saved as csv files in the specified location of the central controller algorithm. The central controller utilizes this information and generates the pseudo price for the grid events. This pseudo price is stored back in the database and send to the controlled homes to optimize the DERs and DRs according to the requirement. The final piece in the central controller architecture is the scheduler, which is developed using APScheduler package, to schedule all the modules according to the design. The central controller architecture overview is given in the Figure 72.

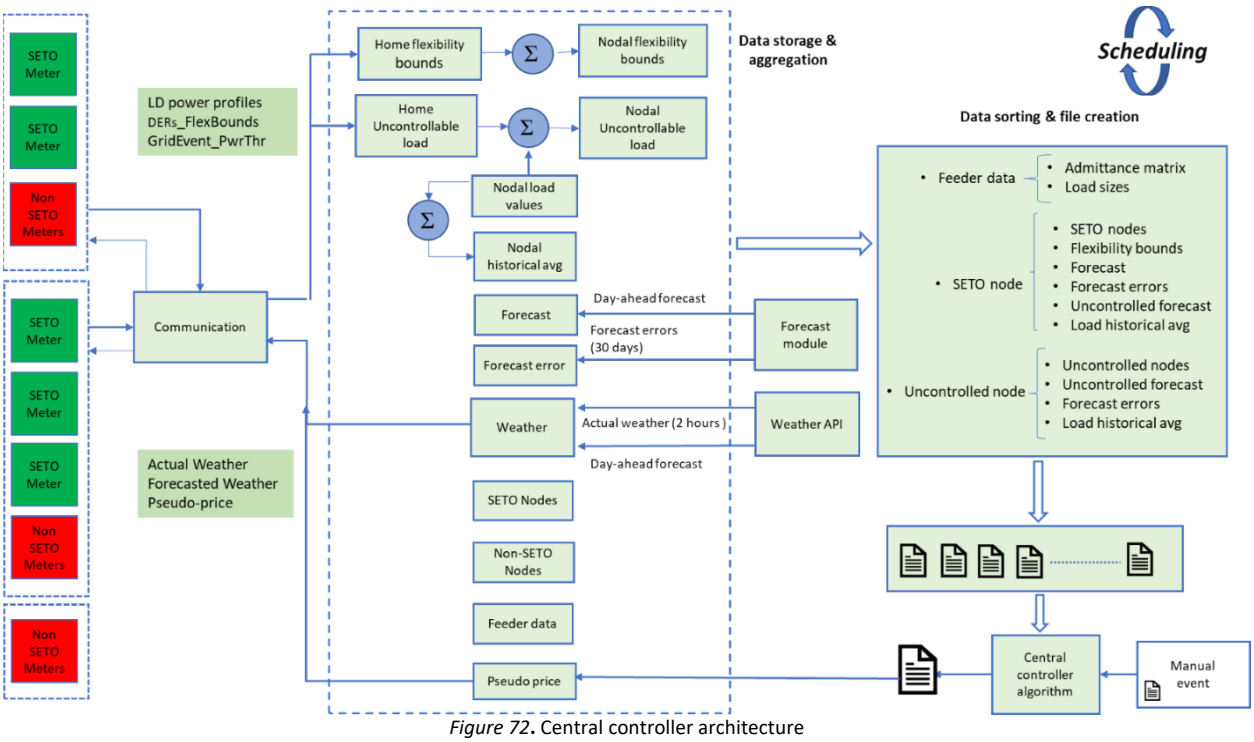

Figure 72. Central controller architecture

Lab Validation: Day-long (24 hour) tests were conducted in NREL's Systems Performance Lab (SPL) to validate the performance of the edge controls strategies and to validate the overall integration of the various hardware and software components on the edge in a laboratory setup. Tests were conducted on a home with controllable Air Conditioner (AC) and Electric Water Heater (EWH) for different scenarios, as shown in Figure 73 and Figure 74. In Figure 73, first a Baseline scenario is tested which mimics how an actual home operates and is based on a home in Austin Texas. Then, a Controlled Grid-Event scenario where the controlled appliances were optimized for a Grid Event between 6PM to 8PM, and a high Time-of-Use pricing for Austin TX between 3PM to 6PM. Test results as summarized in Table 15 shows a 20.4% and 22% savings of energy and cost respectively for the home. It also shows indoor temperature was kept 100% within the desired bounds during the Grid-Event between 6PM-8PM. The indoor temperature was mainly kept within the bounds 99% of the time throughout the whole day. A minor temperature violation occurs at less than 0.2°C temperature difference near the upper-bound at 12:30PM, which is attributed to a communication issue with the LCR that controls the AC during those times. The controlled Grid-Event scenario also achieved 30% reduction of power compared to the Baseline. Hence, the proposed controlled strategy was able to maintain the Quality-of-Service (QoS) while minimizing the cost and energy usage for home and reducing the peak power for the home during the Grid-Event.

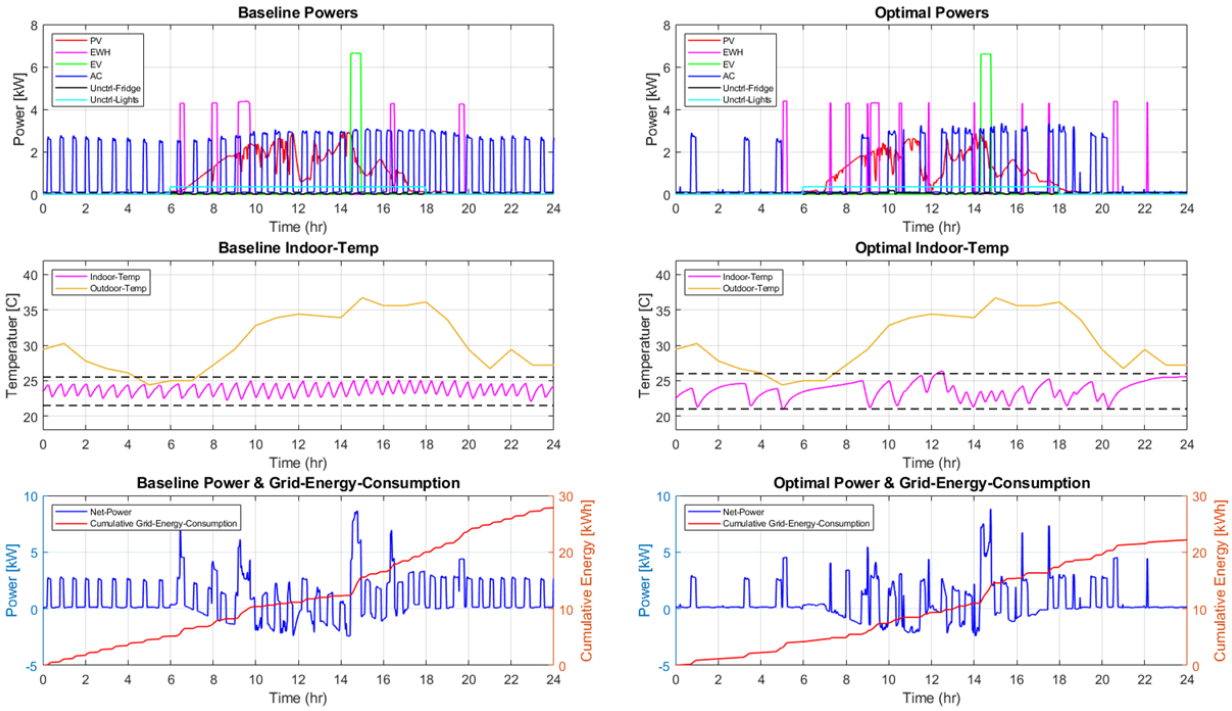

Figure 73. Results for Baseline versus Controlled Grid-Event Scenarios Full-Day Lab Test

Table 15. Performance Metrics for Baseline versus Controlled Grid-Event Scenarios

	Baseline	Optimal	Notes
Energy Import From Grid [kWh]	27.9kWh	22.2kWh	20.4% savings
Energy Cost [$]	$1.00	$0.78	22% savings
Demand during Grid-Event [6-8PM] [kW]	4.4kW	3.1kW	30% reduction
Indoor Temp QoS [%]	100% (no DR)	99%	Violation @ upper bound by < 0.2 °C
Indoor-Temp QoS during Grid-Event [%]	100%	100%	
AC Energy Consumption [kWh]	25.1kWh	16.2kWh	35.5% savings
EWH Energy Consumption [kWh]	6.4kWh	6.2kWh	3.1% savings
Percentage of Following AC Commands	N/A	90.6%	
Percentage of Following EWH Commands	N/A	74.0%	

In Figure 74, the same Baseline scenario as before is shown and compared with an Controlled-Idle scenario where the controlled appliances were optimized for a high Time-of-Use pricing for Austin TX between 3PM to 6PM. Test results as summarized in Table 16shows a 16.1% and 20% savings of energy and cost respectively for the home. The indoor temperature was mainly kept within the bounds 99% of the time throughout the whole day. A minor temperature violation occurs at less than 0.3°C temperature difference near the lower bound at 5:45AM and 9AM, which is attributed to a communication issue with the LCR that controls the AC during those times. Hence, the proposed controlled strategy was able to maintain the Quality-of-Service (QoS) while minimizing the cost and energy usage for the home.

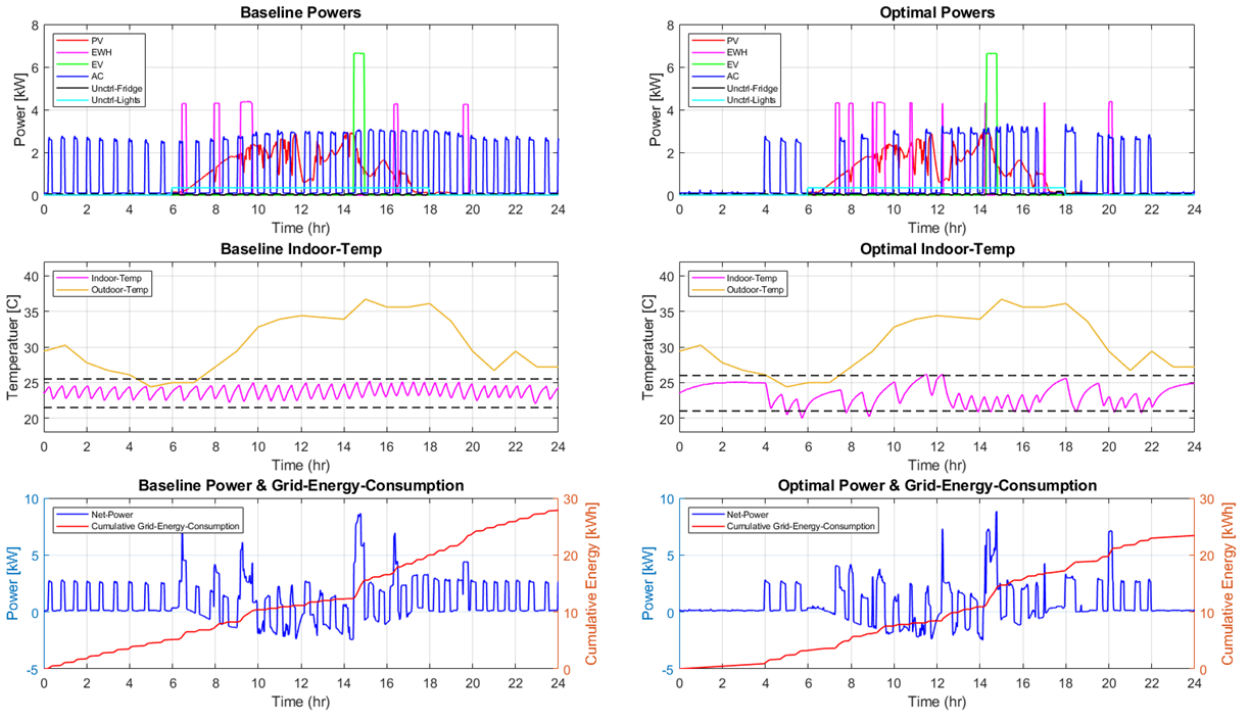

Figure 74. Results for Baseline versus Controlled-Idle Scenarios Full-Day Lab Test

Table 16. Performance Metrics for Baseline versus Controlled-Idle Scenarios

	Baseline	Optimal	Notes
Energy Import From Grid [kWh]	27.9kWh	23.4kWh	16.1% savings
Energy Cost [$]	$1.00	$0.80	20% savings
Indoor Temp QoS [%]	100% (no DR)	99%	Violation @ lower bound by = 0.3 °C
AC Energy Consumption [kWh]	25.1kWh	18.5kWh	26.3% savings
EWH Energy Consumption [kWh]	6.4kWh	5.5kWh	14% savings
Percentage of Following AC Commands	N/A	85.4%	
Percentage of Following EWH Commands	N/A	70.8%	

Electric Water Heater (EWH) Validation

The EWH was controlled based on the strategy to avoid having low hot water temperature in the tank for the homeowners, as have been discussed in previous reports. In the lab test, temperatures at different locations on the EWH tank and the water outlet were measured for the test scenarios discussed above and are shown in Figure 75 and Figure 76. As expected, the average hot water temperature within the EWH tank for the controlled cases were within 3°C of the baseline case with the same water usage, therefore avoiding “cold-showers” for the homeowners.

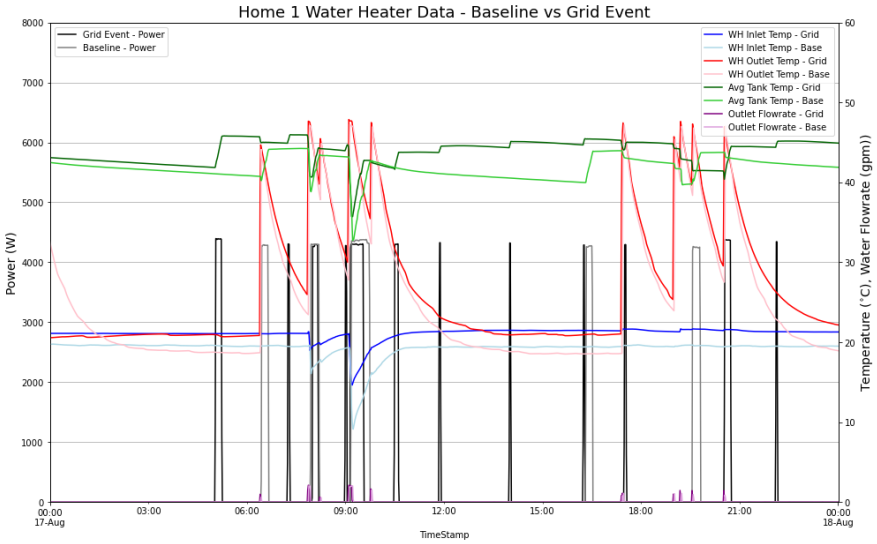

Figure 75. EWH Temperatures & Tank Outlet Flow Rates for Baseline and Grid-Event Scenarios

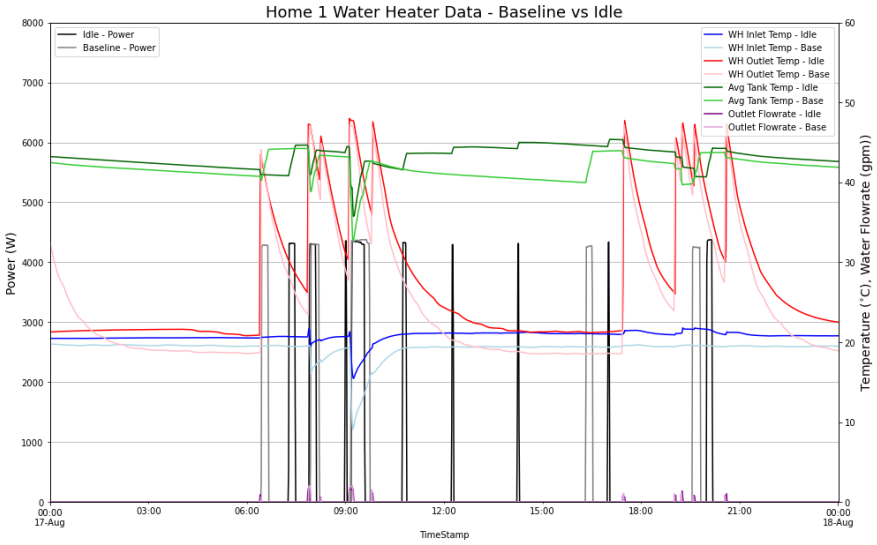

Figure 76. EWH Temperatures & Tank Outlet Flow Rates for Baseline and Idle Scenarios

Based on the temperatures at different locations of the water heater, the power (and energy) consumptions and the mass-flow of hot water measured in the lab, the EWH model as defined in Task 2 is calibrated. First, 18 instances of hot-water usage were identified from the data, similar to the instances shown in Figure 86-87. The estimated mass of hot-water usage using EWH power usage is calculated and the RMSE are calculated against the actual measured mass of hot-water for these 18 instances as shown in Figure 88. The parameter $\Delta T = T_u - T_l$ is the temperatures difference between the two theoretical upper and lower masses of tank volumes in the two-mass model defined in Task 2. Since this method assumes homogenous temperatures in each upper and lower volume of the tank, the temperature measured at specific locations in the tank may not represent the model accurately because the volume separation location is unknown in a real tank. Therefore, the RMSE from the 18 instances of hot water usage are plotted and ΔT = 15.7 °C with lowest RMSE is selected as the best fit for the EWH model. Using a fixed ΔT = 15.7 °C, the mass of hot-water are estimated for all

18 instances as shown in Figure 89. The result shows good correlation between in all 18 instances when EWH was in use, with an RMSE of 11.4 lbs.

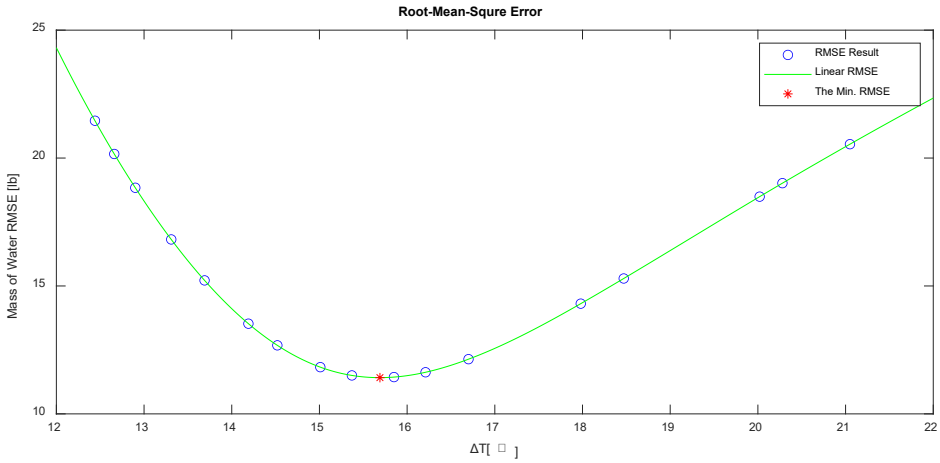

Figure 88. RMSE between Estimated and Actual Mass of Hot-Water in EWH Calibration Process

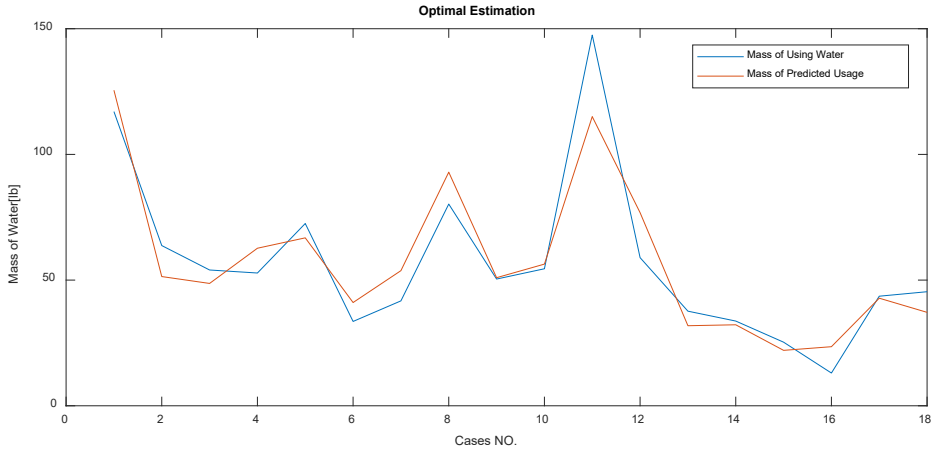

Figure 89. Mass of Hot-Water Usage Comparison with Optimal ΔT

Lab Test Results for Central Controller: One of the main functionalities of the central controller is to monitor the service status and device availability from the multiple test homes in the system. This functionality provides the utility user with an overall system overview at a device level. The premise controller runs three services to control the end devices, premise controller, node controller, and 2030.5 services and an additional service for monitoring. The monitoring service records the status of the other three services at an hourly resolution in the edge database. The recorded service status for a test home in the NREL test bed is given in Figure 77, Figure 78, and Figure 79. The figures depict the availability of the services for the whole test duration.

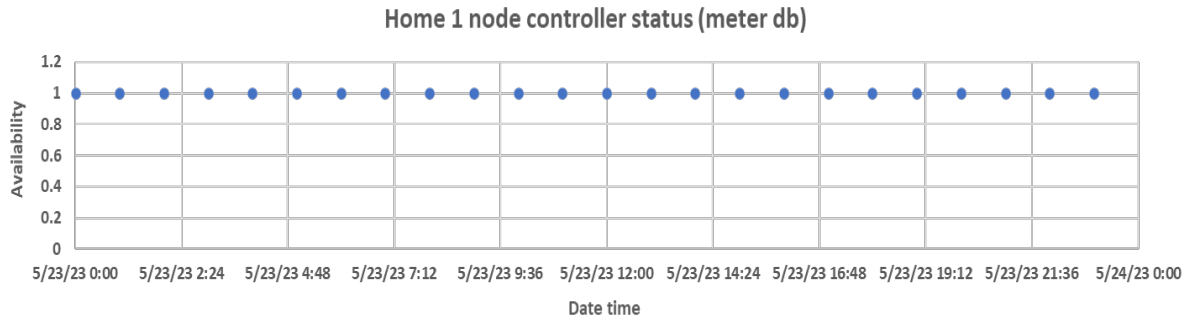

Figure 77. Edge premise controller service status for the test day

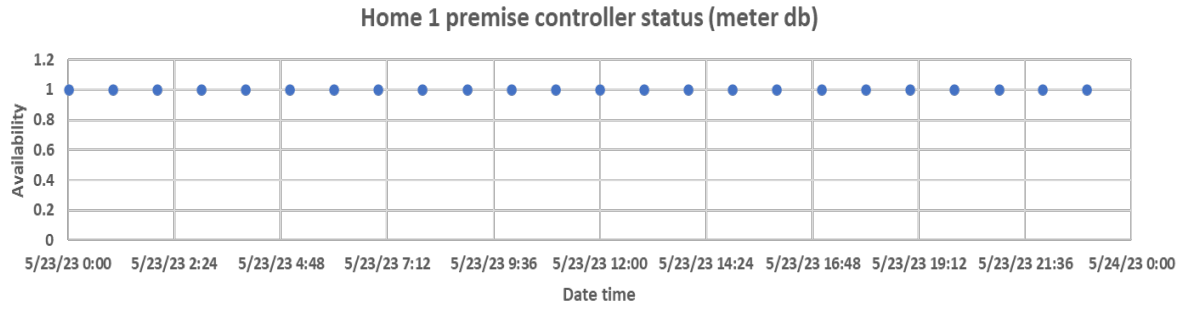

Figure 78. Edge node controller service status for the test day

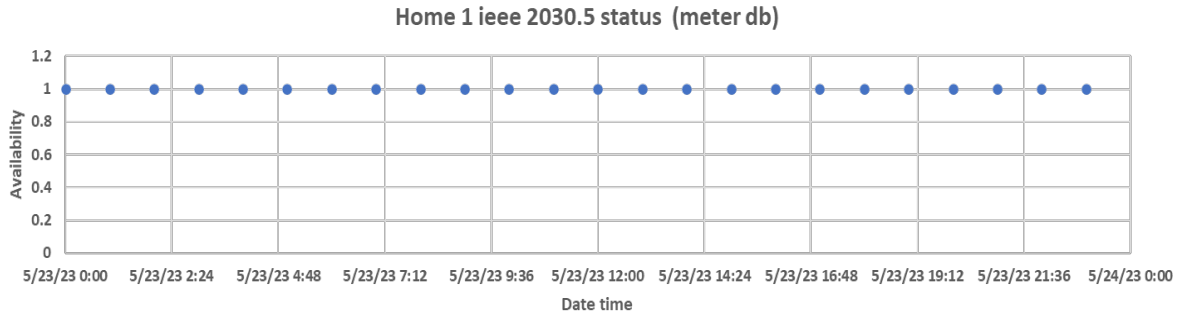

Figure 79. 2030.5 service status for the test day

The premise controller also records the availability of the edge devices (PV, battery) and LCRs (AC, EWH) at a 15-minute resolution in the edge database. The premise will send out the service status along with the device and LCR availability once it receives the statistics request from the central controller. The received PV, battery, LCR availability at the central controller are shown in Figure 80,Figure 81, and Figure 82.

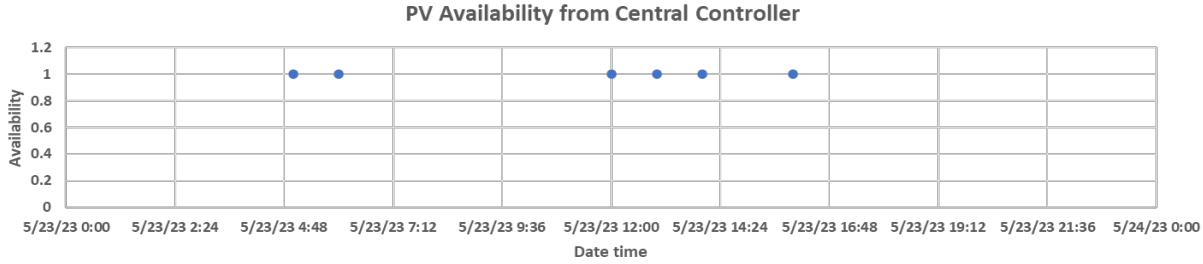

Figure 80. PV availability status for a home received at the central controller

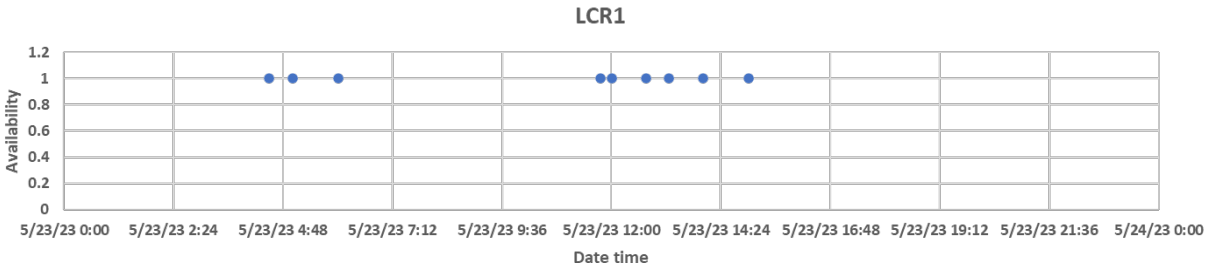

Figure 81. LCR availability status for a home received at the central controller

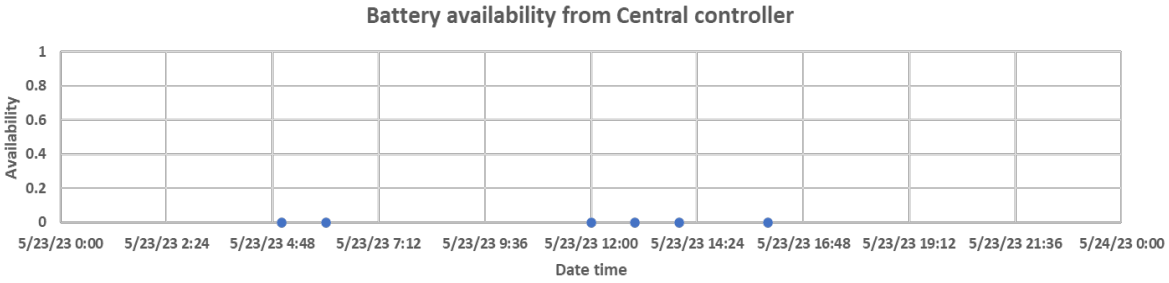

Figure 82. Battery availability status received at the central controller

Task 13.0: Field deployment and demonstration

LCR, GW, and Meter-as-a-controller installation: In the second quarter of 2023 Pecan Street began preparing participants for the field demonstration by sharing more information about the full suite of devices that would be installed at their home and what to expect during the installation. It was at this time that some participants became concerned about a third party controlling their air conditioner and a couple opted out of receiving the LCR. As participants expressed comfort in the full field demonstration, Pecan Street shipped temperature sensors to households for self-installation. A dashboard was developed for the team to internally monitor temperature sensors to confirm when the device was successfully installed by the participant and make sure they remain online with accurate temperature readings reporting in.

Data Id	Mac	Temp_f	Temp_c
1391	562e	71.9	22.2
3540	6c3a	64.8	18.2
4553	5604	69.7	20.9
5763	f8a9	74.0	23.3
5791	5e4e	70.7	21.5
6721	6c56	70.9	21.6
9282	3641	72.2	22.3
10250	6782	70.5	21.3
10496	5a38	68.9	20.5

In the months leading up to the LCR and Gateway installations the Pecan Street team answered questions and hosted zoom meetings with residents to answer questions and prepare them for installation and the field demonstration tests.
LCR and Gateway installations commenced the last week of June 2023. In total Pecan Street was able to coordinate field deployment of load control relays and/or gateways in 12 participating households. Of the 12 houses installed, 10 received the full LCR and gateway kit, 2 received gateways only (because the digital controls on their heat pumps were not compatible with LCR), and 2 received LCR only (because they didn't have solar or had a non-Fronius inverter). The 10 remaining participants were not able to be installed for a variety of reasons, including but not limited to: declining to participate, refusing installation of the DEC meter installation due to minor construction, HVAC issues that couldn't be resolved before the firmware upgrade visit, and inability to align schedules with the installer prior to the teams visit to perform firmware upgrades on the system.

LCR and Solar PV Discoveries through IEEE 2030.5: Within the edge-controller, there are discovery functions to check the availabilities of all LCR and 2030.5 appliances that are communicating to the meter-controller. As previously explained for LCR devices, this is done through broadcasted messages from LCRs to the meter-controller. Once meter-controller receives the broadcast message, it will save the LCR information containing the LCR Device-ID, Device-Type and Device-Availability in a database file ("LCR_IDs.csv"), as shown in Figure 83. Additionally, the LCR information are also passed and stored in the main database ("setoDB.db") as shown in Figure 83. During field commissioning, after the meter-firmware is executed, both "LCR_IDs.csv" and "setoDB.db" will be updated if communication is established. Then, these files were downloaded and checked to ensure the LCR devices are discoverable and available (Availability = 1), as shown in Figure 83.

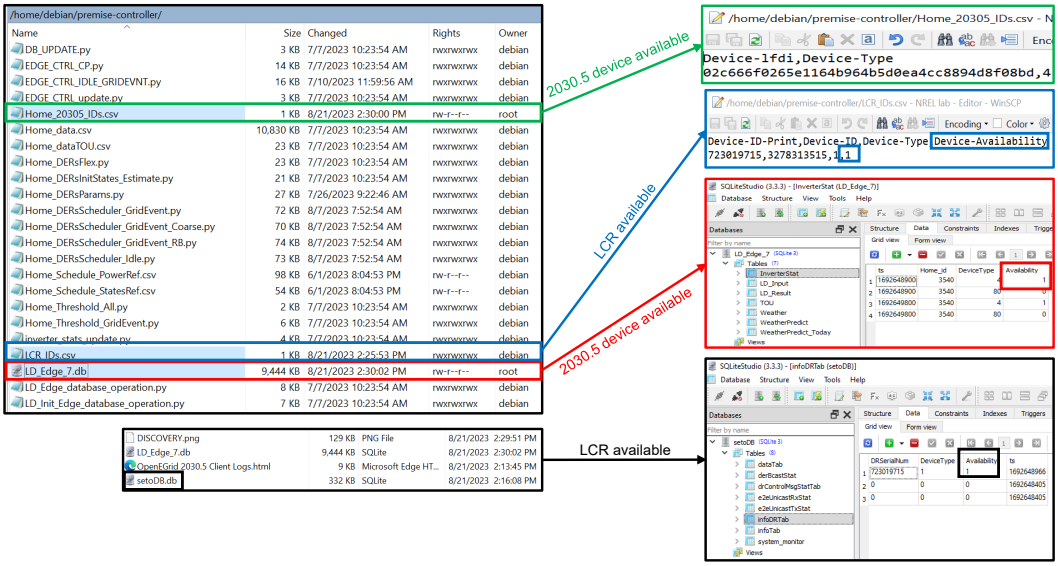

Figure 83. LCR Discovery and 2030.5 Discovery Files Generated in Edge-Controller

Similarly for 2030.5 devices, after the meter-controller is executed, the meter-controller will send a status request to the 2030.5 gateway. If communication is established, the response from the 2030.5 gateway to meter-controller will contain the PV-inverter power-rating and the DER-type (PV-Inverter's DER-type = 4, based on 2030.5 standard). Theses information are stored in two databases in the meter-controller ("Home_20305_IDs.csv" and "LD_Edge_7.db") as shown in Figure 83. As another layer of checking, the 2030.5 gateway can also be accessed to review its event-logs during the status-request and status-response.

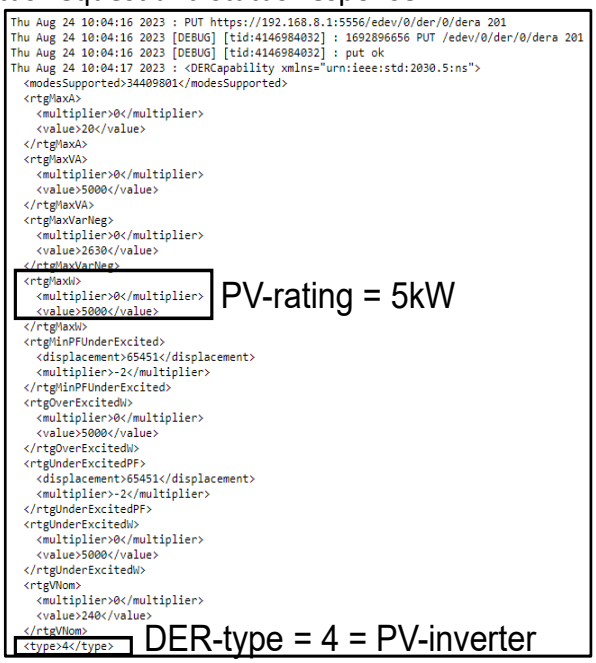

Figure 84.2030.5 Gateway's Event-Log Showing Discoverable PV-Inverter

As shown in
Figure 84, the status-responses from the home's PV-inverter contains the PV-rating of 5kW and DER-type equals of 4. This shows the communication is established between the meter-controller and the 2030.5 PV-Inverter.

Edge to central communication- interconnectivity testing: The central-edge interconnectivity checklist used in the field is given in the table below. The table lists the home ID, the status of the unicast request to the home right after service activation to test the central-edge communication, the response from the device for the unicast request, message reception at the central controller (flexibility bounds, net home load, and controllable home load) and finally the date when we activated the services in the home.

Table 17 Central – Edge communication checklist for the DEC field test

Home ID	Unicast send	Stats Response	Flex bounds	Net home load	Controllable home load	Activation Date

7988	Yes	Yes	✗	✓	✗	21-Aug
3540	Yes	Yes	✓	✓	✓	21-Aug
6568	Yes	Yes	✓	✓	✓	22-Aug
5334	Yes	Yes	✓	✓	✓	22-Aug
4553	Yes	Yes	✓	✓	✓	23-Aug
11410	Yes	Yes	✓	✓	✓	23-Aug
6721	Yes	Yes	✓	✓	✓	23-Aug
9282	Yes	Yes	✓	✓	✓	23-Aug
10250	Yes	Yes	✓	✓	✓	23-Aug
10867	Yes	Yes	✓	✓	✓	24-Aug
7808	Yes	Yes	✓	✓	✓	24-Aug

The central controller sends a status request to all the SETO homes at an hourly resolution and homes as soon they receive the request, will respond back with the control and availability metrics. Figure 85 represents the PV availability in one of the test homes remotely received at the central controller during the field demonstration period. Here, 1 means the PV inverter is available and 0 represents its unavailability. The missing values for a day on Sept 6 were due to a communication disruption caused by Yukon system overload. The availability of LCRs for control in the home 3540 is given in Figure 86. The meter runs 3 services to control and coordinate its activities, and an additional service to monitor the status of the 3 main services. The status of the three services: node controller, premise controller, and the IEEE 2030.5 server are given in Figures
Figure 87 to Figure 89, respectively. The meter also provides the system computing performance to the central controller which is given in Figure 90. Through the completion of this task, we have demonstrated the remote monitoring capabilities of the central controller to send and receive status information from the edge devices on a regular basis.

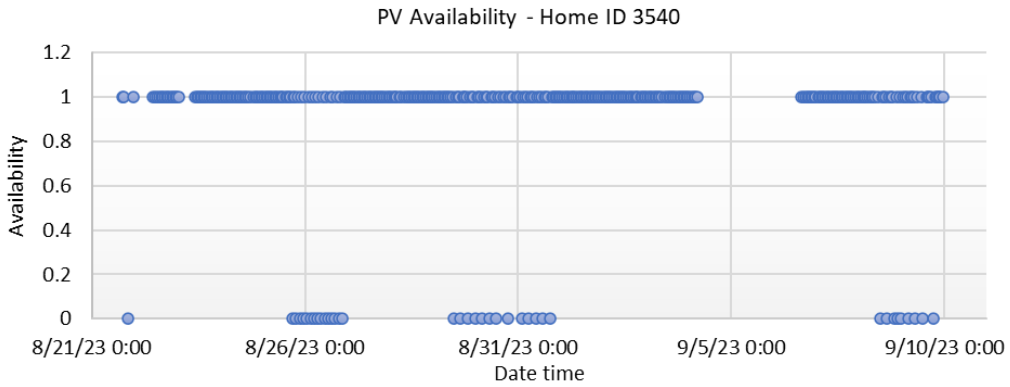

Figure 85.The status PV Inverter received at the central controller from home 3540.

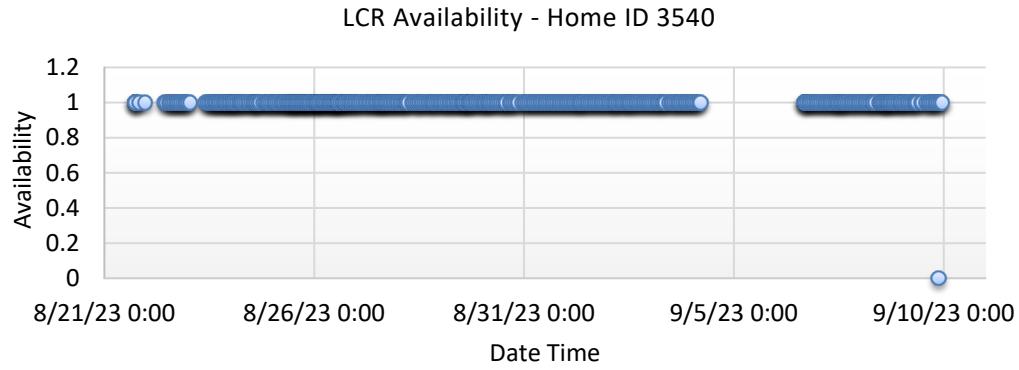

Figure 86.The availability of LCR for control received at the central controller from the 3540.

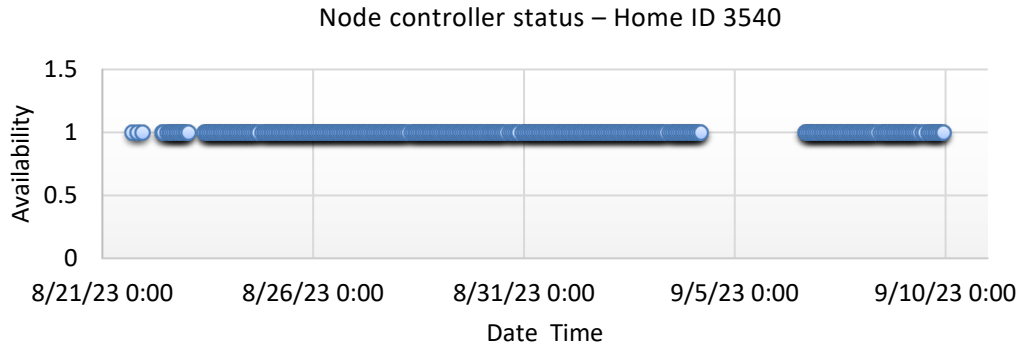

Figure 87. The status of the node controller received at the central controller from the home 3540

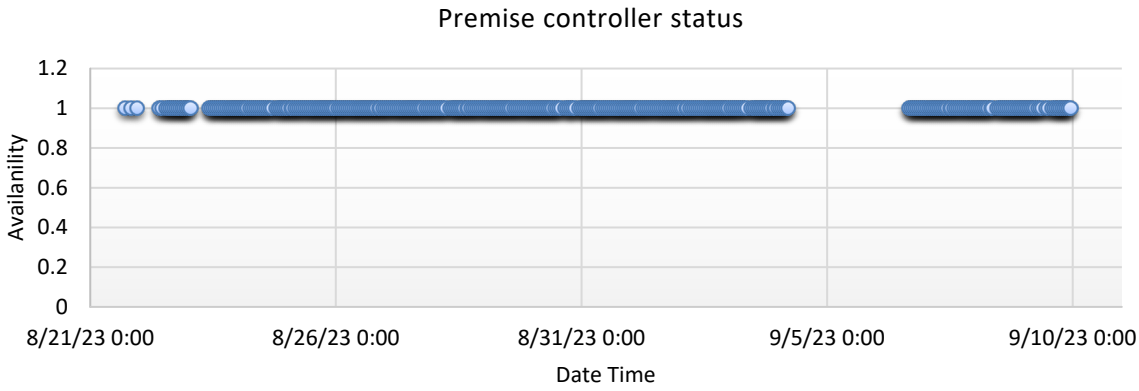

Figure 88. The status of the premise controller received at the central controller from the home 3540

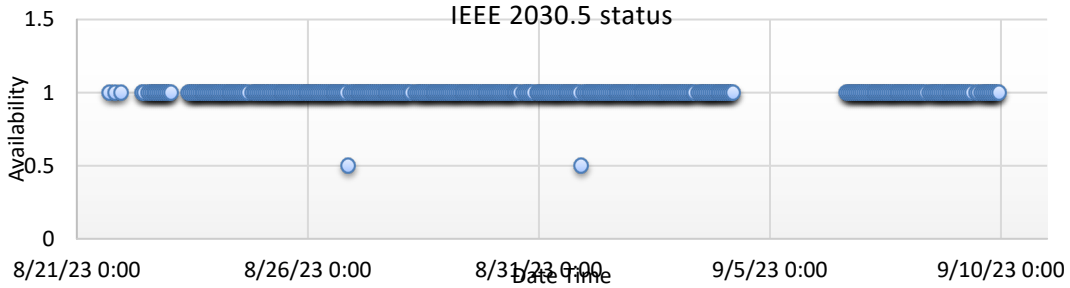

Figure 89. The status of the IEEE 2030.5 server received at the central controller from the home 3540

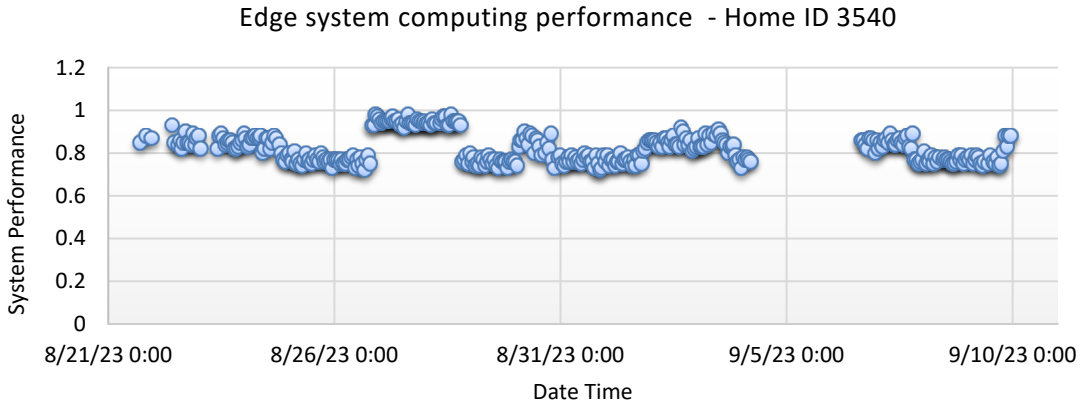

Figure 90. The edge system computing performance received at the central controller from the home 3540

In addition to system performance metrics and status updates, the meter also sends load information to the central controller at regular intervals. The net home load and net controllable load values from the home 3540 received at the central controller are given in Figure 91. The available load for control from the home is calculated from individual device level values which was generated using load disaggregation. We have demonstrated the ability to provide controllable portion of the home load to the utility without installing any additional sensors in the home to record appliance level values.

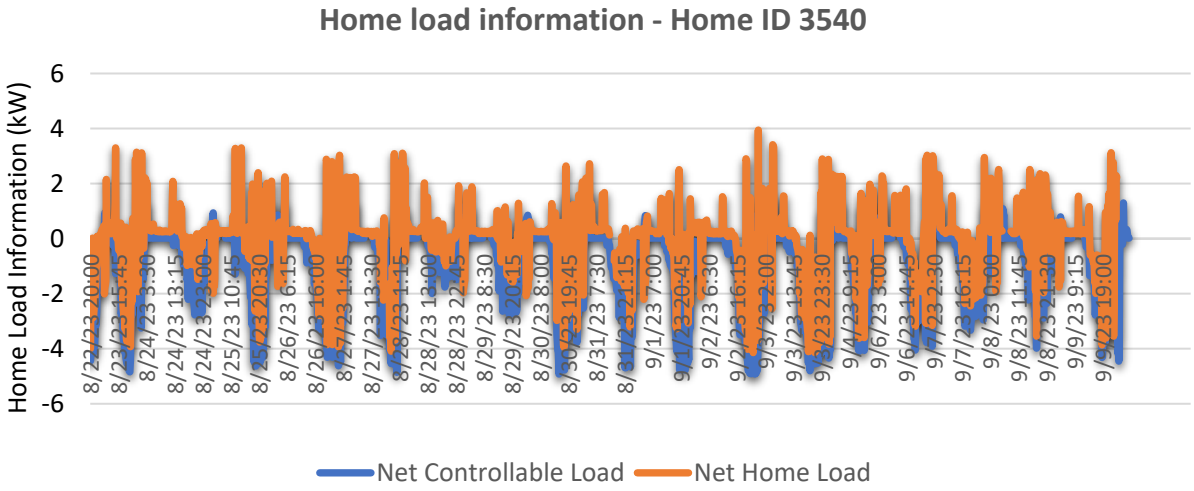

Figure 91. Net controllable and net home load received from the home 3540 at the central controller

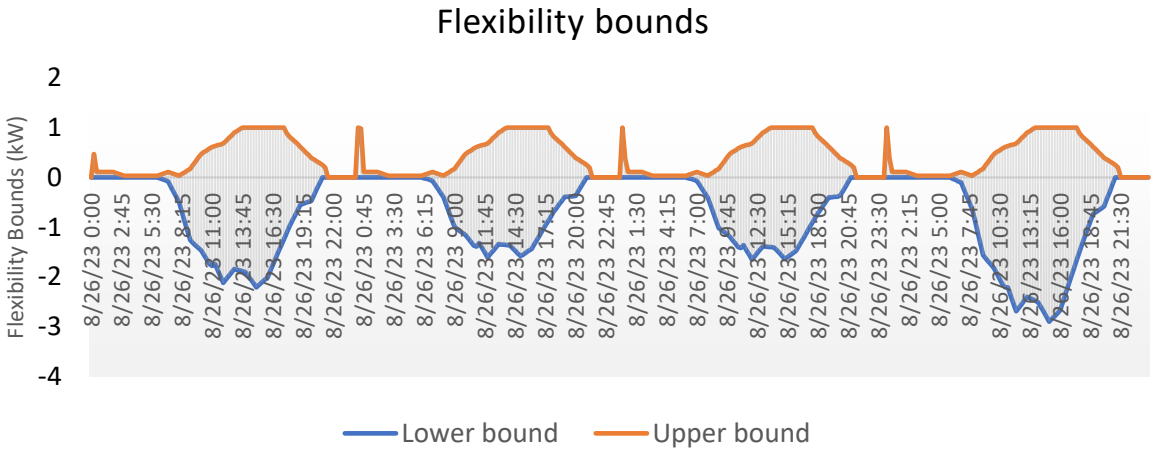

Figure 92. Flexibility bounds received from the homes (9282, 6568, 4553, 7808) on Aug 26th

The meter also sends upper and lower bound flexibility to the central controller, which will provide the utility with the net operating region (power) for appliances (AC, PV) that maintains customer QoS (Quality of Service). An example of the values is given in Figure 92.

Scalability analysis

The SETO control system is architected and executed using a hierarchical communications model. The system is comprised of various elements; the *DR+DER Central Controller, the AMI Yukon service* which provides the entry point into the AMI RF Mesh network. Both services are hosted on either cloud or on-premises compute resources and interact via an IP communication network. RF Gateway appliances are downstream from Yukon and provide a bridge to AMI Field Area Network segments. Yukon and Gateway interface via wired or cellular IP backhaul. Various Endpoint devices including the SETO meter-controller form the RF mesh and operates at data rates between 9.6 - 153.6 Kbps.

Referring the hierarchical structure of the SETO system, as the *meter-controller* can manage the *DR* and *DER* assets at the premise and given the fact that the central controller and Yukon service can readily scale though the addition of server capacity, the scalability of the SETO system is principally limited by the communications bandwidth within the RF Mesh Network.

Table 18: Daily AMI Meter Data Exchange Volume

	Residential Meter	C&I Meter
Interval Data (bytes/day)	3210	9216
Statistics (bytes/day)	3072	3072
Network Data (bytes/day)	2048	2048
Total (bytes/day)	**8330**	**14336**

Table 19: Daily SETO Meter Data Exchange Volume

	Daily Occurrence	Size (bytes)	Daily Total (bytes)
DER Flexibility Bounds Lo	1	710	710
DER Flexibility Bounds Hi	1	760	760
Edge Level Threshold	1	180	180
Net Controllable Load	4	380	1520
Net Home Load	4	380	1520
Edge Level Statistics	24	1000	24000
Weather Actual Data	12	450	5400
Weather Forecast Data	1	1000	1000
Weather Current Day Data	1	1000	1000
Pseudo Price Data	1	100	100
Statistics Requests	24	200	4800
Total (bytes per day)			**40990**

Considering the broad categories of AMI data including interval and billing data, statistics, and network information, the typical AMI residential and commercial meters generate and transfer approximately 8330 and 14,336 bytes daily respectively (See Table 18). Comparatively, ignoring the one-time Discovery messages, a SETO device exchanges approximately 40,990 bytes daily (See Table 19). This represents a 5 and 3 time multiple to that of a typical residential and commercial meter respectively and therefore imposes a heavy burden on the RF AMI network. Such a demand profile may be addressed in the RF Mesh network through the addition/creation of RF gateway appliances and gateway segments to increase bandwidth capacity. Here each gateway segment will support a lesser number of devices to offset the increase in individual device bandwidth. As an example, consider a 10,000 RF AMI meter system. A typical gateway segment will ideally contain 2000 endpoints comprised of 200 C&I meters and 1800 residential meters. The current RF AMI system would require 5 gateways. Substituting residential meters with SETO units would result in a need of 25 RF gateways with each gateway segment consisting of approximately 360 SETO units (See Table 20).

Table 20: Comparison of Standard and SETO RF AMI System

	Standard AMI	SETO AMI
System Size	10000	10000
Gateway Segment Size	2000	500
Residential AMI Meter Count	1800	360 (SETO)
C&I AMI Meter Count	200	40 (Standard)
Number of Gateways	5	25

An alternative approach involves adjusting the frequency of central to edge communications, such as the *Edge Level Statistics* and *Statistics Requests* parameters to a single daily exchange. The resultant required daily bandwidth would reduce to below that of the typical C&I meter. Further reductions of the SETO meter-controller required data capacity is achievable if the message format of the central to edge exchanges utilized binary data formats rather than text-based JSON messages. Lastly, the use of the RF AMI network's broadcast facility to distribute weather information will improve the efficiency of data transmission. The required daily bandwidth would approach levels typical of an AMI residential meter.

To summarize, it is possible to scale the SETO system in the RF Mesh AMI network. The current system as implemented and configured would require a higher number of gateway segments than typical but may be mitigated at some level through reconfiguration of the SETO services. Implementation of a more efficient message data format would allow the SETO system to scale seamlessly within the existing RF AMI Mesh Network. Figure 93 below shows an example of end-to-end deployment of SETO system.

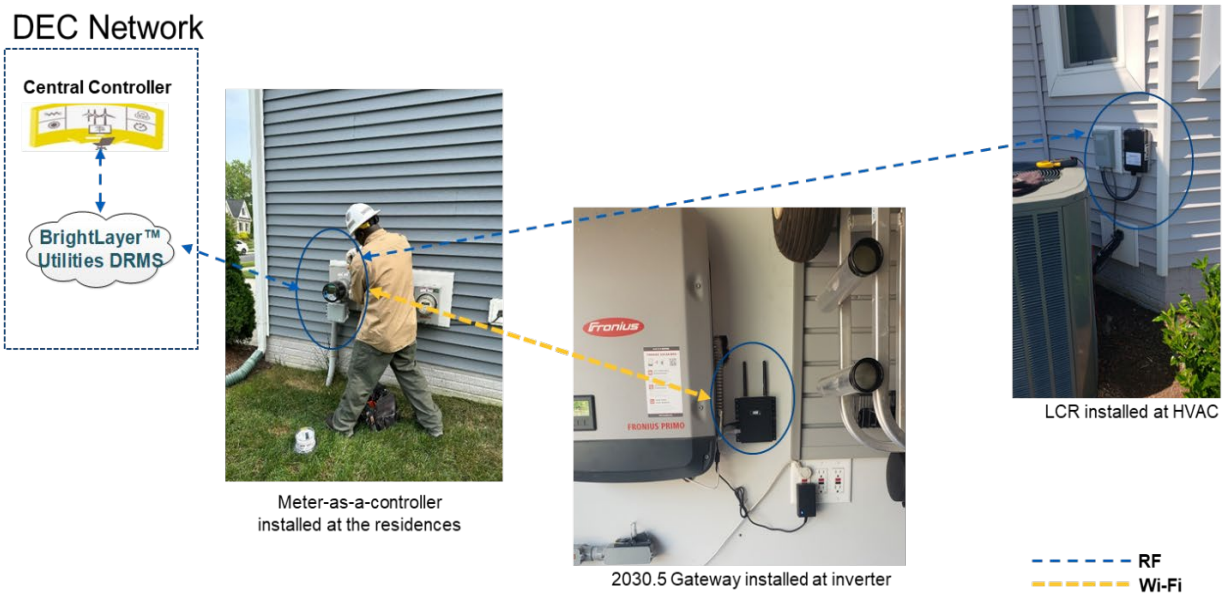

Figure 93. End-to-end system deployment in the DEC network.

After the field demonstration, team has documented some limitations and lessons learned for the technologies developed:

Table 21. Lessons learned/takeaways from the developed technologies

Technology	Limitations/Lessons learned/takeaways
Meter-Controller Prototype	• No Remote Connectivity to update FW • HW watchdog should be included • Software security can be increased • Permanent adapters and extension to fit on a house socket
Premise-Controller Application	• Open sources solvers to fit on single-board processor • Detection of loads • Integration with thermostat and/or auto discovery • Eliminate heat capacity of the electric water heater tank • Integration of EV control
IEEE 2030.5 Service	• Server doesn't support reconnection • Vendors are not open to provide certifications for testing
Central Controller/Yukon	• Nice to have the ability to access the edge FW and update from the central controller • Integration of weather station for more precise and granular data
End-to-end communication	• RF Mesh is hard to debug remotely; WiFi/Cellular can be alternative
Platform OS	• Moving to Ubuntu core or Yocto Linux would provide more benefits over Linux OS

Task 14.0: Stakeholder engagement (Budget Period 3)

In BP3, team focused on demonstrating the outcome of the use cases through lab validation and the update on field trial. Team consequently reported the how the field devices will be installed, and communication will be established. Industry advisory board constantly provided positive feedback on the development. In addition, in many discussion with the stakeholders, the inclusion on electric vehicle in the control and coordination platform. Team acknowledges that it is a gap in the development and would like to put a plan for it in future development.

3. Significant Accomplishments and Conclusions:

The objective of this project was to develop, test, and demonstrate a hierarchical control framework integrating utility DRMS and a meter-as-a-controller protype through AMI. Goal for this end-to-end integration is create observability and controllability of BTM DERs to utilize them for grid services. The major accomplishments in this project are listed below:

- **Algorithms:** A precise load disaggregation, utility level uncontrolled load forecast, and coordinated control algorithms for end-user assets for both utility interfacing and user-focused; a central level control algorithm is also developed to coordinate residential loads in a distribution for achieving necessary load reduction so that voltage profiles don't violate over 90% of the operational time.

- **Hardware prototype:** A hardware/software prototype of meter-as-a-controller to integrate with end-user assets such as HAVC, EWH, and DERs, and utility controller (DRMS); HVAC and EWH are controlled by Eaton load control relay (LCR) based on the command received from meter-as-a-controller; meter-as-a-controller is also able to control the solar PV setpoint as well as battery SOC.
- **Lab testing:** Detailed technology readiness level 5 (TRL 5) level validation plan and successful testing at system performance lab in National Renewable Energy Lab (NREL); The testing included the asset controls in three virtual homes; these homes were also coordinated via Eaton Yukon DRMS to test the interconnectivity, exchange the homes flexibility, and pseudo-price a signal to curtail the load within the home; the validation helped in de-risking the technology prior to field deployment.
- **Field deployment and demonstration**: Successful technology readiness level 6 (TRL 6) field demonstration to show the interconnectivity and scalability at Delaware Electric Co-op; The communication between meter-as-a-controller and home assets were showcased through RF and IEEE 2030.5; Communication between meter-as-a-controller and Yukon DRMS was also demonstrated; the end-to-end interconnectivity is scalable to more than 10000 meters with additional RF gateway.
- **Patent applications:** Generated 7 patent applications for path to commercialization; details of the patent applications are provided in section 5;
- **Papers:** Published three papers and one paper has received the recognition of best paper at IEEE PES GM 2024.

4. Path Forward:

Eaton does not have any smart metering commercial product as such to take the meter-as-a-controller developments to the market right away. However, all the developments have been filed for patent applications. In addition, team is currently working on how portions of these developments can be taken to the available product lines as well what new research can be conducted basing these developments. Few directions that may lead to the next level of research are:

- **Hosting platform:** Enhance the developments and controls in the breaker-based system to reduce dependency on additional controller and communication platforms; breakers are already connected to the home assets which can be controlled and coordinated through a gateway instead of meter-as-a-controller.
- **Algorithms:** Include EV and/or V2X functionalities for providing resilience in a residential home; Current SETO algorithm didn't consider EV as controllable load- considering EV load as a controllable load would provide additional flexibility for home operations as well as grid services.
- **Utility Interfacing:** Make the controller vendor agnostic to interconnect with numerous home assets and ADMS/DRMS/DERMS provided by different vendors; This will ensure the controller has a broader points list and multiple protocols to support different HW/SW manufactures.
- **Firmware Improvement:** Eliminate the firmware related limitations from the lessons learned listed in Table 21; this will enable a close-to-commercial grade product for the end-users.

5. Products:

Throughout the project, the development that team has undergone a significant development which have been disseminated through different publications and intellectual properties. Tables below show the list of publications and patents/Provisionals/disclosures submitted during the project lifetime.

Table 22. Papers published during the project life-time

"Article Title"	Paper Number	Conference/Proceedings Title	Conference Location	Date (MM/DD/YYYY; First day if multiple days)
Secure Control Regions for Distributed Stochastic Systems with Application to Distributed Energy Resources Dispatch	1047	American Control Conference	Atlanta, GA	6/8/2022
A Hierarchical Control Architecture: Utilization of Behind-the-Meter Appliances with Increased Visibility and Controllability	2003	Power and Energy Society General Meeting	Orlando, FL	7/23/2023
Value-based Insights from the Implementation of Hierarchical Control for Energy Savings and Demand Response in Residential Premises	1348	Power and Energy Society General Meeting	Seattle, Washington	7/22/2024

Table 23. Patents/Provisionals/Disclosures submitted during project lifetime

"Patent Title" (Invention Disclosure Tile)	Date Application Filed (Date Disclosure Filed)	Patent Application Number (Invention Disclosure Dock No.)
Control of Electric Water Heater based on Two-Mass Model for Behind-the-Meter Building Energy Management System	31-Mar-22	18/193077
DERs Scheduler with Quality-of-Service Consideration for Behind-the-Meter Building Energy Mgmt System	7-Jul-23	15720.1055USP1
Short-term load prediction of residential appliances using a memory-based method	7-Jul-23	15720.1054USP1
Air Conditioner Predictive Power Management with Quality-of-Service Consideration for Behind-the-Meter Building Energy Mgmt System	31-Mar-22	18/192259

Pseudo Signal Feedback Mechanism for Aggregated Load Regulation in a Hierarchical Distributed Grid Control	31-Mar-22	18/193957
Estimation of Home Indoor Temperature Without Temperature Sensor for Maintaining Quality of Service in Behind-the-Meter Building Energy Management System	7-Jul-23	15720.1056USP1
A Hierarchical Communication and Control Architecture Utilizing Advanced Metering Infrastructure for the Operations of Behind-the-Meter Distributed Energy Resources and Controllable Appliances	11-Jul-23	041-242P01/P23-1504US01PROV

6. Project Team and Roles:

Table below shows the required milestones, teams involved in each milestone, and timelines of the project per SOPO those have been completed:

Table 24. Milestones per SOPO

SOPO/TWP Milestone #	Milestone Description	Performer	Original Planned	Revised Planned	Actual	Percent Complete
M.1.1.1	Data collection and cleaning	NREL, Eaton, Pecan Street	12/31/20		*12/31/20*	*100%*
M.1.1.2	RMS error	NREL, Eaton, Pecan Street	6/30/21		*6/28/21*	*100%*
M.1.1.3	Forecast error reduction	NREL, Eaton, Pecan Street	9/30/21		*9/30/21*	*100%*
M1.2.1	Application and use case definition	Eaton, EPRI	3/31/21		*3/26/21*	*100%*
M1.2.2	Simulation validation	Eaton, EPRI	6/30/21		*6/24/21*	*100%*
M1.3.1	Simulation and data mining	NREL, Eaton	6/30/21		*6/23/21*	*100%*
M1.4.1	Data rate and specs	Eaton, EPRI	9/30/21		*9/30/21*	*100%*
M1.5.1	Industry engagement	Eaton, EPRI, Pecan Street, NREL	9/30/20		*10/1/20*	*100%*
M1.5.1	Industry engagement	Eaton, EPRI, Pecan Street, NREL	12/31/20		*12/10/20*	*100%*
M1.5.1	Industry engagement	Eaton, EPRI, Pecan Street, NREL	3/31/21		*3/26/21*	*100%*
M1.5.1	Industry engagement	Eaton, EPRI, Pecan Street, NREL	6/30/21		*6/28/21*	*100%*

M1.5.1	Industry engagement	Eaton, EPRI, Pecan Street, NREL	9/30/21		*9/27/21*	*100%*
M.2.6.1	Simulation validation	Eaton	9/30/22		*9/30/22*	*100%*
M.2.7.1	Simulation validation	NREL	6/30/22	*7/31/22*	*6/30/22*	*100%*
M.2.8.1	Firmware functionalities	Eaton, EPRI	3/31/22		*3/31/22*	*100%*
M.2.8.2	Hardware/software integration	Eaton, NREL	6/30/22	*10/30/22*	*9/26/22*	*100%*
M.2.9.1	Hardware/software function test	Eaton, Pecan Street	9/30/22	*10/30/22*	*10/30/22*	*100%*
M.2.11.1	Industry engagement	Eaton, EPRI, Pecan Street, NREL	12/31/21		*12/31/21*	*100%*
M.2.11.1	Industry engagement	Eaton, EPRI, Pecan Street, NREL	4/1/22		*4/1/22*	*100%*
M.2.11.1	Industry engagement	Eaton, EPRI, Pecan Street, NREL	6/30/22		*6/30/22*	*100%*
M.2.11.1	Industry engagement	Eaton, EPRI, Pecan Street, NREL	9/30/22		*9/30/22*	*100%*
M.3.12.1	Hardware/software function test	Eaton	12/31/23		*6/15/23*	*100%*
M.3.13.1	Status report	Eaton	3/31/23	*7/15/23*	*7/15/23*	*100%*
M.3.13.2	Field Test	Eaton	6/30/23	*9/30/23*	*8/30/23*	*100%*

7. References:

[1] A. Kahan, “EIA projects nearly 50% increase in world energy usage by 2050, led by growth in Asia,” eia.gov, Sep. 24, 2019. https://tinyurl.com/y6r976c2 (accessed Nov. 07, 2023)

[2] International Energy Agency, “Net Zero by 2050 – Analysis,” IEA, May 2021. https://www.iea.org/reports/net-zero-by-2050

[3] U. S. D. of Energy, “Grid-Scale U.S. Energy Storage Capacity Could Grow Five-Fold By 2050,” *CleanTechnica*, Jun 07, 2021. https://tinyurl.com/yqsattfo (accessed Nov. 07, 2023)

[4] “Summary Report on EVs at Scale and the U.S. Electric Power System,” 2019. Available: https://tinyurl.com/3ypszzhh (accessed Nov. 07, 2023)

[5] C. Qin, A. K. Srivastava and K. L. Davies, "Unbundling Smart Meter Services Through Spatiotemporal Decomposition Agents in DER-Rich Environment," in IEEE Transactions on Industrial Informatics, vol. 18, no. 1, pp. 666-676, Jan. 2022.

[6] Y. Yuan and Z. Wang, "Mining Smart Meter Data to Enhance Distribution Grid Observability for Behind-the-Meter Load Control: Significantly improving system situational awareness and providing valuable insights," in IEEE Electrification Magazine, vol. 9, no. 3, pp. 92-103, Sept. 2021.

[7] P. Paudyal et al., "The Impact of Behind-the-Meter Heterogeneous Distributed Energy Resources on Distribution Grids," 2020 47th IEEE Photovoltaic Specialists Conference (PVSC), 2020, pp. 0857-0862.

[8] W. Liu and F. Ding, "Collaborative Distribution System Restoration Planning and Real-Time Dispatch Considering Behind-the-Meter DERS," in IEEE Transactions on Power Systems, vol. 36, no. 4, pp. 3629-3644, July 2021.
[9] C. Huang et al., "Smart Meter Pinging and Reading Through AMI Two-Way Communication Networks to Monitor Grid Edge Devices and DERs," in IEEE Transactions on Smart Grid, vol. 13, no. 5, pp. 4144-4153, Sept. 2022.
[10] Nalley S, LaRose A. Annual energy outlook 2022 (AEO2022). Energy Information Agency. 2022 Mar 3;23.
[11] Omitaomu OA, Niu H. Artificial intelligence techniques in smart grid: A survey. Smart Cities. 2021 Apr 22;4(2):548-68.
[12] J. Hao, D. W. Gao and J. J. Zhang, "Reinforcement Learning for Building Energy Optimization Through Controlling of Central HVAC System," in IEEE Open Access Journal of Power and Energy, vol. 7, pp. 320-328, 2020, doi: 10.1109/OAJPE.2020.3023916.
[13] Y. Xu and J. V. Milanović, "Artificial-Intelligence-Based Methodology for Load Disaggregation at Bulk Supply Point," in IEEE Transactions on Power Systems, vol. 30, no. 2, pp. 795-803, March 2015, doi: 10.1109/TPWRS.2014.2337872.
[14] S. Kong, Y. Kim, R. Ko and S. -K. Joo, "Home appliance load disaggregation using cepstrum-smoothing-based method," in IEEE Transactions on Consumer Electronics, vol. 61, no. 1, pp. 24-30, February 2015, doi: 10.1109/TCE.2015.7064107.
[15] N. Huang, W. Wang, S. Wang, J. Wang, G. Cai, and L. Zhang, "Incorporating Load Fluctuation in Feature Importance Profile Clustering for Day-Ahead Aggregated Residential Load Forecasting," in IEEE Access, vol. 8, pp. 25198-25209, 2020.
[16] W. Kong, Z. Y. Dong, Y. Jia, D. J. Hill, Y. Xu and Y. Zhang, "Short-Term Residential Load Forecasting Based on LSTM Recurrent Neural Network," in IEEE Transactions on Smart Grid, vol. 10, no. 1, pp. 841-851, Jan. 2019.
[17] M. Sun, T. Zhang, Y. Wang, G. Strbac and C. Kang, "Using Bayesian Deep Learning to Capture Uncertainty for Residential Net Load Forecasting," in IEEE Transactions on Power Systems, vol. 35, no. 1, pp. 188-201, Jan. 2020.
[18] E. Razavi, A. Arefi, D. Smith, G. Ledwich, G. Nourbakhsh and M. Minakshi, "Privacy-Preserved Framework for Short-Term Probabilistic Net Energy Forecasting," in IEEE Transactions on Industrial Informatics, vol. 19, no. 6, pp. 7613-7623, June 2023
[19] S. E. Razavi, A. Arefi, G. Ledwich, G. Nourbakhsh, D. B. Smith and M. Minakshi, "From Load to Net Energy Forecasting: Short-Term Residential Forecasting for the Blend of Load and PV Behind the Meter," in IEEE Access, vol. 8, pp. 224343-224353, 2020.
[20] S. Shao, M. Pipattanasomporn and S. Rahman, "Development of physical-based demand response-enabled residential load models," in IEEE Transactions on Power Systems, vol. 28, no. 2, pp. 607-614, May 2013.
[21] F. Y. Melhem, O. Grunder, Z. Hammoudan and N. Moubayed, "Energy Management in Electrical Smart Grid Environment Using Robust Optimization Algorithm," in IEEE Transactions on Industry Applications, vol. 54, no. 3, pp. 2714-2726, May-June 2018.
[22] N. G. Paterakis, O. Erdinç, A. G. Bakirtzis and J. P. S. Catalão, "Optimal Household Appliances Scheduling Under Day-Ahead Pricing and Load-Shaping Demand Response Strategies," in IEEE Transactions on Industrial Informatics, vol. 11, no. 6, pp. 1509-1519, Dec. 2015.
[23] F. Y. Melhem, O. Grunder, Z. Hammoudan and N. Moubayed, "Optimization and Energy Management in Smart Home Considering Photovoltaic, Wind, and Battery Storage System with Integration of Electric Vehicles," in Canadian Journal of Electrical and Computer Engineering, vol. 40, no. 2, pp. 128-138, 2017.
[24] V. C. Gungor, D. Sahin, T. Kocak, S. Ergut, C. Buccella, C. Cecati, and G. P. Hancke, “A survey on smart grid potential applications and communication requirements,” IEEE Transactions on industrial informatics, vol. 9, no. 1, pp. 28–42, 2012.
[25] D. Henry and J. E. Ramirez-Marquez, “Generic metrics and quantitative approaches for system resilience as a function of time,” Reliability Engineering & System Safety, vol. 99, pp. 114–122, 2012.
[26] K. Baker, A. Bernstein, E. Dall’Anese, and C. Zhao, “Network cognizant voltage droop control for distribution grids,” IEEE Transactions on Power Systems, vol. 33, no. 2, pp. 2098–2108, 2017.
[27] United States Department of State and the United States Executive Office of the President. (2021). THE LONG-TERM STRATEGY OF THE UNITED STATES Pathways to Net-Zero Greenhouse Gas Emissions by 2050. https://www.whitehouse.gov/wp-content/uploads/2021/10/US-Long-Term-Strategy.pdf

[28] Ricketts, S., Bast, C., Argento-McCurdy, H., Hoffman, E., Fowler, N., & Clayton, K. (2023, September 14). Implementing America's Clean Energy Future. Center for American Progress. https://www.americanprogress.org/article/implementing-americas-clean-energy-future/